การกักเก็บเคอร์คิวมินในอนุภาคระดับนาโน

นางสาวณัฐกฤตา สุวรรณทีป

ENCAPSULATION OF CURCUMIN INTO NANOPARTICLES

Miss Natthakitta Suwannateep

A Dissertation Submitted in Partial Fulfillment of the Requirements

for the Degree of Doctor of Philosophy Program in Biotechnology

Faculty of Science

Chulalongkorn University

Academic Year 2010

Thesis Title	ENCAPSULATION OF CURCUMIN INTO NANOPARTICLES
By	Miss Natthakitta Suwannateep
Field of Study	Biotechnology
Thesis Advisor	Associate Professor Supason Wanichwecharungruang, Ph.D.

Accepted by the Faculty of Science, Chulalongkorn University in Partial Fulfillment of the Requirements for the Doctoral Degree

…………………………………………….. Dean of the Faculty of Science

(Professor Supot Hannongbua, Dr. rer. nat.)

THESIS COMMITTEE

…………………………………………... Chairman

(Associate Professor Sirirat Rengpipat, Ph.D.)

………………………………………….……. Thesis Advisor

(Associate Professor Supason Wanichwecharungruang, Ph.D.)

………………………………………….. Examiner

(Professor Dr.med Pravit Asawanonda, Ph.D.)

………………………………………….. Examiner

(Associate Professor Nattaya Ngamrojanavanich, Ph.D.)

…………………………………………….. External Examiner

(Associate Professor Chavanee Tongroach, Ph.D.)

ณัฐกฤตา สุวรรณทีป : การกักเก็บเคอร์คิวมินในอนุภาคระดับนาโน.
(ENCAPSULATION OF CURCUMIN INTO NANOPARTICLES)
อ. ที่ปรึกษาวิทยานิพนธ์หลัก : รศ. ดร. ศุภศร วนิชเวชารุ่งเรือง, 124 หน้า.

การกักเก็บเคอร์คิวมินดำเนินการโดยวิธีไดอะไลซิส โดยใช้พอลิเมอร์ที่แตกต่างกัน คือ เอทิลเซลลูโลส (EC), เมทิลเซลลูโลส (MC), เมทิลอีเธอร์เทอมิเนตเตตพอลิ(เอทิลีนไกลคอล)-4-เมทอกซีซินนาโมอิลพธาโลอิลไคโตซาน (PCPLC), พอลิ(ไวนิลแอลกอฮอล์–โค-ไวนิล-4-เมทอกซีซินนาเมต) ที่มีการแทนที่ของ 4-เมทอกซีซินนาโมอิลสองดีกรี (PB4-I และ PB4-II) พอลิเมอร์ทั้งห้าสามารถกักเก็บเคอร์คิวมินได้และให้อนุภาครูปทรงกลม โดยให้ค่าประสิทธิภาพการกักเก็บมากกว่า 90% กักเก็บเคอร์คิวมินได้ประมาณ 50% โดยน้ำหนัก ที่อัตราส่วนโดยน้ำหนักของพอลิเมอร์ต่อเคอร์คิวมิน 1:1 จากการศึกษาพบว่าเคอร์คิวมินที่ถูกกักเก็บในอนุภาคนาโนมีความเสถียรต่อแสงมากกว่าเคอร์คิวมินอิสระอย่างมีนัยสำคัญ การทดลองควบคุมการปลดปล่อยของเคอร์คิวมินจากอนุภาคทั้งห้าชนิด พบว่าเคอร์คิวมินสามารถถูกปลดปล่อยจากอนุภาค EC และ ECMC ได้ดีที่สุดทั้งในภาวะที่เป็นกรดและเป็นกลาง อีกทั้ง ECMC ยังปลดปล่อยเคอร์คิวมินได้ดีกว่า EC ในภาวะเลียนแบบน้ำย่อยในกระเพาะ การประเมินผลอรรถชีวประโยชน์ของเคอร์คิวมินที่ถูกกักเก็บใน EC (C-EC) และ ECMC (C-ECMC) โดยป้อนให้หนูทางปาก พบว่าอนุภาคมีการยึดเกาะที่เนื้อเยื่อมิวคอซาของกระเพาะอาหารและมีความสามารถในการปล่อยเคอร์คิวมินเข้าสู่กระแสเลือดได้มากกว่าและนานกว่าเคอร์คิวมินอิสระ นอกจากนี้ทั้ง C-EC และ C-ECMC ยังมีความสามารถป้องกันการเกิดอนุมูลอิสระที่ผิวหนังซึ่งให้ผลเทียบเคียงได้กับเคอร์คิวมินอิสระ การศึกษาการซึมผ่านผิวหนังของหูหมู พบสัญญาณการเรืองแสงของเคอร์คิวมินในเนื้อเยื่อผิวและบริเวณรูขุมขนที่ผิวหนัง โดยที่โลชั่นแบบน้ำในน้ำมันช่วยเพิ่มการซึมผ่านของ C - EC และ C - ECMC สู่ชั้นผิวหนังและรูขุมขนที่ผิวหนังได้ดีกว่าโลชั่นแบบน้ำมันในน้ำ ภาพจากการสังเกตด้วยกล้องจุลทรรศน์เลเซอร์สแกนเรืองแสง (LFSM) แสดงให้เห็นว่ารูขุมขนที่ผิวหนังเป็นเส้นทางขนส่งหลักของเคอร์คิวมินที่ถูกกักเก็บในอนุภาคนาโนที่เตรียมได้

สาขาวิชา....เทคโนโลยีชีวภาพ.....ลายมือชื่อนิสิต...
ปีการศึกษา...........2553.............ลายมือชื่อ อ.ที่ปรึกษาวิทยานิพนธ์หลัก...........................

Thesis Title	ENCAPSULATION OF CURCUMIN INTO NANOPARTICLES
By	Miss Natthakitta Suwannateep
Field of Study	Biotechnology
Thesis Advisor	Associate Professor Supason Wanichwecharungruang, Ph.D.

Accepted by the Faculty of Science, Chulalongkorn University in Partial Fulfillment of the Requirements for the Doctoral Degree

……………………………………….. Dean of the Faculty of Science

(Professor Supot Hannongbua, Dr. rer. nat.)

THESIS COMMITTEE

……………………………………... Chairman

(Associate Professor Sirirat Rengpipat, Ph.D.)

………………………………….……. Thesis Advisor

(Associate Professor Supason Wanichwecharungruang, Ph.D.)

………………………………………….. Examiner

(Professor Dr.med Pravit Asawanonda, Ph.D.)

………………………………………….. Examiner

(Associate Professor Nattaya Ngamrojanavanich, Ph.D.)

………………………………………….. External Examiner

(Associate Professor Chavanee Tongroach, Ph.D.)

ACKNOWLEDGEMENTS

CONTENTS

LIST OF TABLES

LIST OF FIGURES

Figure   **Page**

LIST OF ABBREVIATIONS

$^{\circ}C$	degree celsius
mW	milliwatt
cm^2	square centimeter
mm	millimeter
nm	nanometer
s	second
min	minute
h	hour
ppm	part per million
µg	microgram
mg	milligram
µl	microliter
ml	milliliter
DMF	dimethyl formamide
DMSO	dimethyl sulfoxide
LPSSD	low-pressure superheated steam drying
HPLC	high performance liquid chromatography
SEM	scanning electron microscopy
TEM	transmission electron microscopy
LFSM	laser fluorescent scanning microscopy
EPR	electron paramagnetic resonance spectroscopy
RFPC	radical formation protection capacity
PCPLC	methyl ether terminated poly(ethylene glycol)-4-methoxycinnamoyl phthaloylchitosan
PB4-I	poly(vinylalcohol-co-vinyl-4-methoxycinnamate) with degree of 4-methoxycinnamoyl substituion of 0.30
PB4-II	poly(vinylalcohol-co-vinyl-4-methoxycinnamate) with degree of 4-methoxycinnamoyl substituion of 0.44

EC	ethyl cellulose
MC	methyl cellulose
FC	free curcumin
C-EC	curcumin-loaded EC particles
C-ECMC	curcumin-loaded ECMC particles
L1	oil in water lotion pH 5
L2	water in oil lotion pH 5
WS	water suspension
PBS	phosphate buffer solution
SGF	simulated gastric fluid
SIF	simulated intestinal fluid
SBF	suction blister fluid

CHAPTER I

INTRODUCTION

Curcumin

Curcumin [1,7-bis(4-hydroxy-3-methoxyphenyl)-1, 6-heptadiene-3, 5-dione] is the polyphenol active ingredient derived from the rhizome of turmeric (*Curcuma longa*) (Figure 1.1). The powdered turmeric has been used in Asian cookery, medicine, cosmetics and fabric dying for more than twenty centuries. This compound has a long history of use in traditional medicines of India and China. In food and manufacturing, curcumin is currently used in perfumes and as a natural yellow coloring agent, as well as an approved food additive to flavor various types of curries and mustards. Recent emphasis on the use of natural and complementary medicines in Western medicine has drawn the attention of the scientific community to this ancient remedy. Research has revealed that curcumin has a surprisingly wide range of beneficial properties, including anti-inflammatory, antioxidant, chemopreventive and chemotherapeutic activity. These activities have been demonstrated both in cultured cells and in animal models and have paved the way for ongoing human clinical trials [1].

Figure 1.1 *Curcuma longa* (from Koehler's Medicinal-Plants).

Turmeric was isolated and structurally characterized. It contains curcumin, demethoxycurcumin and bisdemethoxycurcumin, which curcumin is the most common structure (Figure 1.2). The stability of curcumin and its chemical degradation has been investigated by several laboratories with varying results. This natural pigment molecule decomposes very rapidly, giving out vanillin, ferulic acid, feruloylmethane and trans-6-(4-hydroxy-3-methoxyphenyl)-2,4-dioxo-5-hexenal as its degradation products. Bis-demethoxycurcumin was the most stable, while curcumin is the fastest decomposed and also photodegradable. Pure turmeric was found to have the highest concentration of curcumin with an average of 3.14% by weight, while curry powders contained relatively low amounts of curcumin. In addition, curcumin itself exists in several forms that exhibit different potencies as antioxidants and anti-tumor agents. Thus, the actual amount of curcumin used in various studies is often unclear [1].
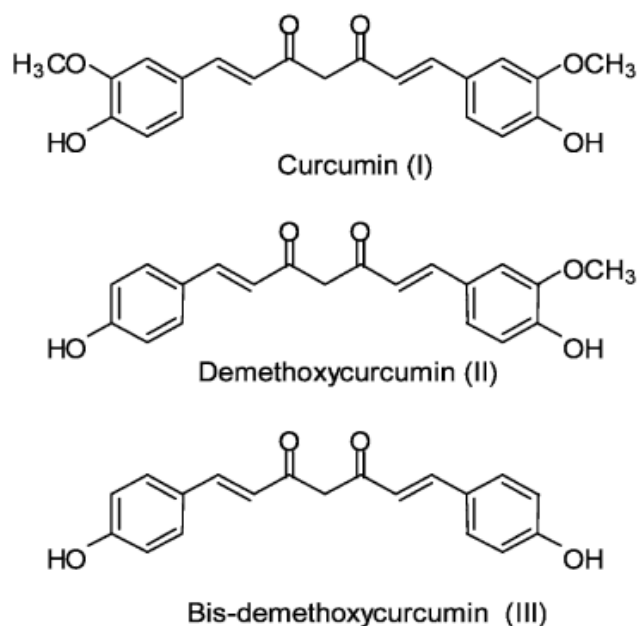
Figure 1.2 Structure of curcumin, demethoxycurcumin and bis-demethyoxycurcumin

Curcumin does not affect to be toxic to animals or humans even at high doses. For centuries, curcumin has been consumed as a dietary spice at doses up to 100 mg/day. Clinical trials phase I indicate that human beings can tolerate a dose as high as

8 g/day with no side effects. Consonant with preclinical demonstrations of curcumin's anti-inflammatory and anti-cancer properties, disease targets include neoplastic and preoplastic diseases such as multiple myeloma, pancreatic cancer, myelodysplastic syndromes, and colon cancer, and conditions linked to inflammation such as psoriasis, and Alzheimer's disease. Curcumin and its disease targets are schematically shown in Figure 1.3 [2]. The desirable preventive or putative therapeutic properties of curcumin have been considered to be associated with its antioxidant and anti-inflammatory properties. Curcumin has been shown to be effective in acute as well as chronic models of inflammation. Several studies have shown that curcumin is a potent antioxidant. In fact, curcumin has been found to be at least 10 times more active as an antioxidant than even vitamin E [2].
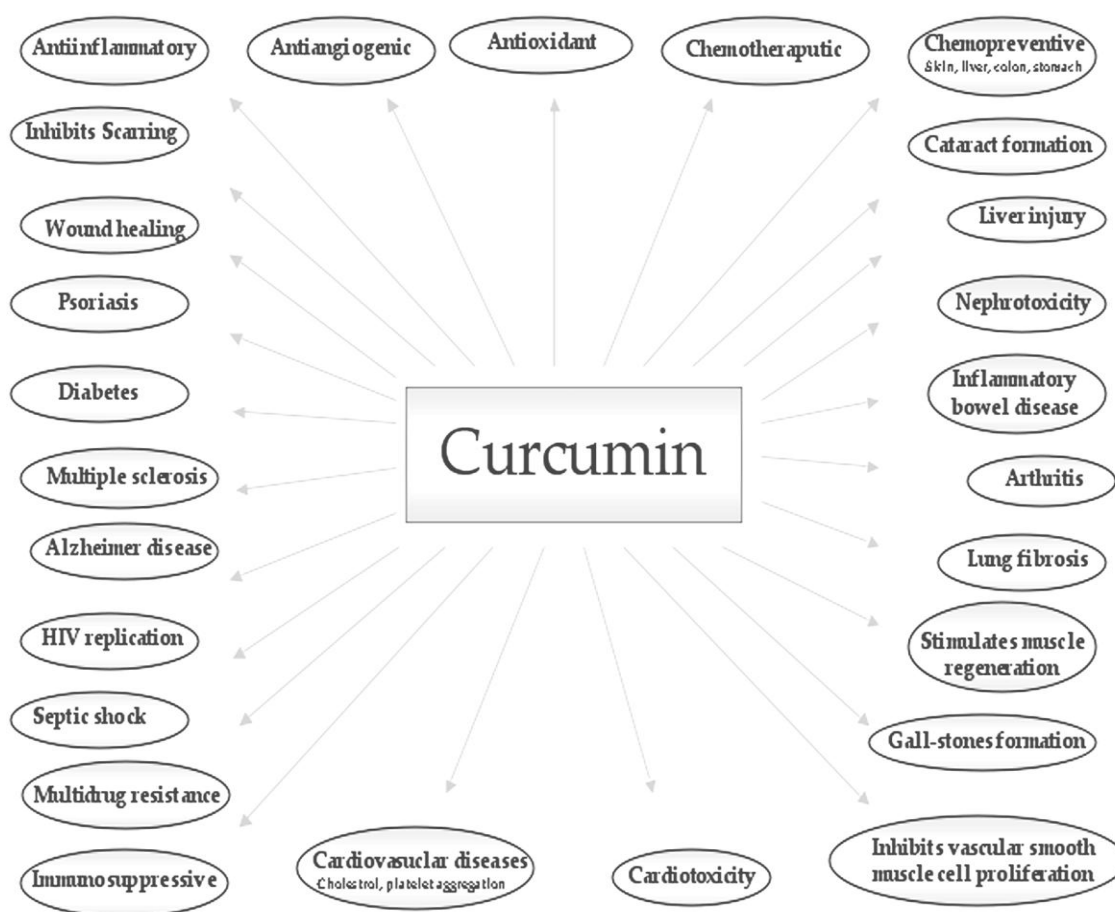
Figure 1.3 Disease targets of curcumin

Various studies have shown that curcumin modulates numerous targets (Figure 1.4). These include the growth factors, growth factor receptors, transcription factors, cytokines, enzymes, and genes regulating apoptosis [2].
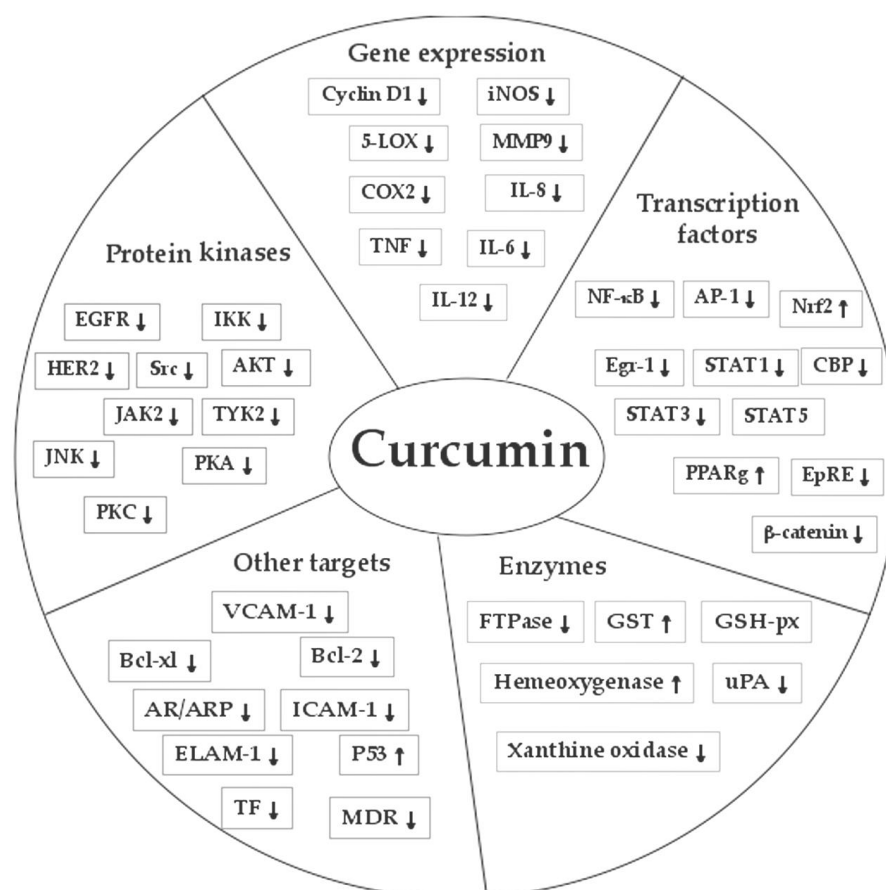
Figure 1.4 Molecular targets of curcumin

Chemically, curcumin is a bis-α,β-unsaturated β-diketone (commonly called diferuloylmethane), which exhibits keto–enol tautomerism having a predominant keto form in acidic and neutral solutions and stable enol form in alkaline medium. Commercial curcumin contains approximately 77% diferuloylmethane, 17% demethoxycurcumin, and 6% bis-demethoxycurcumin. Curcumin and its metabolites are schematically shown in Figure 1.5. Because inflammation is closely linked to tumor promotion, curcumin with its potent anti-inflammatory property is anticipated to exert chemopreventive effects on carcinogenesis. Hence, the past few decades have

witnessed intense research devoted to the antioxidant and anti-inflammatory properties of curcumin. Curcumin, however, is a hydrophobic molecule and is practically insoluble in aqueous solutions, thus, this insolubility not only limits its application but also hampers bioavailability of the compound [3].
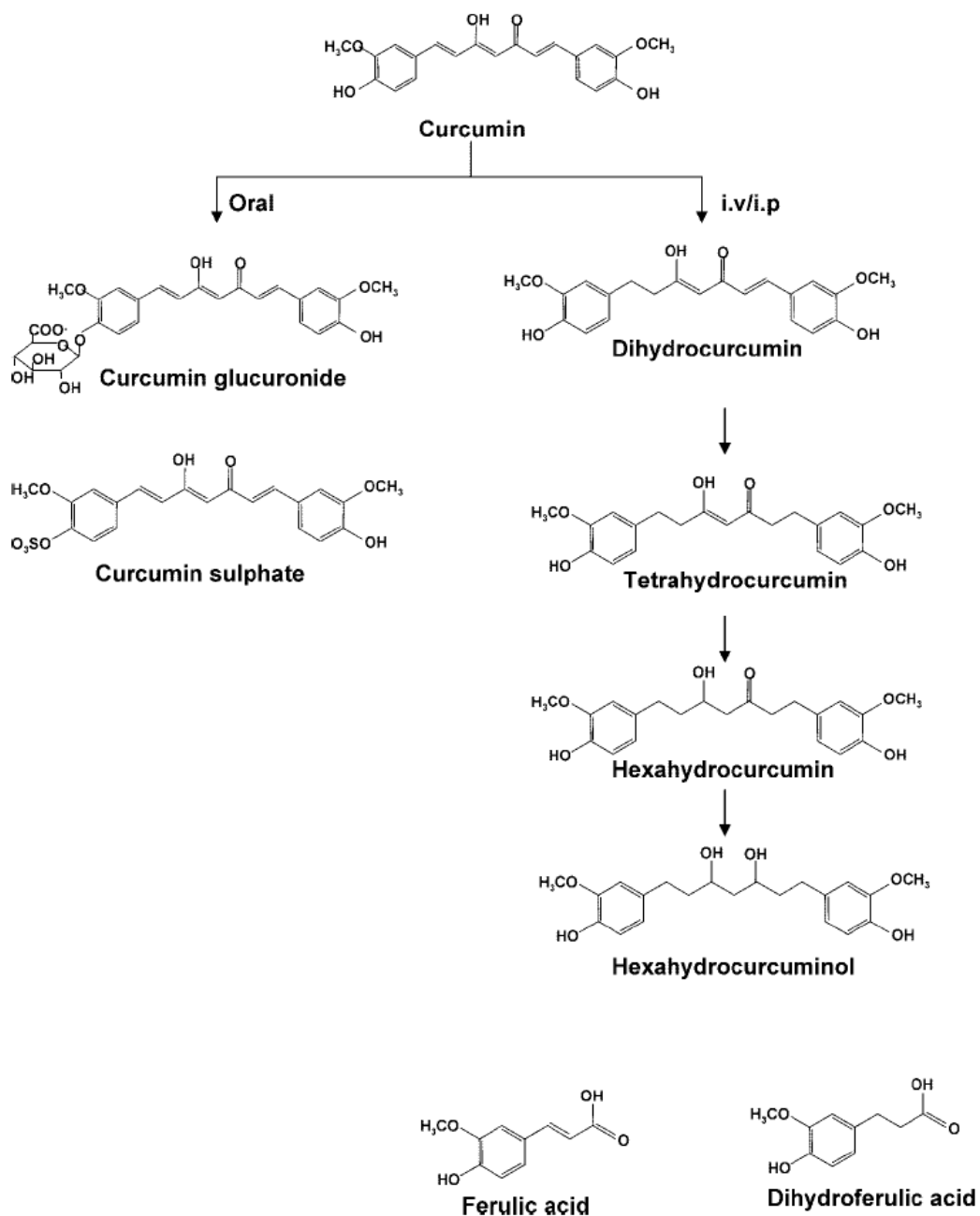
Figure 1.5 Structure of curcumin and its metabolites

The reasons for reduced bioavailability of any agent within the body are low intrinsic activity, poor absorption and high rate of metabolism, inactivity of metabolic products and/or rapid elimination and clearance from the body. Studies to date have suggested a strong intrinsic activity and, hence, efficacy of curcumin as a therapeutic agent for various ailments. However, studies over the past three decades related to absorption, distribution, metabolism and excretion of curcumin have revealed poor absorption and rapid metabolism of curcumin that severely curtails its bioavailability [3]. The tissue and serum distribution of curcumin reported in various animal and human studies is summarized in Table 1.

Table 1.1 Serum and tissue of curcumin in rodents and human after different routes of administration

species	route[a]	dose	plasma/tissue	levels	ref
mice	i.p.	100 mg/kg	plasma	2.25 μg/mL	
			intestine	117 $\pm$ 6.9 μg/g	
			spleen	26.1 $\pm$ 1.1 μg/g	34
			liver	26.9 $\pm$ 2.6 μg/g	
			kidney	7.5 $\pm$ 0.08 μg/g	
			brain	0.4 $\pm$ 0.01 μg/g	
mice	oral	100 mg/kg	plasma	0.22 μg/mL	
mice	i.p.	100 mg/kg	plasma	25 $\pm$ 2 nmol/mL	
			intestinal mucosa	200 $\pm$ 23 nmol/g	
			liver	73 $\pm$ 20 nmol/g	
			brain	2.9 $\pm$ 0.4 nmol/g	35
			heart	9.1 $\pm$ 1.1 nmol/g	
			lungs	16 $\pm$ 3 nmol/g	
			muscle	8.4 $\pm$ 6 nmol/g	
			kidney	78 $\pm$ 3 nmol/g	
rat	oral	2 g/kg	stomach	53.3 $\pm$ 5.1 (μg/g)	
			small intestine	58.6 $\pm$ 11.0 (μg/g)	32
			cecum	51.5 $\pm$ 13.5 (μg/g)	
			large intestine	5.1 $\pm$ 2.5 (μg/g)	
rat	oral	340 mg/kg	serum	6.5 $\pm$ 4.5 nM	39
rat	oral	1g/kg	serum	0.5 μg/mL	38
rat	oral	2 g/kg	serum	1.35 $\pm$ 0.23 μg/mL	28
rat	oral	500 mg/kg	plasma	0.06 $\pm$ 0.01 μg/mL	37
rat	i.v.	10 mg/kg	plasma	0.36 $\pm$ 0.05 μg/mL	
human	oral	2 g/kg	serum	0.006 $\pm$ 0.005 μg /mL	28
human	oral	4–8 g	serum	0.4–3.6 μM	27
human	oral	10 g	serum	50.5 ng/m	26
human	oral	12 g	serum	51.2 ng/mL	
human	oral	3.6 g	plasma	11.1 $\pm$ 0.6 nmol/mL	36
human	oral	0.4–3.6 g	colorectum	7–20 nmol/g	42

[a] Key: i.p., intraperitoneal; i.v., intravenous.

Numerous approaches have been undertaken to improve the bioavailability of curcumin. These approaches involve, (i) the use of adjuvant like piperine that interferes with glucuronidation; (ii) the use of liposomal curcumin; (iii) curcumin nanoparticles; (iv) the use of curcumin phospholipid complex; and (v) the use of structural analogues of curcumin. Modulation of route and medium of curcumin administration, blocking of metabolic pathways by concomitant administration with other agents, and structural modifications are the main strategies now being explored in attempts to improve the bioavailability of curcumin. Attempts at enhanced *in vitro* and *in vivo* efficacies of curcumin through structural modifications of the molecule and/or new formulations have been recently reported. However, the limited literature evidence devoted to show improvements in curcumin bioavailability reveals that the curcumin bioavailability enhancement has not gained significant attention. Yet, novel delivery strategies including those of nanoparticles, liposomes, and defined phospholipid complexes offer significant promise and are worthy of further exploration which appear to provide longer circulation, better permeability and resistance to metabolic processes in attempts to enhance the bioavailability, medicinal value and application of this interesting molecule [3].

Nanoparticles as Drug Carrier System

Nanoparticles are defined as particulate dispersions or solid, submicron-sized particles that may or may not be biodegradable. The term nanoparticles is a collective name for both nanospheres and nanocapsules. Nanospheres have a matrix type of structure. Drugs may be absorbed at the sphere surface or encapsulated within the particle. Nanocapsules are vesicular systems in which the drug is confined to a cavity consisting of an inner liquid core surrounded by a polymeric membrane. In this case the active substances are usually dissolved in the inner core but may also be adsorbed to the capsule surface. Nanoparticles are receiving considerable attention for the delivery of therapeutic drugs [4]. Nanoencapsulation of drugs involves forming drug loaded particles with diameters ranging from 1 to 1000 nm. The drug is dissolved, entrapped,

encapsulated or attached to a nanoparticles matrix. Depending upon the method of preparation, nanoparticles, nanospheres or nanocapsules can be obtained. In facts, polymeric nanoparticles have become a popular choice of carrier for the topical administration of cosmetics and pharmaceuticals due to their superior physical stability over not only liposomes but also microemulsions, multiple emulsions, solid lipid particles and nanostructured lipid carriers. Liposome have been used as potential drug carriers instead of conventional dosage forms because of their unique advantages which include ability to protect drugs from degradation, target the drug to the site of action and reduce the toxicity or side effects. However, developmental work on liposome has been limited due to inherent problems such as low encapsulation efficiency, rapid leakage of water-soluble drug in the presence of blood components and poor storage stability. On the other hand, polymeric nanoparticles offer some specific advantages over liposomes. For instance, nanoparticles help to increase the stability of drugs/proteins and possess useful controlled release properties [5]. The advantages of using nanoparticles as a drug delivery system include the following:

1. Particle size and surface characteristics of nanoparticles can be easily manipulated to achieve both passive and active drug targeting after parenteral administration.

2. They control and sustain release of the drug during the transportation and at the site of localization, altering organ distribution of the drug and subsequent clearance of the drug so as to achieve increase in drug therapeutic efficacy and reduction in side effects.

3. Controlled release and particle degradation characteristics can be readily modulated by the choice of matrix constituents. Drug loading is relatively high and drugs can be incorporated into the systems without any chemical reaction; this is an important factor for preserving the drug activity.

4. Site-specific targeting can be achieved by attaching targeting ligands to surface of particles or use of magnetic guidance.

5. The system can be used for various routes of administration including oral, nasal, parenteral, intra-ocular etc.

In spite of these advantages, nanoparticles do have limitations. For example, their small size and large surface area can lead to particle aggregation, making physical handling of nanoparticles difficult in liquid and dry forms. Effect of characteristics of nanoparticles on drug delivery includes particle size and size distribution, surface properties of nanoparticles, drug loading and drug release. In fact, small particles size and large surface area readily result in limited drug loading and burst release. These practical problems have to be overcome before nanoparticles can be used clinically or made commercially available [6].

The Skin Barrier and Transdermal Drug Delivery

The skin consists of 4 basic layers: the stratum corneum, viable epidermis, dermis and subcutaneous tissues (Figure 1.6). In addition to these structures, there are also several associated appendages: hair follicles, sweat glands, apocrine glands, and nails. During the differentiation process the epidermal layers (stratum spinosum, granulosum, lucidum and corneum) are converted to corneocytes. Herein cellular changes include the extrusion of lamellar bodies, loss of the nucleus and an increase in the keratin amount until the stratum corneum is formed. The functions of the skin have been classified as protective, homeostatic or sensorial. The first two mentioned are mainly function of its barrier properties [7]. Due to its barrier properties, the skin membrane is equally capable at limiting the molecular transport from and into the body. Overcoming this barrier function will be the purpose of transdermal drug delivery [8, 14].
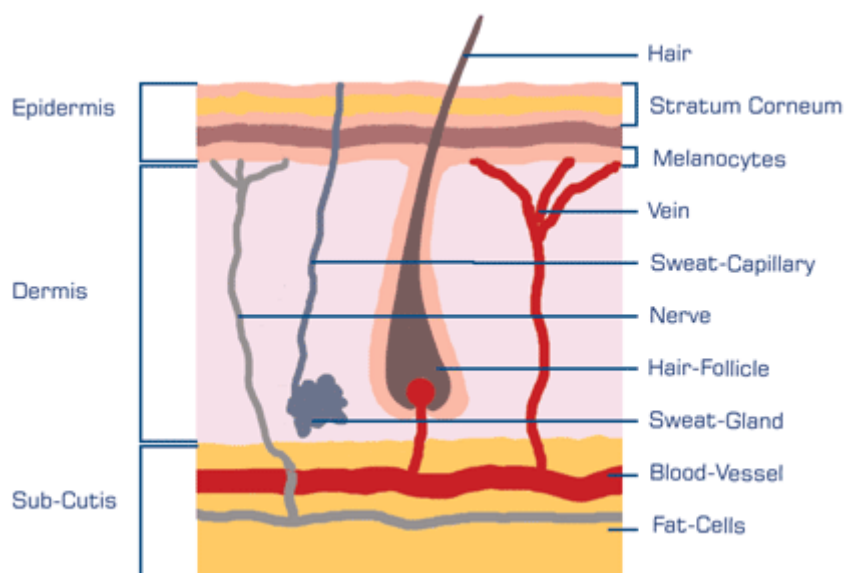
Figure 1.6 Simplified schematic cross-section of the human skin (available at http://www.swiss-creations.com/sc-14story.htm#The Human Skin)

The differentiation process of the epidermal layers (strtum spinosum, granulosum, lucidum and corneum) is changed to corneocytes and increase in the keratin amount until the stratum corneum is formed [9]. The stratum corneum (SC) is the outermost layer of the epidermis, also called non viable epidermis, has an approximately thickness of 10 – 20 μm that can vary from one body site to the other. It consists, in a given cross-section, of 15 – 25 flattened, stacked, hexagonal, and cornified cells (corneocytes, also called horny cells) anchored in a mortar of highly organized intercellular lipids. This structure has been described as brick and mortar model and is considered the rate controlling barrier in the transdermal absorption of substances (Figure 1.7) [10]. The intercellular matrix consists of lipids and desmosomes for the corneocyte cohesion [7, 14]. The lipids of this area provide the only continuous phase (diffusion pathway) from the skin surface to the base of the SC. The intercellular lipid layer is considered the most important transdermal absorption pathway for small substances [11]. The SC by its composition and structure is considered to act as the main barrier for the exchange of substances between the body and the environment. And therefore became the real challenge on drug delivery into and through the skin [12].

There are three pathways postulated for the absorption of substances through the SC under normal conditions: transcellular, intercellular (Figure 1.7) and transappendageal [13, 14].
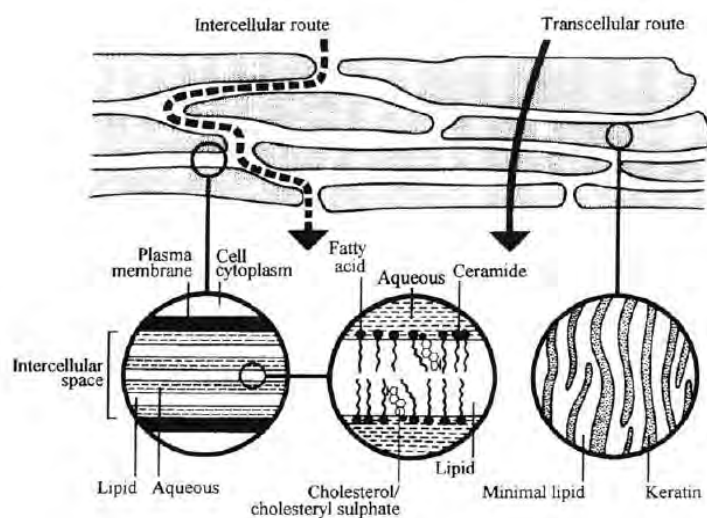
Figure 1.7 Model of stratum corneum, lipid bilayer organization and possible pathway

The predominant route of transdermal penetration of the majority of the applied drugs is through intercellular spaces; therefore, the transdermal pathway is much longer than the normal stratum corneum thickness (~20 µm) which was estimated as long as 500 µm [15]. The transdermal absorption process requires drug characteristics or an appropriate carrier which should be able to deliver the drug to the desired skin deepness to reach topical or systemic effects [14]. A good transdermal delivery system must not only provide an adequate drug release over long periods of time from the formulation, but also allow considerable amounts of drug to overcome the skin barrier, ensure a non-irritancy of the skin, and also ensure that the drug will not be inactivated on the skin's surface or during the permeation process [16]. In the past, it was assumed that the intercellular route was the only relevant penetration pathway. Originally, it was assumed that the hair follicles play a minor role in skin penetration by representing only 0.1% of the total skin surface. The results of different investigations imply that the follicles do in fact play an important role in penetration processes [17]. The hair follicle delivery has several pharmacokinetic advantages as a reduction or bypass of the

tortuous pathway of the transepidermal absorption, decrease of the drug systemic toxicity when the follicle act as long term delivery reservoir and increasing additionally the therapeutic index of some drugs as well as reducing the applied dose or frequency of administration [18]. Micro- as well as nanoparticles have been demonstrated to reach deep into the hair follicles, where the barrier posses only a few layers of differentiated corneocytes and can be considered highly permeable, and additionally the hair follicles can act as long-term reservoir, beneficial condition when transdermal delivery is intended [19]. Nanoparticles are well suited to penetrate efficiently into the hair follicles, reaching deeper functional structures, where they can be stored for some days. In the case of non-particle substances, such a long-term effect cannot be observed, either in the hair follicles or in the stratum corneum. As described before, follicular penetration of nanoparticles (Figure 1.8) [13] appear to be a promising mechanism for transdermal drug delivery [14].
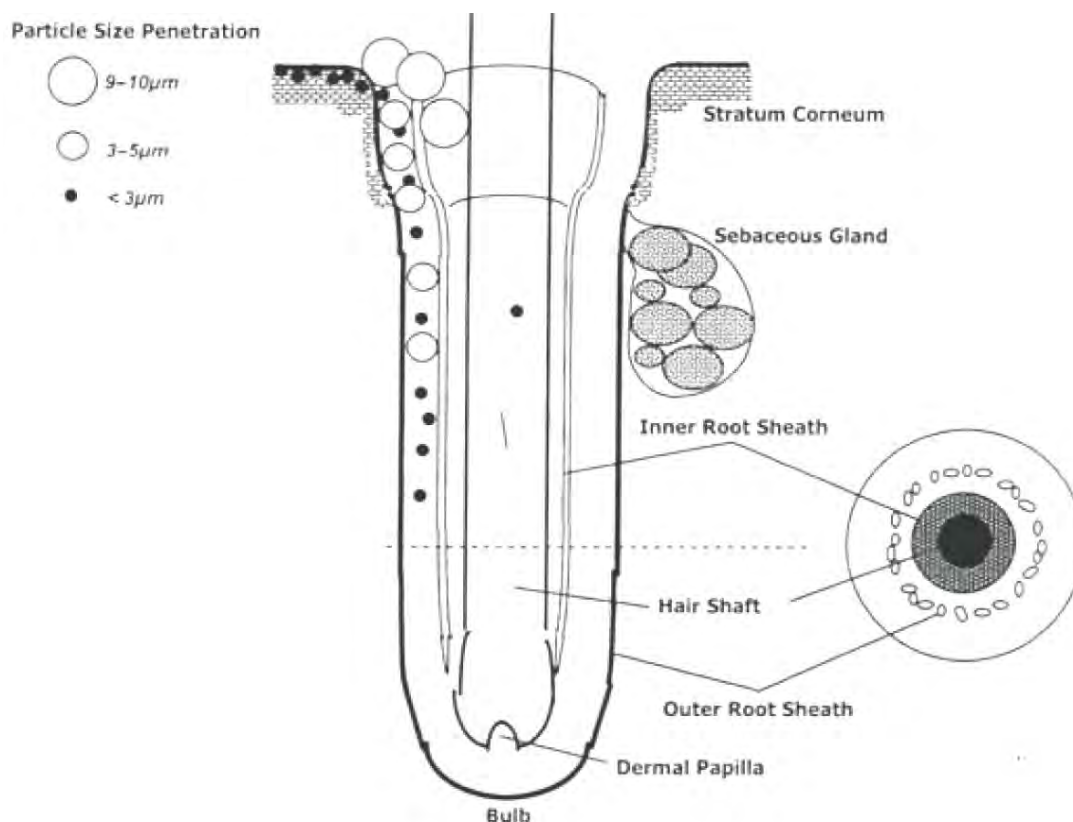
Figure 1.8 Size dependence of hair follicle particle penetration

Literature Reviews

Curcumin Derivatives

In 2000, Kumar *et al.* synthesized and characterized di-O-glycinoyl curcumin (I), di-O-glycinoyl-C4-glycyl-curcumin (II), 5'-deoxy-5'-curcuminyl thymidine (5'-cur-T) (III) and 2'-deoxy-2'-curcuminyl uridine (2'-cur-U) (IV) by elemental analysis & $_1$H NMR. The antibacterial activities of these four bioconjugates have been tested particularly for multi resistant micro-organisms. Best results are shown by I & IV. These bioconjugates serve dual purpose of systemic delivery as well as therapeutic agents against viral diseases [20].

In 2005, Venkateswarlu *et al.* synthesized series of curcumin analogs through the condensation of appropriately protected hydroxybenzaldehydes with acetylacetone, followed by deprotection. The antioxidant activity of these analogs was determined by superoxide free radical nitroblue tetrazolium and DPPH free radical scavenging methods and the polyhydroxycurcuminoids displayed excellent antioxidant activity. These analogs showed cytotoxicity to lymphocytes and promising tumor-reducing activity on Dalton's lymphoma as cites tumor cells [21].

In 2007, Safavy *et al.* synthesized conjugates of curcumin to two differently sized poly(ethylene glycol) molecules in an attempt to overcome the low aqueous solubility of this natural product with cytotoxic activity against some human cancer cell lines. The soluble conjugates exhibited enhanced cytotoxicity as compared to that of the parent drug. Synthesis, analyses of the rate of drug release, and cytotoxicity studies are reported. The water-soluble conjugates may provide information useful for the development of injectable curcumin conjugates [22].

In 2011, KIM *et al.* developed conjugation of curcumin (CCM) by polyethylene glycol (PEG) to improve water solubility of the natural form of CCM and its antiproliferative role in some human cancer cell lines. This study examined the cellular uptake kinetics of the natural form of CCM and CCM-PEG. Their cytotoxic effect in

proliferating preadipocytes and antiadipogenic property in differentiating preadipocytes had also been investigated. These results suggest that pegylation-improved water solubility and cellular retention of CCM may be uniquely useful for improving the delivery of CCM in preadipocytes and its antiadipogenic ability [23].

Curcumin-Cyclodextrin Inclusion Complexation

In 2002, Tonneson *et al.* prepared cyclodextrin complexes of the natural compound curcumin in order to improve the water solubility and the hydrolytic and photochemical stability of the compound. Complex formation resulted in an increase in water solubility at pH 5 by a factor of at least 10^4. The hydrolytic stability of curcumin under alkaline conditions was strongly improved by complex formation, while the photo decomposition rate was increased compared to a curcumin solution in organic solvents. The cavity size and the charge and bulkiness of the cyclodextrin side-chains influenced the stability constant for complexation and the degradation rate of the curcumin molecule [24].

In 2005, Baglole *et al*. studied the effect of α-, β-, and γ-cyclodextrin (CD) and their hydroxypropylated (HP) derivatives on the solubility and fluorescence of the compound curcumin. All of those six cyclodextrins significantly increase the aqueous solubility of curcumin, with the greatest solubility observed in HP-γ-CD. Curcumin forms 2:1 host–guest inclusion complexes with these cyclodextrins, with the strongest complexes formed in the case of HP-β-CD. These 2:1 complexes are postulated to form when a cyclodextrin host encapsulates each of the two phenyl rings at the ends of the curcumin molecule. The equilibrium constant for encapsulation by the second cyclodextrin host is significantly smaller than that for the first in each case [25].

In 2008, Hegge *et al*. investigated the effect of different combinations of cyclodextrins and alginates on curcumin release towards hydrophilic membranes *in vitro*. The results indicate that the unrestricted curcumin flux (e.g. in the case of wounded skin) is rather independent of the composition of the hydrophilic vehicle and mostly limited by the viscosity. In conclusion, a combination of hydroxypropyl-β-

cyclodextrin and propylene glycol alginate seemed to be the best choice with respect to curcumin solubility and release from the vehicle [26].

Curcumin Complexation with Protein and Fat

In 2006, Maiti *et al*. prepared curcumin–phospholipid complex to overcome the limitation of absorption and to investigate the protective effect of curcumin–phospholipid complex on carbon tetrachloride induced acute liver damage in rats. The antioxidant activity of curcumin–phospholipid complex (equivalent of curcumin 100 and 200 mg/kg body weight) and free curcumin (100 and 200 mg/kg body weight) was evaluated by measuring various enzymes in oxidative stress condition. The complex provided better protection to rat liver than free curcumin at same doses and maintained effective concentration of curcumin for a longer period of time in rat serum. The result proved that curcumin–phospholipid complex has better hepatoprotective activity, owe to its superior antioxidant property, than free curcumin at the same dose level [27].

In 2010, Sneharani *et al*. investigated the complex formation of curcumin with β-Lactoglobulin (βLG) employing spectroscopic techniques. The stability of curcumin bound to βLG in solution is enhanced 6.7 times, in comparison to curcumin alone (in aqueous solution). βLG interacts with curcumin at pH 7.0 with an association constant of $1.04 \pm 0.1 \times 10^{5}$ M^{-1} to form a 1:1 complex at 25 °C. These binding studies have prompted the preparation and encapsulation of curcumin in βLG nanoparticles. Nanoparticles of βLG prepared by desolvation are found to encapsulate curcumin with >96% efficiency. The solubility of curcumin in βLG nanoparticle is significantly enhanced to 625 μM in comparison with its aqueous solubility (30 nM) [28].

Curcumin Encapsulation

In 2002, Tonnesen incorporated curcumin into various surfactant micellar systems in order to improve the water solubility and the hydrolytic and photochemical stability. The presence of micellar structures resulted in an increase in water solubility at

pH 5 by a factor of at least 10^5. The hydrolytic stability of curcumin under alkaline conditions was strongly improved by incorporation into micelles while the photo decomposition rate was increased compared to curcumin in hydrogen bonding organic solvents or aqueous solutions. The ability of curcumin to act as a photosensitizer was dependent on the type of micelles and pH of the medium [29].

In 2008, Wang *et al.* prepared oil-in-water (O/W) emulsions of different sizes, using medium chain triacylglycerols (MCT) as oil and Tween 20 as emulsifier, to encapsulate curcumin in order to improve its anti-inflammation activity, which was evaluated by using a mouse ear inflammation model. In the case of O/W emulsion preparations, stir-only and high-speed homogenization at low speed (<13,000 rpm) could not form stable emulsions, eventually phase separated within 24 h. When high-speed homogenization was carried out at 24,000 rpm, stable O/W emulsions were obtained. It is found that 1% curcumin can be successfully encapsulated in O/W emulsions. The nearly-unchanged absorption peak of curcumin indicates that at a pH between 5.0 and 5.5, the stability of curcumin can be maintained in O/W emulsions [30].

In 2009, Jing Cui *et al*. developed selfmicroemulsifying drug delivery system (SMEDDS) to improve the solubility and oral absorption of curcumin. The optimal formulation of SMEDDS was comprised of 57.5% surfactant (emulsifier OP:Cremorphor EL = 1:1), 30.0% co-surfactant (PEG 400) and 12.5% oil (ethyl oleate). The solubility of curcumin (21 mg/g) significantly increased in SMEDDS. The average particle size of SMEDDS-containing curcumin was about 21nm when diluted in water. The dissolution study *in vitro* showed that more than 95% of curcumin in SMEDDS could be dissolved in pH 1.2 or pH 6.8 buffer solutions in 20 min, however, less than 2% for crude curcumin in 60 min. The *in situ* absorption property of curcumin-loaded SMEDDS was evaluated in intestines of rats. The results showed the absorption of curcumin in SMEDDS was *via* passive transfer by diffusion across the lipid membranes. The results of oral absorption experiment in mice showed that SMEDDS could significantly increase the oral absorption of curcumin compared with its suspension [31].

In 2009, Lin *et al*. constructed the ternary phase diagram of a curcumin-encapsulated O/W microemulsion system using lecithin and Tween 80 as the surfactants and ethyl oleate as the oil phase. The results indicated that a composition of curcumin microemulsion (DI water: surfactants (the mole ratio of lecithin/Tween 80 was 0.3): EO = 10:1.7:0.4 in wt ratio) was stable for 2 months with an average diameter of 71.8 ± 2.45 nm, as detected by UV–Vis spectra and diameter distributions. The microemulsion possesses an ability to be diluted with aqueous buffer without destroying its structure for 48 h. The *in vitro* skin permeation study, both the dose–response and time-dependent studies of the encapsulated curcumin formula showed that MEC2 was the most suitable formulation with reduced particle diameter and maximum permeation capability [32].

In 2008, Chen *et al.* reported the effects of different liposome formulations on curcumin stability in phosphate buffered saline (PBS), human blood, plasma and culture medium RPMI-1640+10% PBS (pH 7.4, 37 C). Liposomal curcumin had higher stability than free curcumin in PBS. Liposomal and free curcumin had similar stability in human blood, plasma and RPMI-1640 + 10% FBS. Liposomal curcumin had similar or even stronger inhibitory effects on concanavalin A (Con A)-stimulated human lymphocyte, splenocyte and LCL proliferation. They conclude that liposomal curcumin may be useful for intravenous administration to improve the bioavailability and efficacy, facilitating *in vivo* studies that could ultimately lead to clinical application of curcumin [33].

In 2009, Takahashi *et al*. prepared liposome-encapsulated curcumin (LEC) from commercially available lecithins (SLP-WHITE and SLP-PC70) and examined for its interfacial and biochemical properties. A LEC prepared from 5 wt % of SLP-PC70 and 2.5 wt % of curcumin gave a good dispersibility with 68.0% encapsulation efficiency for curcumin, with a diameter of approximately 263 nm, while those from SLP-WHITE did not. Three forms of curcumin [curcumin, a mixture of curcumin and SLP-PC70 (lecithin), and LEC] were then administered orally to Sprague-Dawley rats at a dose of 100 mg curcumin/kg body weight. High bioavailability of curcumin was evident in the case of oral LEC; a faster rate and better absorption of curcumin were observed as compared to

the other forms. Oral LEC gave higher Cmax and shorter Tmax values, as well as a higher value for the area under the blood concentration-time curve, at all time points. In addition, the plasma antioxidant activity following oral LEC was significantly higher than that of the other treatments [34].

In 2009, Patel *et al*. investigated the potential of a tranfersomes formulation for transdermal delivery of curcumin. The entrapment efficiency was found to be PC (Lecithin): Edge Activator (Tween 80 & Span 80) ratio dependent. Higher entrapment was found to be 89.6±0.049 within T8 formulation. The average size of the vesicle also correlated with the entrapment efficiency of the formulation and found to be 339.9nm with formulation T8. Permeation was also dependent on PC (Lecithin):Edge Activator ratio(Tween 80 & Span 80). The formulation T8 provides higher permeation of drug from transfersomal gel [35].

In 2007, Tiyaboonchai *et al.* prepared curcuminoids loaded solid lipid nanoparticles (SLNs) by a microemulsion technique at moderate temperature. At optimal conditions, the mean particle size of curcuminoids loaded SLNs was 447 nm and incorporation efficacy of curcuminoids was 70% (w/w). This study demonstrates that the stability of curcuminoids in a cream containing curcuminoids incorporated into SLNs was significantly improved as compared to free curcumoids in the cream formulation. The light and oxygen sensitivity of curcuminoids was strongly reduced by incorporating curcuminoids into SLNs [36].

In 2009, Onoue *et al*. designed formulations of curcumin, including nanocrystal solid dispersion (CSD-Cur), amorphous solid dispersion (ASD-Cur), and nanoemulsion (NE-Cur), with the aim of improving physicochemical and pharmacokinetic properties. In dissolution tests, all curcumin formulations exhibited marked improvement in the dissolution behavior when compared with crystalline curcumin. Significant improvement in pharmacokinetic behavior was observed in the newly developed formulations, as evidenced by 12- (ASD-Cur), 16- (CSD-Cur), and 9-fold (NE-Cur) increase of oral

bioavailability. Upon photochemical characterization, curcumin was found to be photoreactive and photodegradable in the solution state, whereas high photochemical stability was seen in the solid formulations, especially CSD-Cur [37].

In 2007, Aziz *et al.* studied to reduce the color staining effect and enhance the stability of curcumin via microencapsulation using gelatin coacervation method. As for curcumin, ethanol and acetone were used as coacervating solvents. Curcumin was dispersed in ethanol while dissolved in acetone. Irrespective of the types of coacervating solvents used, microencapsulation resolved the color-staining problem and enhanced the flow properties and photo-stability of curcumin. Nevertheless, it was found that more spherical curcumin microcapsules with higher yield, higher curcumin loading, and higher entrapment efficiency were obtained with acetone than ethanol. The *in vitro* release of curcumin after microencapsulation was slightly prolonged [38].

In 2009, Wang *et al.* prepared curcumin microcapsules by spray drying process using porous starch and gelatin as wall material. Results showed optimal condition as follows: the ratio of core and wall material of 1/30, embedding temperature of 70 $^{\circ}$C, embedding time 2 h, inlet gas temperature of 190 $^{\circ}$C, feed flow rate 70 mL/min and drying air flow 70 m^{3}/h, at which the microencapsules had good encapsulation efficiency. The stability of microencapsulation curcumin against light, heat, pH was effectively improved and its solubility was increased greatly [39].

In 2007, Bisht *et al.* synthesized polymeric nanoparticle encapsulated formulation of curcumin –nanocurcumin – utilizing the micellar aggregates of cross-linked and random copolymers of Nisopropylacrylamide with N-vinyl-2-pyrrolidone and poly(ethyleneglycol) monoacrylate. Nanocurcumin, size distribution in the 50 nm range, is readily dispersed in aqueous media. Nanocurcumin demonstrates comparable *in vitro* therapeutic efficacy to free curcumin against a panel of human pancreatic cancer cell lines, as assessed by cell viability and clonogenicity assays in soft agar. Further, nanocurcumin's mechanisms of action on pancreatic cancer cells mirror that of free curcumin, including induction of

cellular apoptosis, blockade of nuclear factor kappa B activation, and down regulation of steady state levels of multiple proinflammatory cytokines [40].

In 2008, Abhishek *et al*. synthesized a novel polymeric amphiphile, mPEG–PA, with methoxy poly(ethylene glycol) (mPEG) as the hydrophilic and palmitic acid (PA) as the hydrophobic segment. mPEG–PA conjugate undergoes self-assembly in an aqueous environment. The micelles were spherical in shape, with a mean diameter of 41.43 nm. The utility of mPEG–PA to entrap curcumin in the core of nanocarrier was investigated. Drug-loaded micelle nanoparticles showed good stability in physiological condition (pH 7.4), in simulated gastric fluid (pH 1.2) and in simulated intestinal fluid (pH 6.8). This micellar formulation can be used as an enzyme-triggered drug release carrier, as suggested by *in vitro* enzyme-catalyzed drug release using pure lipase and HeLa cell lysate. The IC_{50} of free curcumin and encapsulated curcumin was found to be 14.32 and 15.58 lM, respectively [41].

In 2009, Shaikh *et al*. encapsulated curcumin into poly (lactide-co-glycolide) (PLGA) nanoparticles by emulsion technique. The obtained nanoparticles were spherical in shape with particle size of 264 nm (polydispersity index 0.31) and 76.9% entrapment at 15% loading. X-ray diffraction analysis revealed the amorphous nature of the encapsulated curcumin. The *in vitro* release was predominantly by diffusion phenomenon and followed Higuchi's release pattern. The *in vivo* pharmacokinetics revealed that curcumin entrapped nanoparticles demonstrate at least 9-fold increase in oral bioavailability when compared to curcumin administered with piperine as absorption enhancer [42].

In 2010, Das *et al*. prepared the composite nanoparticles (NPs) by using three polymers-alginate (ALG), chitosan (CS), and pluronic-by ionotropic pre-gelation followed by polycationic cross-linking. Pluronic F127 was used to enhance the solubility of curcumin in the ALG-CS NPs. The particles were nearly spherical in shape with an average size of 100 ± 20 nm. Encapsulation efficiency (%) of curcumin in composite

NPs showed considerable increase over ALG-CS NPs without pluronic. The *in vitro* drug release profile along with release kinetics and mechanism from the composite NPs were studied under simulated physiological conditions for different incubation periods. A cytotoxicity assay showed that composite NPs at a concentration of 500 μg/mL were nontoxic to HeLa cells. Cellular internalization of curcumin-loaded composite NPs was confirmed from green fluorescence inside the HeLa cells. The half-maximal inhibitory concentrations for free curcumin and encapsulated curcumin were found to be 13.28 and 14.34 μM, respectively [43].

In 2010, Anand *et al*. encapsulated curcumin in nanoparticulate formulation based on poly (lactide-co-glycolide) (PLGA) and a stabilizer polyethylene glycol (PEG)-5000 with 97.5% efficiency and particle diameter of 80.9 nm. Overall they demonstrated that curcumin-loaded PLGA nanoparticles formulation has enhanced cellular uptake, and increased bioactivity in vitro and superior bioavailability and had a longer half-life in vivo over curcumin [44].

In 2010, Feng *et al*. developed a novel curcumin nanoparticle system (CURN) using nanoprecipitation technique with polyvinylpyrrolidone (PVP) as the hydrophilic carrier. The results indicated that CURN improved the physicochemical properties of CUR, including a reduction in particle size and the formation of an amorphous state with hydrogen bonding, both of which increased the drug release of the compound. Moreover, in vitro studies indicated that CURN significantly enhanced the antioxidant and antihepatoma activities of curcumin ($P < 0.05$). Consequently, they suggest that CURN can be used to reduce the dosage of curcumin and improve its bioavailability and merits further investigation for therapeutic applications [45].

Mucoadhesive of Polymeric Nanoparticles

In 2002, Sakuma *et al*. examined the behavior of nanoparticles having surface hydrophilic poly(N-isopropylacrylamide), poly(N-vinylacetamide), poly(vinylamine) or poly(methacrylic acid) chains in the intestin. The permeability of salmon calcitonin (sCT)

from the mucosal to serosal side of the everted jejunum was enhanced in the presence of nanoparticles. This enhancement, which correlated with the amount of sCT incorporated in nanoparticles, disappeared completely after removal of the mucous layer. When fluorescein isothiocyanate–dextran (FD-4) was used instead of sCT, its permeability through the everted jejunum with and without mucous layer was not enhanced by any nanoparticles, because FD-4 was not incorporated in nanoparticles at all. These findings indicated that the accumulation of nanoparticles incorporating sCT in the mucous layer resulted in the enhancement of sCT permeability. It was concluded that mucoadhesion of nanoparticles incorporating sCT to the gastrointestinal mucosa contributed to the absorption enhancement of sCT [46].

In 2004, Umamaheshwari *et al*. designed mucoadhesive gliadin nanoparticles (GNP) containing amoxicillin and evaluated their effectiveness in eradicating *Helicobacter pylori*. GNP-bearing amoxicillin (AGNP) was prepared by desolvation method. Rhodamine isothiocyanate-entrapped GNP formulations were prepared to evaluate their *in vivo* gastric mucoadhesive property in albino rats. With increasing gliadin concentration, the mucoadhesive property of GNP increased. Typically, the maximum amount of nanoparticles remaining was 82±4%, which represented a stronger mucoadhesive propensity and specificity of GNP toward the stomach. *In vitro* antimicrobial activity of AGNP was evaluated by growth inhibition studies on an isolated *H. pylori* strain. The time required for complete eradication was higher in AGNP than in amoxicillin because of the controlled drug delivery of amoxicillin from AGNP. *In vivo* clearance of *H. pylori* following oral administration of AGNP to infected Mongolian gerbils was examined. Amoxicillin and AGNP both showed anti-*H. pylori* effects in this experimental model of infection, but the required dose for complete eradication was less in AGNP than in amoxicillin. In conclusion, AGNP eradicated *H. pylori* from the gastrointestinal tract more effectively than amoxicillin because of the prolonged gastrointestinal residence time attributed to mucoadhesion [47].

In 2007, Sarmento *et al*. evaluated the pharmacological activity of insulin-loaded alginate/chitosan nanoparticles following oral dosage in diabetic rats. Nanoparticles were prepared by ionotropic pre-gelation of an alginate core followed by chitosan polyelectrolyte complexation. Nanoparticles were negatively charged and had a mean size of 750 nm. The insulin association efficiency was over 70% and insulin was released in a pH-dependent manner under simulated gastrointestinal conditions. Orally delivered nanoparticles lowered basal serum glucose levels by more than 40% with 50 and 100 IU/kg doses sustaining hypoglycemia for over 18 h. Pharmacological availability was 6.8 and 3.4% for the 50 and 100 IU/kg doses respectively, a significant increase over 1.6%, determined for oral insulin alone in solution and over other related studies at the same dose levels. Confocal microscopic examinations of FITC-labelled insulin nanoparticles showed clear adhesion to rat intestinal epithelium, and internalization of insulin within the intestinal mucosa. The results indicated that the encapsulation of insulin into mucoadhesive nanoparticles was a key factor in the improvement of its oral absorption and oral bioactivity [48].

In 2007, Bravo-Osuna *et al*. evaluated the potential bioadhesive behaviour of chitosan and thiolated chitosan (chitosan-TBA)-coated poly(isobutyl cyanoacrylates) (PIBCA) nanoparticles. Mucoadhesion was *ex vivo* evaluated under static conditions by applying nanoparticle suspensions on rat intestinal mucosal surfaces and evaluating the amount of nanoparticles remaining attached to the mucosa after incubation. The analysis of the results obtained demonstrated that the presence of either chitosan or thiolated chitosan on the PIBCA nanoparticle surface clearly enhanced the mucoadhesion behaviour thanks to non-covalent interactions (ionic interaction and hydrogen bonds) with mucus chains. Both, the molecular weight of chitosan and the proportion of chitosan-TBA in the formulation influenced the nanoparticle hydrodynamic diameter and hence their transport through the mucus layer. Improved interpenetration ability with the mucus chain during the attachment process was suggested for the chitosan of high molecular weight, enhancing the bioadhesiveness of the system. The presence of thiol groups on the nanoparticle surface at high concentration (200 x 10(-6)

micromol SH/cm2) increased the mucoadhesion capacity of nanoparticles by forming covalent bonds with the cysteine residues of the mucus glycoproteins [49].

In 2008, Thirawong *et al*. prepared pectin-liposome nanocomplexes (PLNs) by mixing of cationic liposomes with pectin solution, in order to improve intestinal absorption of calcitonin (eCT). Both *in vitro* and *in vivo* evaluations for PLNs were evaluated. The results showed that average particle size of PLNs was significantly larger than that of initial cationic liposomes. The surface charges were shifted from positive to negative after mixing with pectin. The PLNs made of high degree of esterification (DE) pectin showed less negatively charged values than those made of low DE pectin. The entrapment efficiency in cationic liposomes was in the same range even if the drug loading was increased. The *in vivo* mucoadhesive test of pectin by confocal laser scanning microscopy demonstrated stronger mucoadhesive properties of PLNs made of low DE pectin, compared to cationic liposomes and PLNs made of other pectins. Moreover, high intensities of a fluorescent marker could be observed throughout the small intestines (i.e. duodenum, jejunum and ileum) and remained at the site of mucoadhesion even after 6 h of administration of PLNs made of low DE pectin. The eCT-loaded PLNs demonstrated a strong pharmacological action over the eCT solution and eCT-loaded liposomes, in which an enhanced and prolonged reduction in plasma calcium concentration of rats was observed. This was attributed to the ability of pectin to adhere to the mucus layer and prolong retention in the intestinal mucosa [50].

In 2009, Moghaddam *et al*. evaluated the *in vitro* mucoadhesion and permeation enhancement properties of thiolated chitosan (chitosan-glutathione) coated poly(hydroxyl ethyl methacrylate) nanoparticles. Core-shell nanoparticles were prepared by radical emulsion polymerization method initiated by cerium(IV) ammonium nitrate. Different molecular weights of chitosan were utilized for nanoparticles preparation. The physicochemical properties of nanoparticles were characterized by size, zeta potential, and thiol content. Incorporation of fluorescein isothiocyanate dextran (FD4, MW 4400 Da), which was used as the model macromolecule, was achieved by incubation method.

The intestinal mucoadhesion and penetration enhancement properties of nanoparticles were investigated using excised rat jejunum. All nanoparticle systems showed mucoadhesion and improved apparent permeation coefficient (P(app)) of FD4. Nanoparticles prepared by thiolated chitosan with medium molecular weight revealed the most mucoadhesion and penetration enhancement properties [51].

In 2010, Chang *et al*. developed chitosan/poly-gamma-glutamic acid nanoparticles incorporated into pH-sensitive hydrogels as an efficient carrier for amoxicillin delivery. The results indicate that hydrogels are pH-sensitive, leading to protecting nanoparticles from being destructed by gastric acid. The results of drug releasing in vitro study clearly indicate that the amount of amoxicillin released from nanoparticles incorporated in hydrogels at pH 1.2 was relatively low (14%), compared to that from only nanoparticles (50%). Confocal laser scanning microscopy revealed that nanoparticles could infiltrate cell-cell junctions and interact with *H. pylori* infection sites in the intercellular spaces. Additionally, the incorporation of amoxicillin-loaded nanoparticles in a hydrogel protected the drug from the actions of the gastric juice and facilitated amoxicillin interaction specifically with intercellular spaces, the site of *H. pylori* infection [52].

In 2011, Makhlof *et al*. investigated the feasibility of combining safe permeation enhancers in a mucoadhesive particulate system for the oral delivery of peptide drugs. Polyelectrolyte complex nanoparticles (NPs) were prepared by ionic interaction of spermine (SPM) with polyacrylic acid (PAA) polymer. Cytotoxicity studies in Caco-2 monolayers revealed the safety of the delivery system in the concentration range used for permeation enhancement. The cellular transport of fluorescein isothiocyanate dextran (FD4) showed higher permeation enhancing profiles of SPM–PAA NPs, as compared to SPM solution or PAA NPs prepared by ionic gelation with MgCl2 (Mg-PAA NPs). Furthermore, confocal microscopy results revealed strong association of the NPs prepared using fluorescence labeled PAA to Caco-2 cells. The permeation enhancing properties of SPM–PAA NPs were further evaluated *in vivo* after oral administration to

rats, using FD4 and calcitonin as models of poorly permeating drugs. Confocal microscopy images of rats' small intestine confirmed previous findings in Caco-2 cells and revealed a strong and prolonged penetration of FD4 from the mucosal to the basolateral side of the intestinal wall. In addition, the proposed NPs were efficient in improving the oral absorption of calcitonin, as evidenced by the significant and prolonged reduction of the blood calcemia in rats [53].

Transdermal Penetration of Nanoparticles

In 2004, Alvarez-Román *et al*. investigated the penetration of octylmethoxy cinnamate (OMC; Parsol MCX) from poly(ε-caprolactone) nanoparticles into and across porcine ear skin in vitro. Confocal laser scanning microscopy (CLSM) was used to visualize the distribution of nanoparticles, charged with Nile red (NR), a lipophilic and fluorescent dye. Quantification of OMC in the skin using tape-stripping demonstrated that nanoparticulate encapsulation produced a 3.4-fold increase in the level of OMC within the stratum corneum (SC), although the use of nanoparticles did not appear to increase skin permeation (it was not possible to detect OMC in the receiver compartment after 6 h). The confocal images showed that the fluorescence profile observed in the skin after application of NR containing nanoparticles was clearly different from that seen following application of NR dissolved in propylene glycol. Two hours postapplication of NR-containing nanoparticles, fluorescence was perceptible at greater depths (up to 60 μm) within the skin [54].

In 2004, Alvarez- Román *et al*. used confocal laser scanning microscopy (CLSM) to visualize the distribution of non-biodegradable, fluorescent, polystyrene nanoparticles (diameters 20 and 200 nm) across porcine skin. The surface images revealed that (i) polystyrene nanoparticles accumulated preferentially in the follicular openings, (ii) this distribution increased in a time-dependent manner, and (iii) the follicular localization was favoured by the smaller particle size. Apart from follicular uptake, localization of nanoparticles in skin furrows was apparent from the surface images. However, cross-

sectional images revealed that these nonfollicular structures did not offer an alternative penetration pathway for the polymer vectors, whose transport was clearly impeded by the stratum corneum [55].

In 2005, Olvera-Martínez *et al*. prepared polymeric nanocapsules (NCs) containing octylmethoxycinnamate (OMC), and determined *in vivo* distribution profile through the stratum corneum (SC). Penetration degree of OMC formulated in NCs was compared with that obtained for a nanoemulsion (NE), and a conventional oil-in-water (o/w) emulsion (EM). *In vivo* percutaneous penetration, evaluated by the tape-stripping technique, demonstrated that NE increased the extent of OMC penetration relative to the penetration achieved by NCs or EM, with relative penetration depths through the SC of 0.86 0.1, 0.64 0.11, and 0.57 0.08, respectively. In the same manner, the accumulation in the skin of OMC was significantly greater with NE than with EM or NCs. OMC penetration depth was strongly dependent upon the size of the colloidal particles and their flexibility [56].

In 2006, Vogt *et al*. investigated the suitability of nanoparticles in transcutaneous route of vaccine administration approach. A high density of Langerhans cells (LCs) were found around hair follicles that, when sorted, readily internalized all size particles. However, flow cytometry after transcutaneous application of 40, 750, or 1,500nm nanoparticles on human skin samples revealed that only 40nm particles entered epidermal LC. Fluorescence and laser scan microscopies revealed that only 40nm particles deeply penetrate into vellus hair openings and through the follicular epithelium. They conclude that 40nm nanoparticles, but not 750 or 1,500nm nanoparticles, may be efficiently used to transcutaneously deliver vaccine compounds via the hair follicle into cutaneous antigen-presenting cells [57].

In 2006, Lademann *et al*. investigated the *in vitro* penetration of dye-containing nanoparticles (diameter 320 nm) into the hair follicles on porcine skin. The results were compared to the findings obtained with the same amount of dye in the non-particle form.

It was found that the nanoparticles penetrate much deeper into the hair follicles than the dye in the non-particle form, if a massage had been applied. Without massage, similar results were obtained for both formulations. The storage behavior of both formulations in the hair follicles was analyzed *in vivo* on human skin by differential stripping. Using the same application protocol, the nanoparticles were stored in the hair follicles up to 10 days, while the non-particle form could be detected only up to 4 days [58].

In 2008, Liu *et al.* prepared solid lipid nanoparticles hydrogel containing the drug triamcinolone acetonide acetate (TAA-SLN). The transdermal iontophoretic delivery of TAA was evaluated in vitro using horizontal diffusion cells fitted with porcine ear skin. The TAA-SLN gel possessed good stability, rheological properties, and high electric conductance. Transdermal penetration of TAA from TAA-SLN gel cross the skin tissue was significantly enhanced by iontophoresis. The enhancement of the cumulative penetration amount and the steady-state penetration flux of the penetrated drug were related to the particle size of TAA-SLN and the characteristics of the applied pulse electric current, such as density, frequency, and on/off interval ratio. These results indicated that SLN carbopol gel could be used as a vehicle for transdermal iontophoretic drug delivery under suitable electric conditions [59].

In 2009, Ghouchi Eskandar *et al.* investigated the dermal delivery of all-trans-retinol from nanoparticle-coated submicron oil-in-water emulsions as a function of the initial emulsifier type, the loading phase of nanoparticles, and the interfacial structure of nanoparticle layers. In-vitro release and skin penetration of all-trans-retinol were studied using Franz diffusion cells with cellulose acetate membrane, and excised porcine skin. The distribution profile was obtained by horizontal sectioning of the skin using microtome-cryostat and HPLC assay. The results indicated that the steady-state flux of all-trans-retinol from silica-coated lecithin emulsions was decreased (up to 90%) and was highly dependent on the initial loading phase of nanoparticles; incorporation from the aqueous phase provided more pronounced sustained release. For oleylamine emulsions, sustained release effect was not affected by initial location of nanoparticles.

The skin retention significantly (p < or = 0.05) increased and was higher for positive oleylamine-stabilised droplets. All-trans-retinol was mainly localized in the epidermis with deeper distribution to viable skin layers in the presence of nanoparticles, yet negligible permeation (approximately 1% of topically applied dose) through full-thickness skin [60].

In 2010, Zhang *et al*. investigate the penetration and the distribution of poly(d,l-lactic-co-glycolic acid) (PLGA) nanoparticles in the human skin treated with microneedles. The distribution of nanoparticles, visualizing by confocal laser scanning microscopy (CLSM) showed that nanoparticles were delivered into the microconduits created by microneedles and permeated into the epidermis and the dermis. The quantitative determination by high performance liquid chromatography showed that (i) the permeation of nanoparticles into the skin was enhanced by microneedles, but no nanoparticle reached the receptor solution; (ii) much more nanoparticles deposited in the epidermis than those in the dermis; (iii) the permeation was in a particle size-dependent manner; and (iv) the permeation increased with the nanoparticle concentration increasing until a limit value was reached. The biodegradable nanoparticles would sustain drug release in the skin and supply the skin with drug over a prolonged period [61].

In 2010, Senzui *et al*. determined skin penetration of four different types of rutile titanium dioxide (TiO(2)) (T-35, 35 nm, non-coating; TC-35, 35 nm, with almina/silica/ silicon coating; T-disp, 10 x 100 nm, mixture of almina coated and silicon coated particles, dispersed in cyclopentasiloxan; T-250, 250 nm, non-coating) with *in vitro* intact, stripped, and hair-removed skin of Yucatan micropigs to study the effect of dispersion and skin conditions. The TiO(2) was suspended in a volatile silicone fluid used for cosmetics, cyclopentasiloxane, at a concentration of 10%. The suspension was applied at a dose 2 microl/cm(2) for 24 hr, followed by cyanoacrylate stripping. The Ti concentration in skin was determined by ICP-MS. T-35 and T-250 easily aggregated in suspension with a mean diameter greater than 1 microm. TC-35 and T-disp showed good dispersion properties with a mean diameter in suspension of approximately 100

nm. No penetration was observed regardless of TiO(2) type in intact and stripped skin. The concentration of Ti in skin was significantly higher when TC-35 was applied on hair-removed skin. SEM-EDS observation showed that Ti penetrated into vacant hair follicles (greater than 1 mm below the skin surface), however, it did not penetrate into dermis or viable epidermis [62].

In 2010, Zhao *et al.* determined how the physicochemical properties of nanoparticles influence minoxidil release pre and post dose application when formulated as a simple aqueous suspension compared to dynamic hydrofluoroalkane (HFA) foams. Minoxidil loaded lipid nanoparticles (LN, 1.4 mg/ml, 50 nm) and polymeric nanoparticles with a lipid core (PN, 0.6 mg/ml, 260 nm) were produced and suspended in water to produce the aqueous suspensions. These aqueous suspensions were emulsified with HFA using pluronic surfactant to generate the foams. Approximately 60% of the minoxidil loaded into the PN and 80% of the minoxidil loaded into the LN was released into the external aqueous phase 24 h after production. Drug permeation was superior from the PN irrespective of the formulation method. Premature drug release resulted in the performance of the topical formulation being dictated by the thermodynamic activity of the solubilised drug not the particle properties [63].

In 2011, Schlupp *et al.* studied the influence of the drug-particle interaction on penetration enhancement. The 3 glucocorticoids (GCs), prednisolone (PD), the diester prednicarbate (PC) and the monoester betamethasone 17-valerate (BMV), were loaded onto SLNs. Theoretical permeability coefficients (cm/s) of the agents rank BMV (-6.38) > PC (-6.57) > PD (-7.30). GC-particle interaction, drug release and skin penetration were investigated including a conventional oil-in-water cream for reference. Both with SLN and cream, PD release was clearly superior to PC release which exceeded BMV release. With the cream, the rank order did not change when studying skin penetration. Interestingly, PC and PD uptake from SLN even resulted in epidermal targeting. Thus, SLNs are not only able to improve skin penetration of topically applied drugs, but may also be of particular interest when specifically aiming to influence epidermal dysfunction [64].

Although encapsulations of curcumin have been reported, the loading capacity, encapsulation efficiency and stability assessment are rarely reported. Thus a more efficient system with better loading is still being needed. This present work reports a high loading, highly efficient curcumin nanoencapsulation system using biocompatble, safe and inexpensive polymer. The result also includes comparison of encapsulation using different polymers, ethyl cellulose (EC), methylcellulose (MC), chitosan derivative and poly(vinylalcohol) derivatives. Improvement of curcumin photostability upon nanoencapsulation, the release characteristics and physical stability of curcumin-loaded particles are also being reported. Moreover, oral bioavailability, free radical formation protection and skin penetration of loaded curcumin were investigated.

Research Objectives

The objectives of this research can be summarized as follows:

1. To encapsulate curcumin into nanoparticles prepared from different polymers namely; ethyl cellulose (EC), methylcellulose (MC), methyl ether terminated poly(ethylene glycol)-4-methoxycinnamoylphthaloylchitosan (PCPLC), Poly(vinylalcohol-co-vinyl-4-methoxycinnamate) with degree of 4-methoxy cinnamoyl substituion of 0.30 (PB4-I) and 0.44 (PB4-II).

2. To characterize morphology of the obtained curcumin-loaded nanoparticles.

3. To compare the stability of the loaded curcumin with that of free curcumin.

4. To study the *in vitro* release of the obtained products under different pH.

5. To evaluate oral bioavailability and mucoadhesive of the curcumin-loaded nanoparticles.

6. To investigate skin and hair follicle penetration of the loaded curcumin.

7. To determine free radical formation protection of the loaded curcumin.

CHAPTER II

EXPERIMENTAL

Materials and Chemicals

Curcumin (98+% w/w purity) was purchased from ACROS Organics (Geel, Belgium). Ethyl cellulose (EC) (48 % w/w ethoxy content, MW 170.000, viscosity 100 cp) and methyl cellulose (MC) (Mn 40.000 with a degree of methoxy substitution of 1.60-1.90) were purchased from Sigma-Aldrich (St. Louis, USA). Methyl ether terminated poly(ethylene glycol)-4-methoxycinnamoylphthaloylchitosan (PCPLC) was provided by Anumansirikul [65] by grafting m-PEGphthaloylchitosan derivative with the 4-methoxy cinnamoyl group. Poly(vinylalcohol-co-vinyl-4-methoxycinnamate) with degree of 4-methoxycinnamoyl substituion of 0.30 (PB4-I) and 0.44 (PB4-II) were provided by Luadthong [66] by grafting poly(vinylalcohol) with the 4-methoxycinnamoyl group, at two different degrees of substitution. Ethanol (EtOH), dimethyl formamide (DMF), dimethyl sulfoxide (DMSO) and ethyl acetate (EtOAc), analytical grade reagent, were purchased from Labscan (Bangkok, Thailand). HPLC grade reagent was purchased from Merck (Darmstadt, Germany). 2,2-Diphenyl-1-picrylhydrazyl (DPPH) and 3-Carboxy-2,2,5,5-tetramethylpyrrolidine-1-oxyl (PCA) were purchased from Sigma-Aldrich (Muenchen, Germany). Cellulose membrane (MWCO 12,400 Daltons, 49mm flat width, purchased from Sigma-Aldrich, Steinheim, Germany) was used to perform nanoparticles by dialysis method. CelluSep T4, MWCO 12000–14000, 45 mm flat width, 6.42 ml cm^{-1} volume capacity (Seguin, TX, USA) was used for controlled release study. The oil in water, water in oil lotions and Printus tape were provided by Beiersdorf (Hamburg, Germany). Permanent marker (edding 140 S, OHP-marker permanent) was purchased from Edding (Ahrensburg, Germany) and Finn Chamber was purchased from Epitest Ltd., Oy. (Tuusula, Findland).

Instruments and Equipments

Determination of Curcumin Content

Curcumin content was determined by UV/VIS absorption spectroscopy (UV 2500 UV–vis spectrophotometer, Shimadzu Corporation, Kyoto, Japan). High Performance Liquid Chromatography (HPLC) analyses were performed using HPLC system, Hypersil ODS-C$_{18}$ column (5 µm, 4.6 mm x 150 mm, Shandon, U.K.) with a UV/VIS detector (SPD-10A, Shimadzu, Tokyo, Japan).

Morphology Characterization of Particles

Morphology of particles was characterized by scanning electron microscope (SEM) with an accelerating voltage of 15 kV (JSM-6400, JEOL, Tokyo, Japan). The nanoparticles were coated with a gold layer under vacuum at 15 kV for 90 s (IB-3 ion coater, Eiko, Tokyo, Japan). TEM photographs were performed on a transmission electron microscope (JEM-2100, JEOL, Tokyo, Japan) with an accelerating voltage of 100–120 kV in conjunction with selected area electron diffraction (SAED). The particle size and zeta potential of aqueous particles were determined by a dynamic light scattering method with Zetasizer Nano series model (Malvern Instruments, Worcestershire, UK) equipped with a He–Ne laser beam at 632.8 nm (scattering angle of 173˚).

Drying Instruments

Freeze dry/shell freeze system model 7753501 (Labconco Corp., Kansus, MI, USA), Spray Dryer (L-8, Ohkawara Kakohki, Yokohama, Japan), low-pressure superheated steam drying and vacuum drying, homemade instrument as previously developed by Devahastin [67], were used in stability studies of the obtained curcumin-loaded nanoparticles upon various drying method.

Equipments for Free Radical Formation Measurement

Free radical scavenging activity of curcumin was measured using Electro Paramagnetic Resonance (EPR) spectrometer (LBM MT 03, Magnettech, Berlin, Germany). UV irradiation device TH-1E (Cosmedico Medizintechnik GmbH, Schwenningen, Germany) was used to generate UV radiation to skin samples.

Equipments for Skin and Hair Follicle Penetration Experiment

Laser Fluorescent Scanning Microscope (LFSM) photograph was performed using Stratum confocal imaging system with an Ar^+ laser beam at 488 nm (Optiscan Pty, Notting Hill, Australia). Hand-held device (Massagegerät PC 60, Petra-electric Elektrogeräte Fabrik, Burgau, Germany) was used to massage pig ear skin after sample application. Frozen biopsied skin was cryosectioned using microtome cryostat (Microm HM 560 CryoStar, MICROM International GmbH, Walldorf, Germany). Fluorescence microscope, Olympus BX60 (Olympus optical co., (EUROPA) GmbH, Hamburg, Germany) was used to observe penetration of curcumin into skin and hair follicle.

Nanoparticle Formation and Curcumin Encapsulation

Five polymers namely; ethyl cellulose (EC), Methylcellulose (MC), methyl ether terminated poly(ethylene glycol)-4-methoxycinnamoylphthaloylchitosan (PCPLC), poly (vinylalcohol-co-vinyl-4-methoxycinnamate) with degree of 4-methoxycinnamoyl substitution of 0.30 (PB4-I) and 0.44 (PB4-II) were used for curcumin encapsulation by dialysis method at the similar concentration, the polymer and curcumin concentration ratio of 1: 1.

Nanoparticle Formation of Polymeric Suspensions

Five polymeric nanosuspensions were prepared by dialysis method. Briefly, EC was dissolved in ethanol at $70^{\circ}C$, PCPLC was dissolved in dimethyl formamide (DMF) and dimethyl sulfoxide (DMSO) was used to dissolve PB4-I and PB4-II, to give a polymer

concentration of 3000 ppm, while ECMC particles were performed by dissolving EC (150 mg) in ethanol (75 ml). MC (150 mg) was dissolved in water (25 ml) then poured into the solution of EC (the polymer concentration of 3000 ppm). Each polymer solution were placed into cellulose membrane tube and then were dialyzed against distilled water (5 x 1000 ml), stirring rate of 250 rpm at room temperature. Since, the final volume of the suspension usually doubles the volume of the polymer solution used at the beginning. Therefore, water was added to the obtained suspension to get the final polymer concentration of 1500 ppm. Subsequently, the obtained aqueous suspensions of curcumin-loaded nanoparticles were then subjected to determine their morphology by SEM, TEM, particle size and zeta potential analyses.

Encapsulation of Curcumin

Curcumin was loaded into nanoparticles by dialysis method. Each polymer was dissolved in solvent. EC was dissolved in ethanol, PCPLC was dissolved in DMF and DMSO was used to dissolve PB4-I and PB4-II, to get the polymer concentration of 3000 ppm. The mixture was stirred and heated at 70°C until clear solution was obtained and curcumin was added, to get curcumin concentration of 3000 ppm, and sonicated until clear solution was obtained. While encapsulation of curcumin into ECMC particles was performed by dissolving EC (150 mg) and curcumin (300 mg) in ethanol (75 ml). MC (150 mg) was dissolved in water (25 ml) then poured into the solution of EC and curcumin (the polymer and curcumin concentration of 3000 ppm). Subsequently, each resulting solution was transferred into cellulose membrane tube and was dialyzed against distilled water (5 x 1000 ml), stirring rate of 250 rpm at room temperature, to obtain colloidal suspension. Dialysate water were collected and directly subjected to quantify curcumin content by UV/VIS absorption analysis at 425 nm, with the aids of a calibration curve (0.1, 0.2, 0.4, 0.6, 0.8 and 1.0 ppm curcumin solutions) freshly prepared in ethanol (see calibration curve in appendix A). The morphology of the obtained aqueous suspension of curcumin-loaded nanoparticles was characterized by SEM, TEM, and dynamic light scattering technique.

The final concentration of curcumin in the obtained suspension, the encapsulation efficiency and loading of curcumin were calculated as following equations:

$$\text{Curcumin concentration (ppm)} = A/V_f \times 1000$$

$$\text{Encapsulation efficiency (\%)} = (A/B) \times 100$$

$$\text{Loading (\%w/w)} = [A/(B+C)] \times 100$$

A = weight of loaded curcumin (mg) = weight of curcumin used (mg) − weight of curcumin found in dialysate (mg); B = weight of curcumin used (mg); C = weight of polymer used (mg); V_f = final volume of the obtained suspension (ml).

Release of Curcumin from Curcumin-Loaded Polymeric Particles

Sample Preparation

The curcumin-loaded EC, ECMC, PCPLC, PB4-I and PB4-II suspension were performed by dialysis method as previously described to get final curcumin concentration of 1500 ppm (loading of 50%w/w). The curcumin-loaded EC, ECMC, PCPLC, PB4-I and PB4-II suspensions were determined the release of curcumin from particles under acidic and neutral condition by dialysis method.

Release by Dialysis Method

Five milliliters of each curcumin-loaded suspension were placed into a regenerated dialysis membrane tube (CelluSep T4) and then immersed in 100 ml of release medium (10:15:75 v/v of ethanol/tween 20/0.01 mM aqueous phosphate buffer pH 5.5 or pH 7). Dialysis was carried out against release medium under stirring rate of 250 rpm at room temperature. At 1, 2, 4, 6, 8, and 24 h, 5 ml of the medium were withdrawn, and the same volume of fresh release medium was replaced.

Quantification of Curcumin

The amount of curcumin in withdrawn release medium were determined by UV/VIS spectroscopy at 425 nm with the aids of a calibration curve constructed from a series of free curcumin solutions prepared in the same release medium. Usually the concentration range of the calibration standards was 0.1, 0.2, 0.4, 0.6, 0.8 and 1.0 ppm (see calibration curve in appendix B). The percentage of curcumin released was calculated with the following equation:

$$\text{Release (\%)} = \frac{\text{Released curcumin}}{\text{Total curcumin used}} \times 100$$

Stability of Curcumin-Loaded Particles

Photostability of Five Curcumin-Loaded Particles

Ten milliliters of aqueous nanosuspension of i) curcumin-loaded EC ii) ECMC iii) PCPLC iv) PB4-I v) PB4-II particles and vi) free curcumin solution (in ethanol), at curcumin concentration of 1000 ppm, were placed into a glass vial (diameter 2.0 cm, height 5.0 cm). The vial was sealed and exposed to sunlight for 4 hours (11.00 am – 15.00 pm). At 0 and 4 h, each samples (0.1 ml) were diluted in ethanol (10ml) prior subjected to determination of curcumin content using UV/VIS spectroscopy at 425 nm with the aid of a calibration curve (1.0, 2.0, 4.0, 6.0, 8.0 and 10.0 ppm curcumin solutions) freshly prepared in ethanol (see calibration curve in appendix A).

Stability of Curcumin-Loaded EC and ECMC Particles in various pH values

The stability of curcumin-loaded EC and curcumin-loaded ECMC particles in the 0.01 M phosphate buffer of pH 4, 5.5, 7 and 10 (see phosphate buffer preparation at various pH values in appendix C), were evaluated. Curcumin-loaded EC and curcumin-loaded ECMC aqueous suspensions, at curcumin concentration of 3000 ppm (loading of 50%), were diluted with each phosphate buffer to get the final curcumin concentration of

1000 ppm. Subsequently, each aqueous nanosuspensions at various pH values (10ml) were placed into a glass vial (diameter 2.0 cm, height 5.0 cm). The vial was sealed and placed at room temperature. The dispersibility of nanosuspensions at various pH values were observed by vision after 24 h, 4 and 7 days.

Stability of Curcumin-Load EC and ECMC Particles under Various Drying Conditions

Freeze Drying

One hundred milliliters of aqueous suspension of curcumin-loaded EC and ECMC particles, at curcumin concentration of 3000 ppm, were subjected to quick deep freezing at $-80^{\circ}C$ using acetone-dry ice bath, and the frozen suspension was then being vacuumed with a freeze dry/shell freeze system overnight or until the dried product was obtained. The obtained dried particles were redispersed in water by sonication and then subjected to SEM analysis.

Spray Drying

One liters of aqueous suspension of curcumin-loaded EC and ECMC particles, at curcumin concentration of 3000 ppm, were subjected to spray-drying at 130 $^{\circ}C$. The suspension was stirred and sprayed through nozzle, at speed of 40 round/s, into hot gas chamber. The dried product was collect at cyclone. The obtained dried particles were redispersed in water by sonication and then subjected to SEM analysis.

Low-Pressure Superheated Steam Drying and Vacuum Drying

Twenty milliliters of aqueous suspension of curcumin-loaded EC and ECMC particles, at curcumin concentration of 3000 ppm, were placed into glass Petri dish and then subjected to low-pressure superheated steam drying and vacuum drying using home-made instruments under the pressure of 8 kPa 80 $^{\circ}C$. The drying was processed until the dried product was obtained. The obtained dried particles were redispersed in water by sonication and then subjected to SEM analysis.

In vitro Release of Curcumin from EC and ECMC Particles in Simulated Gastric Fluid
and Simulated Intestinal Fluid

Sample Preparation

The curcumin-loaded EC and ECMC nanosuspensions were fabricated by
dialysis method as previously described to get final curcumin concentration of 5000
ppm and the freshly obtained sample was used for the release study.

In Vitro Release by Dialysis Method

Five milliliters of curcumin-loaded EC or ECMC suspensions were placed into a
dialysis cellulose membrane tube and then immersed in 100 ml of simulated gastric fluid
(SGF, pH 1.2) or simulated intestinal fluid (SIF, pH 6.8), which prepared according to
USP (see SGF and SIF preparation in appendix C). Dialysis was carried out against SGF
or SIF under stirring rate of 100 rpm and maintained at 37 $^{\circ}$C. At 1, 2, 4, 6, 8 and 24 h, 5
ml of the release medium were withdrawn, and the same volume of fresh SGF or SIF
(37°C) was replaced.

Quantification of Curcumin

The amount of curcumin in each withdrawn SGF and SIF were determined by
UV/VIS spectroscopy at 425 nm with the aids of a calibration curve constructed from a
series of free curcumin solutions (concentration of 0.1, 0.2, 0.4, 0.6, 0.8 and 1.0 ppm)
prepared in the same release medium (see calibration curve in appendix B). The
percentage of curcumin released was calculated with the following equation:

$$\text{Release (\%)} = \frac{\text{Released curcumin}}{\text{Total curcumin used}} \times 100$$

Oral Bioavailability of Curcumin-Loaded EC and ECMC Particles in Mice

Mice

Bioavailability of curcumin-loaded particles was investigated by oral administration of samples in ICR mice, strain ICR/Mlac, with 30 ± 2 g body weight, 8 weeks old (National Laboratory Animal center, NLCA, Nakornpathom, Thailand) under permission from the animal care and use committee in the Faculty of Veterinary Science, Chulalongkorn University (IACUC). One hundred and sixty ICR mice of both sexes were randomly divided into three groups. The animal groups were orally fed 100 mg/kg body weight, with aqueous suspension of curcumin-loaded EC, ECMC particles or free curcumin dispersing in water using feeding tube. The mice was fed with distilled water is control of each group.

Sample for Oral Administration

The curcumin-loaded EC and ECMC nanosuspensions were performed by dialysis method as previously described to get final curcumin concentration of 0.5 %w/v. Free curcumin water suspension (0.5% w/v) was prepared by dissolved free curcumin (0.5 g) in ethanol (5 ml) and water (95ml) was added and the mixture was sonicated until the suspension was obtained. Distilled water is used as control.

Blood and Organs Sampling

At 15, 30, 60, 90, 120, 180 and 300 min, the animals of each group were sacrificed, respectively, blood and their visceral organs were collected in 2.5% (w/v) aqueous gluteraldehyde. Plasma was separated by centrifuging the blood samples at 4000 rcf for 10 min at 4°C and subjected to quantification of curcumin by HPLC analysis. Stomach and intestine samples were kept at -20 $^{\circ}$C, soaked in water before being freeze-dried and then subjected to SEM analysis.

HPLC Quantification of Curcumin

To quantify curcumin content in plasma, 500 µl of ethyl acetate was added to 200 µl of plasma and the mixture was vortexed for 60s. The supernatant was filtered through a nylon membrane filter (0.2 µm pore size), 20 µl of the filtrant was then injected into the HPLC Hypersil ODS-C_{18} column at room temperature. The mobile phase was a mixture of methanol/3.6% aqueous acetic acid (73:27 %v/v) and was delivered at a flow rate of 0.8 ml min^{-1}. The eluent was monitored with a UV/VIS detector at 425 nm. The retention time for curcumin was ∼ 2.5-3.0 min. The amounts of curcumin in each sample were determined by triplicate injections and were calculated from peak area with the aids of a calibration curve constructed from a series of free curcumin standards (0.01, 0.02, 0.04, 0.06, 0.08 and 0.10 ppm curcumin solutions) freshly prepared in methanol [68].

To quantify curcumin content that had attached to the stomach tissue and the curcumin in the stomach tissue, the freeze-dried sample (~10–20 mg) was accurately weighed and then soaked in 2.0 ml of ethyl acetate (overnight). The suspension was then vortexed and centrifuged at 8000×g for 10 min to pellet the solid. The liquid was collected, filtered through a nylon membrane filter (0.2 µm pore size) and dried under nitrogen. The solid residue was then solvated in 1.0 ml of methanol and subjected to quantification of the curcumin content by HPLC at the similar protocol as described above [68].

Free Radical Formation Protection of Curcumin-Loaded EC and ECMC Particles

The free radical formation protection capacity of free curcumin (FC), curcumin-loaded EC (C-EC, 50% w/w curcumin loading) and curcumin-loaded ECMC particles (C-ECMC, 50% w/w curcumin loading), was being evaluated *in vitro* and *ex vivo* when mixed into oil in water pH5 lotion (L1) and water in oil pH5 lotion (L2), using EPR technique [69].

Lotions

The L1 and L2 lotions were obtained from Beiersdorf (Hamburg, Germany). Their formulations are as follows:

Lotion 1 (L1), oil in water pH 5 lotion, consists of aqua, glycerin, cetyl palmitate, paraffinum liquidum, panthenol, cyclomethicone, cetyl alcohol, sorbitan stearate, aluminum starch octenylsuccinate, phenoxyethanol, tocopheryl acetate, citric acid, carbomer, sodium citrate, methylparaben, propylparaben, perfume, linalool, hydroxyisohxyl 3-cyclohexene carboxaldehyde, hexyl cinnamal, benzyl salicylate, alpha-isomethyl ionone, butylphenyl methylpropional and limonene.

Lotion 2 (L2), water in oil pH 5 lotion, consists of aqua, isopropyl stearate, paraffinum liquidum, glycerin, panthenol, polyglyceryl-2 dipolyhydroxystearate, polyglyceryl-3 diisostearate, tocopheryl acetate, phenoxyethanol, magnesium sulfate, sodium citrate, citric acid, methylparaben, propylparaben, perfume, linalool, hydroxyisohxyl 3-cyclohexene carboxaldehyde, hexyl cinnamal, benzyl salicylate, alpha-isomethyl ionone, butylphenyl bethylpropional, limonene trisodium EDTA, silica, acrylates/C10–30 alkyl acrylate crosspolymer, propylparaben and BHT.

Sample Preparation

Six lotion samples containing curcumin were prepared as following, i) FC (0.25 g) was dispersed in L1 (50 ml), (FC-L1), ii) FC (0.25 g) was dispersed in L2 (50 ml), (FC-L2), iii) C-EC (0.5 g) was dispersed in L1 (50 ml) (C-EC-L1), iv) C-EC (0.5 g) was dispersed in L2 (50 ml) (C-EC-L2), v) C-ECMC (0.5 g) was dispersed in L1 (50 ml) (C-ECMC-L1) and vi) C-ECMC (0.5 g) was dispersed in L2 (50 ml) (C-ECMC-L2). The final concentration of curcumin in the obtained lotion was 5 mg/ml.

Skin Pretreatment

The study was performed on the upper side skin of the excised freshly porcine ears, which were obtained from freshly slaughtered pigs. Skin pretreatment of the porcine ears consisted of washing with cold water and the hairs of the ears were carefully shaved by razor. The ears were then washed and dried with paper towels. The skin was stripped with Printus tape to remove the stratum corneum in part. Ten tape strips were taken from the same skin area. Approval for these experiments had been obtained from the Government Office of Veterinary Medicine in Berlin-Treptow, Germany.

In vitro EPR Experiments

The lotion sample i) to vi) was dispersed in ethanol to give the final curcumin concentration of 0.5 mg/ml. The mixture was mixed well by vortex shaking for 5 min in the dark. One millilitre of the mixture were withdrawn and added with the same volume of 6 mM DPPH in ethanol. The mixture was allowed to react for 30 min by vortex shaking at dark room temperature. Subsequently, the mixture was centrifuged for 5 min. The upper layer of the centrifuged mixture was taken and 200 μL of withdrawn samples in appendorf were subjected to EPR measurement. The EPR parameters were chosen as follows: attenuation 04, BO-field 46.0 mT, sweep 12 mT, sweep time 10 s, gain 2000. The EPR signal results were calculated and expressed as radical formation protection capacity (RFPC). The RFPC is expressed by a positive number N with the measuring unit 10^{14} radicals/mg, which means: RFPC = N $\cdot$ [10^{14} radicals/mg].

The number of reduced test radicals represents the radical scavenging activity that is normalized to 1 mg input of the respective formulation. The RP is calculated by the following equation:

$$RFPC = (RC \times RF)/PI$$

RC = concentration of the test radical [radicals/ml]

RF = The reduction factor represents the difference between the untreated test radical intensity and the decreased signal intensity after treatment with the antioxidant normalized to the signal of the untreated test radical.

PI = Product input represents the amount of the substance/product measured in [mg/ml]

Ex vivo EPR Experiments

For each experiment, three punch biopsies (diameter 14 mm) were taken from the stripped skin and fixed on microscopic slides. Subsequently, a filter paper disk was placed on the skin samples and 50 μL of 10 mM PCA in water/ethanol (ratio 1:1 v/v) solution was applied. Then, skin samples were covered with a Finn Chamber and PCA was allowed to penetrate for 30 min. The remaining of PCA solution on the skin surface was removed with paper towels before the initial EPR measurement. The EPR parameters were chosen as follows: attenuation 04, BO-field 46.0 mT, sweep 8 mT, sweep time 10 s, gain 2000. Subsequently, three of skin biopsied samples were applied with FC, C-EC or C-ECMC lotion, sample i) to iii), using skin biopsied samples without lotion application as negative control and lotion base (lotion 1 or 2) application as positive control. After 15 minutes of lotion penetration time, the skin samples were subjected to EPR measurements. Whereupon, the lotion applied skin samples were UV irradiated for 3 min, using UV irradiation device, irradiation intensity was 3.8 mW/cm^2 measured by the power meter HBM-1, before subjected to final EPR measurement. The sample iv) to vi) were performed as similar procedure on the same porcine skin. The obtained EPR signal results were normalized to their initial value before irradiation and expressed as relative signal intensity.

Skin and Hair Follicle Penetration of Curcumin-Loaded EC and ECMC Particles

The experiment to investigate penetration of curcumin-loaded particles into skin and hair follicle of pig ear skin were adopted from previously described [70] with slight modification.

Sample Preparation

Six topical samples for skin application were prepared, including; i) curcumin-loaded EC water suspension (C-EC-WS), ii) curcumin-loaded ECMC water suspension (C-ECMC-WS), iii) curcumin-loaded EC in o/w lotion (C-EC-L1), iv) curcumin-loaded ECMC in o/w lotion (C-ECMC-L1), v) curcumin-loaded EC in w/o lotion (C-EC-L2) and vi) curcumin-loaded ECMC w/o lotion (C-ECMC-L2). Each water suspension and lotion samples contain curcumin with a final concentration of 5 mg/ml. The water suspension of curcumin-loaded particles was prepared by dispersing 50% loading curcumin-loaded EC (C-EC) or ECMC nanoparticles (C-ECMC) dried powder in water, using sonication (40 kHz, room temperature). The lotions containing loaded curcumin were prepared by stirring the dried powder curcumin-loaded EC or ECMC particles (both with 50% w/w curcumin loading) in oil in water pH 5 lotion, (L1) and water in oil pH 5 lotion, (L2) (Beiersdorf, Hamburg, Germany).

Skin Pretreatment

Approval for these experiments had been obtained from the Government Office of Veterinary Medicine in Berlin-Treptow, Germany. The study was performed on the upper side of freshly porcine ears, which were obtained from freshly slaughtered pigs. The porcine ears were pre-treated by washing with cold water and drying with paper towels. The hairs of the ears were also carefully removed by scissors.

Laser Scanning Microscopy Observation

The skin penetration was investigated on 6 upper porcine ears. Six skin areas of 3 cm × 2 cm were separated on each skin ear using a permanent marker. Subsequently, tape stripping was performed three times on the same skin area. The sample i) and ii) were applied 20 μL/cm^2 on the first and the second skin area. The third to sixth area were treated with 2 mg/cm^2 of sample iii), iv), v) and vi), respectively. After a 30 minutes penetration time, at room temperature, excess water or lotion was carefully removed with

a paper towel. From each application area, the penetration of the loaded curcumin into stratum corneum and hair follicle was scanned and observed by detecting the fluorescent signal at the wavelength of 488 nm using laser fluorescent scanning microscopy (LFSM). The selected LFSM photographs of each application area were stored. The stratum corneum penetration intensity and the aggregation of curcumin-loaded particles were observed and estimated semi-quantitatively in strong, weak or no fluorescence signal.

Biopsy/Cryosectioning/Fluorescence Microscopy Observation

Six skin areas of 3 cm × 2 cm were separated on upper porcine ears. A silicon barrier was applied around each selected skin area. The first and second area was treated with 20 µl/cm^2 of loaded curcumin aqueous suspension sample i) and ii). The third to sixth skin area were treated with 2 mg/cm^2 of the loaded curcumin sample iii) to vi) lotion, respectively. The formulations were massaged for 2 min using a hand-held device, with speed 2. After a 60-min penetration time at room temperature, excess water or lotion was carefully removed with a paper towel. From each application area, five biopsies of 0.5 cm × 0.5 cm were removed and shock frozen in liquid nitrogen. Each frozen biopsy was cryosectioned into 10 µm thin slices using microtome cryostat. Sections containing follicles were marked and observed using a fluorescence microscope. The penetration depth of the loaded curcumin was measured on each fluorescent picture and penetration depth was estimated quantitatively in µm.

Transdermal Penetration of Curcumin-Loaded EC Particles by Suction Blister Technique

The transdermal penetration of loaded curcumin was carried out by suction blister technique under approval from the ethics committee of King Chulalongkorn Memorial Hospital/Chulalongkorn University. Informed consent was obtained from each volunteer. The experiments were carried out on 5 volunteers and six blister roofs were formed for each volunteer. The lotion containing free curcumin or curcumin-loaded particles were tested on every volunteer as following.

Sample Preparation

The dried powder of curcumin-loaded EC (C-EC, 50% w/w curcumin loading) (or free curcumin) was dispersed in lotion base (JOHNSON'S® Baby Lotion, Johnson & Johnson, Indonesia) consisting aqua, petrolatum, isopropyl palmitate, paraffinum liquidum, glyceryl stearate, ceteth-20, anhydrous lanolin, methylparaben, propylparaben and sodium hydroxide. The concentration of the curcumin in the obtained lotion was 10mg/ml.

Suction Blister Roof Performing

The volunteer's inner thigh skin area was pressed with the end of 5 ml plastic syringes, the other end was connected to intravenous tube and was pumped with negative pressure 200 mm Hg by suction pump (as shown in Figure 2.1). After suction for 2-3 h, the epidermis was separated from the underlying dermis forming the roof of the blisters with the diameter at the blister's base of approximately 10 mm.

Sample Application

Six blister roof of each volunteer skin were applied with C-EC lotion (20 μg) at first and second blister roof and the third and fourth blister roofs were applied with FC lotion (20 μg), giving approximately 2 mg/cm^2. The fifth and sixth blister roof of each volunteer skin was not applied lotion sample. Suction blister fluid (SBF) from unapplied roofs was used as control for determination of curcumin in SBF.

Suction Blister Fluid Sampling

After 3 h lotion application, the blister roofs were cleaned with water to avoid lotion contamination in SBF. Each SBF was collected using a fine needle and appendorf of samples were kept in refrigerator at 4-10°C, and then subjected to quantify curcumin content by UV/VIS absorption analysis.

Quantification of Curcumin in Suction Blister Fluid

The withdraw SBF (0.5 ml) was diluted with 2.5 ml of the isotonic phosphate buffer solution (PBS) prior to measurement. The mixture was subjected to determine the curcumin content in SBF using UV/VIS spectroscopy at 425 nm with the aids of a calibration curve constructed from a series of free curcumin solutions (0.01, 0.02, 0.04, 0.06, 0.08 and 0.10 ppm curcumin solutions) prepared in isotonic PBS (see calibration curve in appendix B). The curcumin content in SBF was compared with SBF without lotion application for each individual volunteer.

CHAPTER III

RESULT AND DISCUSSION

Amongst many polymers used in the pharmaceutical industry, the most widely used are the cellulose derivatives: methylcellulose, hydroxypropyl methylcellulose, hydroxypropyl cellulose, ethylcellulose, cellulose acetate phthalate and hydroxypropyl methylcellulose phthalate [71]. The high thermal softening points or glass-transition temperatures of hydroxypropylcellulose (120°C), hydroxypropyl methylcellulose (180°C) and ethylcellulose (140°C) make them ideal polymers for use in a variety of pharmaceutical application, such as film coatings either during high temperature drying or during the heat sealing process used in strips or blister packing. Application of heat up to its softening point has little effect on ethylcellulose. Light, visible or ultraviolet, has no discoloring action on ethylcellulose [72]. Examples of application of ethylcellulose in pharmaceutical formulations are binder in tablets, coating material for stabilization, slow drug release from films, coating for drug microcapsules and beads, thickening agent in creams, lotions or gels, coating material for tablets and controlled release. Ethylcellulose by itself forms a water-soluble film. However, it is commonly used with hydroxypropyl methylcellulose to alter the solubility of the film [73]. Methylcellulose polymers are a broad range of water-soluble cellulose ethers. They enable pharmaceutical developers to create formulas for tablet coatings, granulation, controlled release, extrusion, molding, and for controlled viscosity in liquid formulations. Methyl cellulose is also an important emulsifier, preventing the separation of two mixed liquids [74]. Example of ethylcellulose microparticles and nanoparticles containing drug or active ingredients, were prepared and evaluated in many previously studied [75-81].

In the present work, ethylcellulose (EC) and EC blended with methylcellulose (MC) were compared with three different polymers, namely; poly(ethylene oxide)-4-methoxy cinnamoylphthaloylchitosan (PCPLC), poly(vinylalcohol-co-vinyl-4-methoxycinnamate) with two degrees of 4-methoxycinnamoyl substitution (PB4-I and PB4-II) for encapsulation of

curcumin by solvent displacement, using dialysis method. Improvement of curcumin photostability upon nanoencapsulation, the release characteristics and physical stability of curcumin loaded particles are evaluated. In addition, oral bioavailability, bioactivity and application of the obtained curcumin loaded particles in cosmetic formulation were also investigated.

Nanoparticle Formation, Curcumin Encapsulation and Characterization

Previously, UV screening chitosan derivative (PCPLC) and poly(vinylalcohol-co-vinyl-4-methoxycinnamate) (PB4) were synthesized and were evaluated as an effectively nanocarriers for unstable compound such as sunscreen agent (EHMC) [65] and retinyl acetate [82], while EC was used to encapsulate astaxanthin [79]. Since, the encapsulation of curcumin into polymeric nanoparticles is promised to improve its solubility and bioavailability. Therefore, in this work, five polymers were used for curcumin encapsulation and determined encapsulation efficiency, loading and morphology characterization. Firstly, the nanoformation of five polymers namely; ethylcellulose (EC), methylcellulose (MC), methyl ether terminated poly(ethylene glycol)-4-methoxycinnamoylphthaloylchitosan (PCPLC), poly(vinylalcohol-co-vinyl-4-methoxy cinnamate) with degree of 4-methoxycinnamoyl substitution of 0.30 (PB4-I) and 0.44 (PB4-II), was carried out at the polymer concentration of 3000 ppm by solvent displacement using dialysis method. Since, each polymer could dissolve in different solvent to provide particles, ethanol was used for EC and ECMC polymer, PCPLC was dissolved in DMF and DMSO was used to dissolve PB4-I and PB4-II. During self-assembly of each of the amphiphilic polymer, it was assumed that when solvent was displaced by water, the hydrophobic part were directed to the inside of the particle, while the hydrophilic part arranged them at the outer surface of the particle to provide interaction with water molecules [83], leading to spontaneous particle formation which appeared as white aqueous colloidal particles suspension, at the final polymer concentration of 1500 ppm (Figure 3.1).
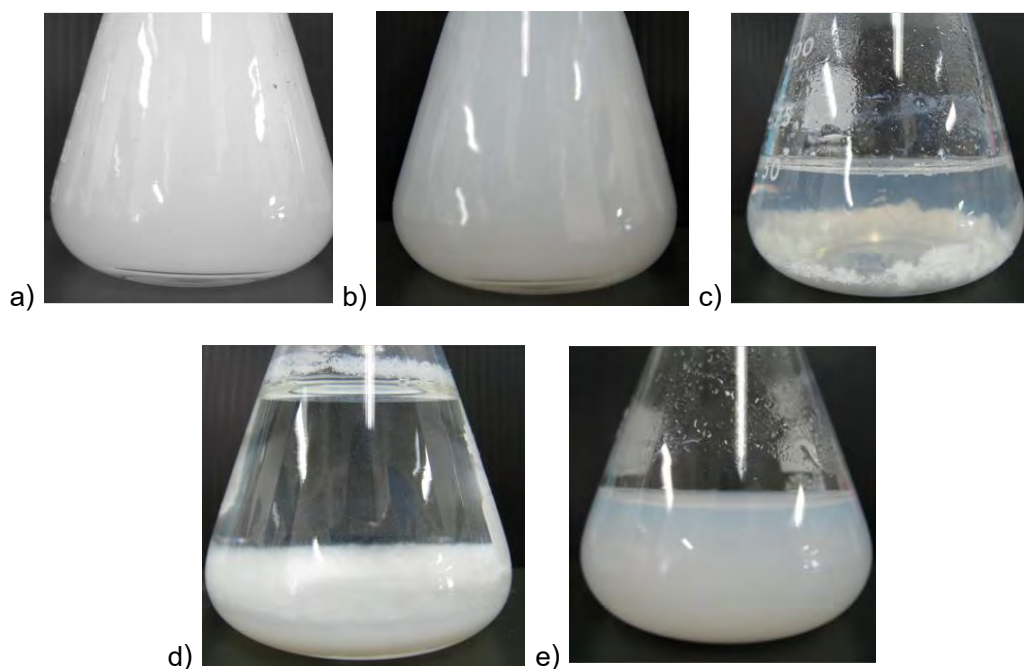
Figure 3.1 The aqueous colloidal suspensions of a) EC, b) ECMC, c) PCPLC, d) PB4-I and e) PB4-II particles

Subsequently, the encapsulation of curcumin into EC, PCPLC, PB4-I and PB4-II, were performed by solvent displacement using dialysis method at the polymer and curcumin concentration of 3000 ppm, and each polymer use the similar solvent as mentioned above. Since curcumin is water insoluble compound, therefore, curcumin was encapsulated at the core of particles during self-assemble of each amphiphilic polymer. To determine the concentration of curcumin in the obtained suspension, encapsulation efficiency and the curcumin loading, the dialysate water was collected and subjected to UV/VIS absorption analysis directly at 425 nm with the aids of calibration curve with the aid of a calibration curve (0.1, 0.2, 0.4, 0.6, 0.8 and 1.0 ppm curcumin solutions) freshly prepared in ethanol (see calibration curve in appendix A). The process gave a turbid yellow aqueous suspension, at the final curcumin concentration of ∼1400-1500 ppm (Figure 3.2). The encapsulation efficiency and the curcumin loading of the obtained particles was 98.67 ± 0.68% and 49.34 ± 0.92%(w/w) for EC polymer, 97.79 ± 1.05% and 48.90 ± 0.53%(w/w) for ECMC polymer, 96.62 ± 1.11% and 48.31 ± 1.01%(w/w) for PCPLC polymer, 91.69 ± 1.09% and 45.61 ±

1.19%(w/w) for PB4-I polymer and 91.22 ± 1.15% and 45.85 ± 1.05%(w/w) for PB4-II polymers, respectively (Table 3.1).
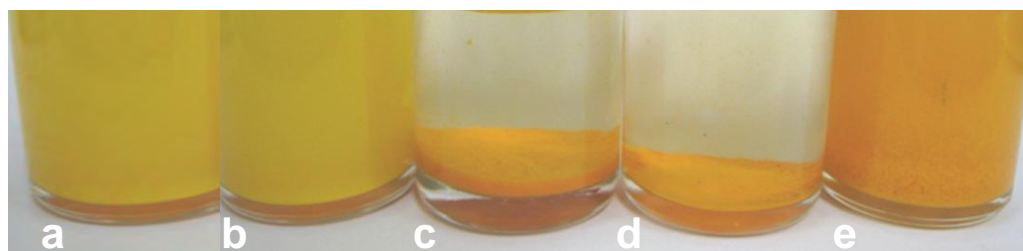
Figure 3.2 The aqueous suspensions of curcumin-loaded a) EC, b) ECMC, c) PCPLC, d) PB4-I and e) PB4-II particles

Table 3.1 The encapsulation efficiency (% EE) and curcumin loading of curcumin loaded EC, PCPLC, PB4-I and PB4-II nanoparticles

Polymer	% EE	% loading (w/w)	Final curcumin concentration (ppm)
EC	98.67 ± 0.68	49.34 ± 0.92	1480 ± 13
ECMC	97.79 ± 1.05	48.90 ± 0.53	1467 ± 18
PCPLC	96.62 ± 1.11	48.31 ± 1.01	1450 ± 22
PB4-I	91.22 ± 1.09	45.61 ± 1.19	1369 ± 27
PB4-II	91.69 ± 1.15	45.85 ± 1.05	1376 ± 26

The aqueous suspension of the resulting nanoparticles was then subjected to SEM, TEM and dynamic light scattering analyses. SEM analyses indicated that the curcumin loaded particles obtained from all five polymers were spherical or semi-spherical shape with larger diameters than their corresponding unloaded particles (Figure 3.3). The fact that the size of curcumin loaded nanoparticles was larger than that of unloaded nanoparticles implies a weak hydrophobic interaction at particles' cores in the presence of curcumin (Table 3.2).
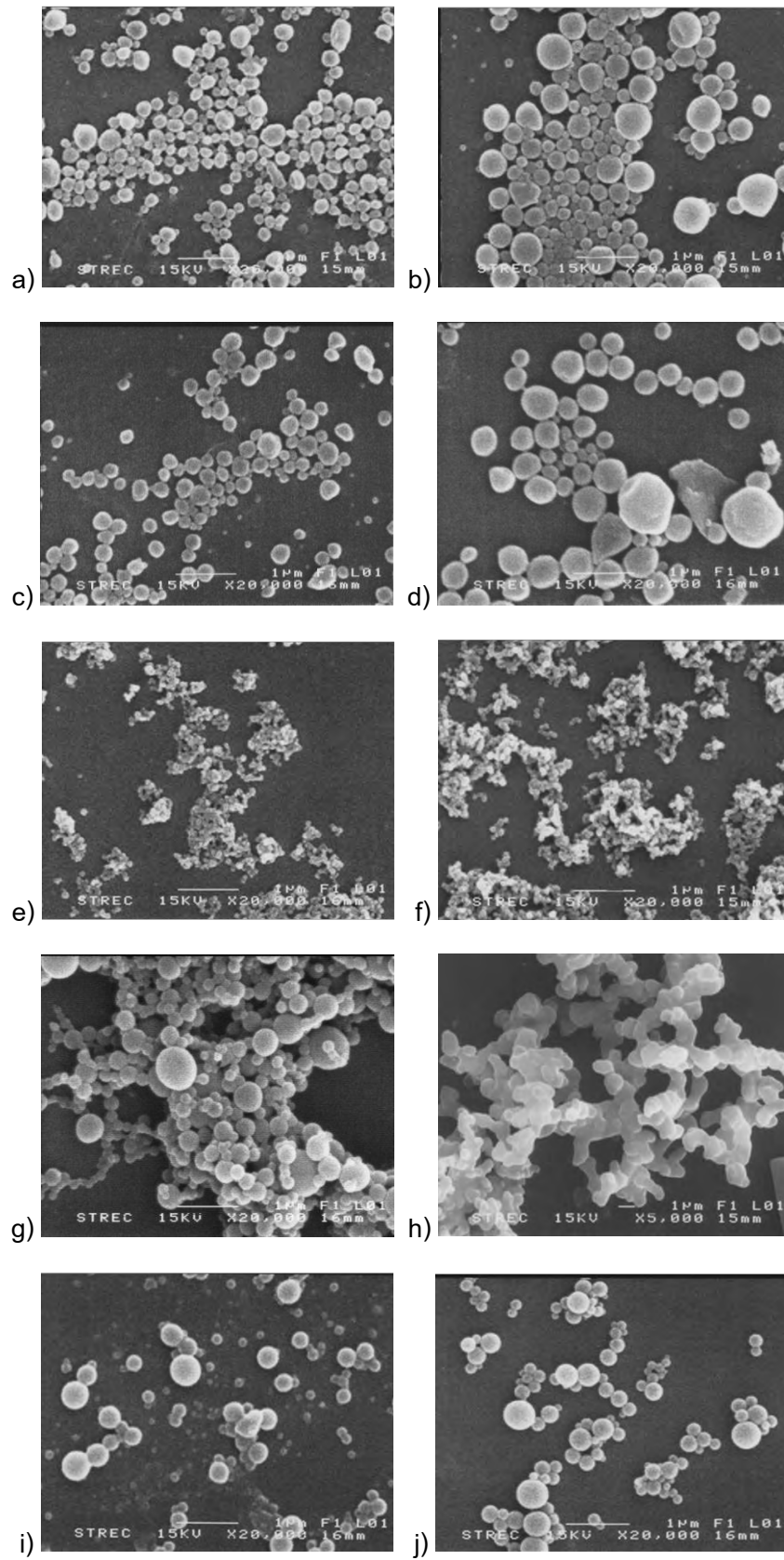
Figure 3.3 SEM photographs of a) empty EC, b) curcumin-loaded EC, c) empty ECMC, d) curcumin-loaded ECMC, e) empty PCPLC, f) curcumin-loaded PCPLC, g) empty PB4-I, h) curcumin-loaded PB4-I, i) empty PB4-II and j) curcumin-loaded PB4-II particles

Table 3.2 Average size by SEM of unloaded and curcumin loaded particles of various polymers

Polymer	Average size by SEM (nm)	
	unloaded	curcumin-loaded
EC	100-300	150-350
ECMC	100-300	150-350
PCPLC	50-100	50-150
PB4-I	100-500	700-800
PB4-II	100-400	150-500

SEM photograph also revealed tight aggregation of curcumin-loaded PB4-I and curcumin-loaded PCPLC particles. This aggregation observation agreed well with the fact that the two suspensions were not stable and fast settling of agglomerated particulates were witnessed (Figure 3.2b and c). Therefore, only curcumin-loaded EC, ECMC and PB4-II nanoparticles could be subjected to dynamic light scattering analyses. Hydrodynamic diameters of 287.37 ± 2.10 nm, 264.82 ± 2.61 and 712.40 ± 2.80 nm were obtained for curcumin-loaded EC, ECMC and PB4-II particles, respectively. The polydispersity index (PDI) of 0.15 ± 0.03 for curcumin-loaded EC, PDI of 0.24 ± 0.01 for curcumin-loaded ECMC and PDI of 0.56 ± 0.10 for curcumin-loaded PB4-II particles. The curcumin-loaded EC particles showed much narrower size distribution than the curcumin-loaded ECMC and PB4-II (Figure 3.4).
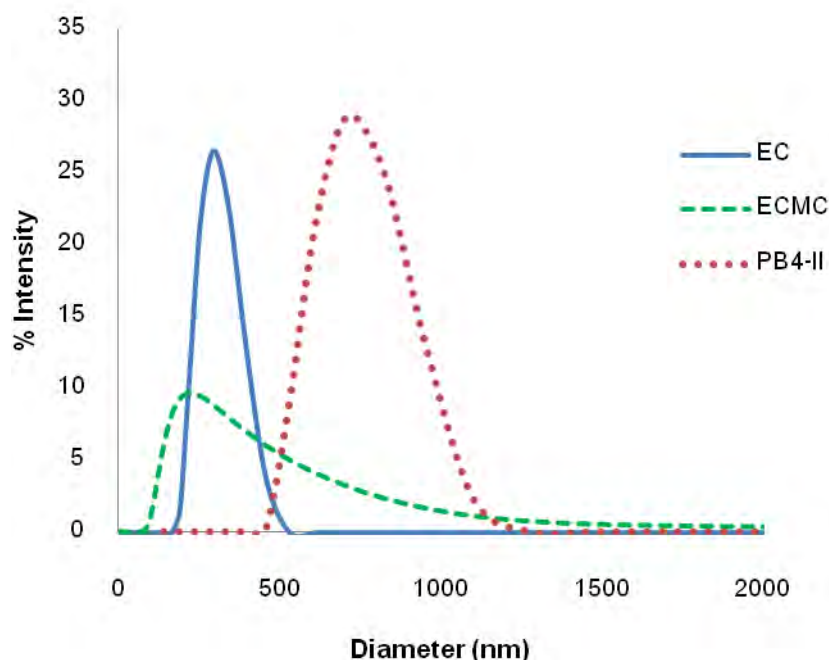
Figure 3.4 Size distributions of curcumin-loaded EC, ECMC and PB4-II particles

Zeta potential of nanoparticles is commonly used for measuring a net charge density of the particle surface. This surface charge directly affects the distribution of particle in the surrounding interfacial region and influences their aggregation behaviors. The decided value of stable and unstable suspensions is generally taken at either +30 mV or -30 mV [84]. In this work, the zeta potential of -30.80 ± 0.68 mV for curcumin-loaded EC particles and -31.57 ± 0.43 mV for curcumin-loaded ECMC particles indicated acceptable stability of suspension, whereas the zeta potential of -1.42 ± 0.31 mV was obtained for curcumin-loaded PB4-II, indicating poor stability of suspension. Even though, SEM photograph of curcumin-loaded PB4-II revealed the particles size smaller than their hydrodynamic size but agglomeration of particles were observed in the photograph (Figure 3.3f). This observation agreed well with the absolute low value of zeta potential of curcumin-loaded PB4-II. In most circumstances, the higher the absolute value of the zeta potential of the particles, the larger amount of charge on their surface. These might result in stronger repellent interactions among the particles, and hence, higher stability of the curcumin-loaded EC and ECMC than PB4-II suspension. Upon

leaving for several months, the curcumin-loaded PB4-II particle suspension showed significant settling of the particles while well dispersed suspension could still be observed for curcumin-loaded EC and ECMC particles. Moreover, TEM photograph of curcumin-loaded EC and ECMC particle (Figure 3.5) revealed distinct core of the particle comparing to unloaded particle. Homogenity of the core probably implies solid solution of curcumin within the polymer matrix. In other words, no individual curcumin crystal could be observed inside the particle's core.
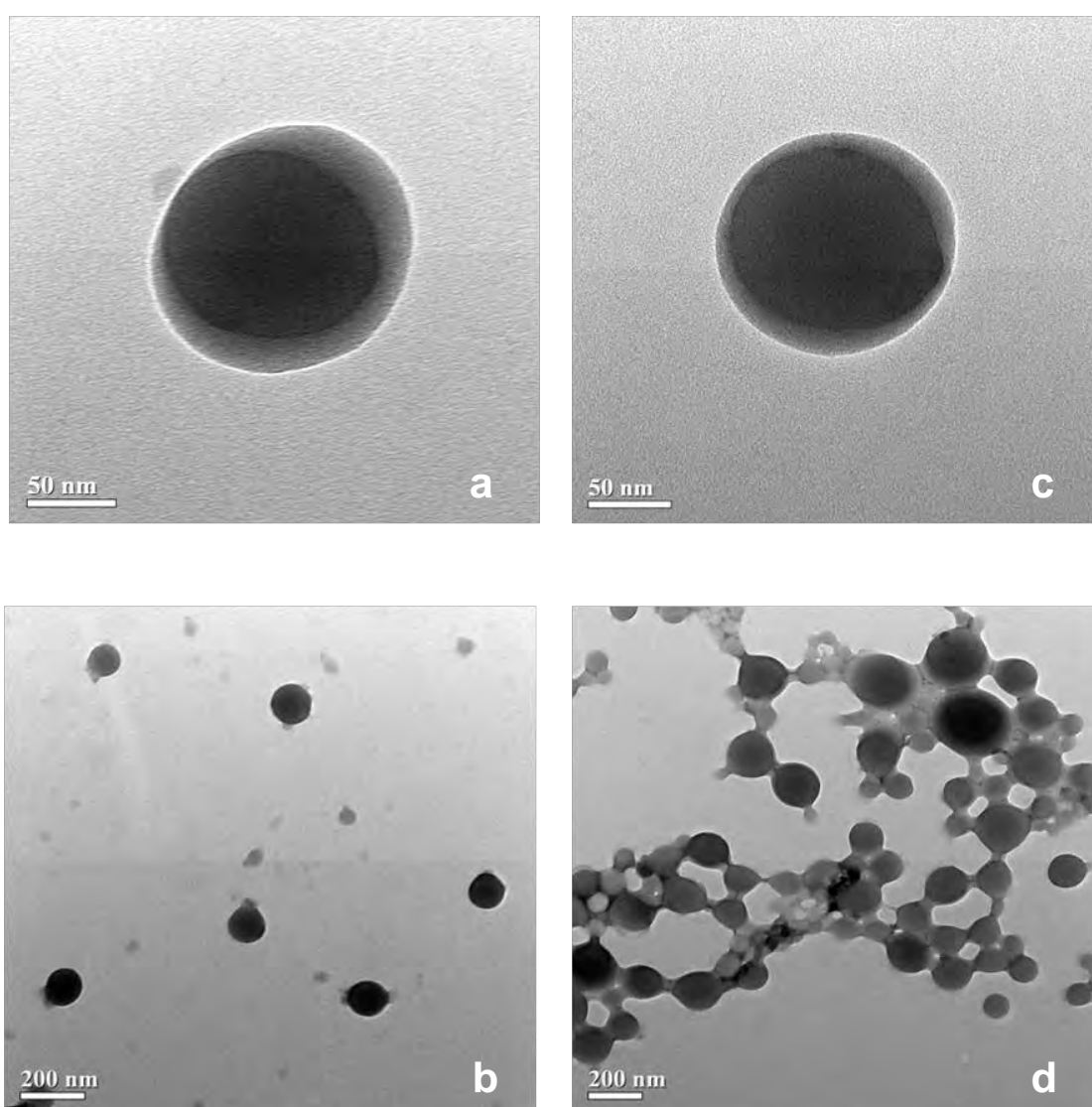
Figure 3.5 TEM photographs of a) empty EC, b) curcumin-loaded EC, c) empty ECMC and d) curcumin-loaded ECMC particles

Thus, based on the morphology, encapsulation efficiency and loading of curcumin, it could be concluded that curcumin nanoencapsulation was successfully performed by dialysis method using the UV-screening PCPLC, PB4-I and Pb4-II polymer and the best resulting curcumin-loaded nanosuspension was achieved using the biocompatible, safe, inexpensive and commercially available ethyl cellulose and methylcellulose polymer.

Release of Curcumin from Curcumin-Loaded Polymeric Particles

The release of curcumin from EC, ECMC, PCPLC, PB4-I and PB4-II nanoparticles in phosphate buffer at pH 5.5 and 7 were performed with a dialysis method for 192 h. The release of curcumin could be observed from the EC, ECMC, PCPLC, PB4-I and PB4-II nanoparticles under all two pH conditions (Figure 3.6). The releases of curcumin under acidic condition were more and faster than neutral condition except that the releases under acidic and neutral conditions were similar for PB4-I nanoparticles. The fastest release was attained from ECMC nanoparticles under all acidic and neutral conditions. The slowest release rate was observed under neutral conditions for PCPLC and corresponds well with the fact that chitosan polymers are least swollen in neutral-basic media and PCPLC gave the least particles size in comparison from four polymers which used for nanoparticles preparation. The release curves also indicated that EC and ECMC particles released curcumin more quickly than PCPLC particles did, implying a good interaction between curcumin molecules and the grafted cinnamoyl moieties in the PCPLC polymer. In addition, comparison between EC and ECMC, the releases of curcumin under acidic condition were more and faster than neutral condition whereas curcumin could released from ECMC more than EC under all acidic and neutral conditions (Figure 3.7). It should be noted here that, since the release mediums of different pH values can all solubilize curcumin well, even at the highest possible release concentration, the differences in release profiles among the two pH conditions are related to the diffusion of curcumin from particles.
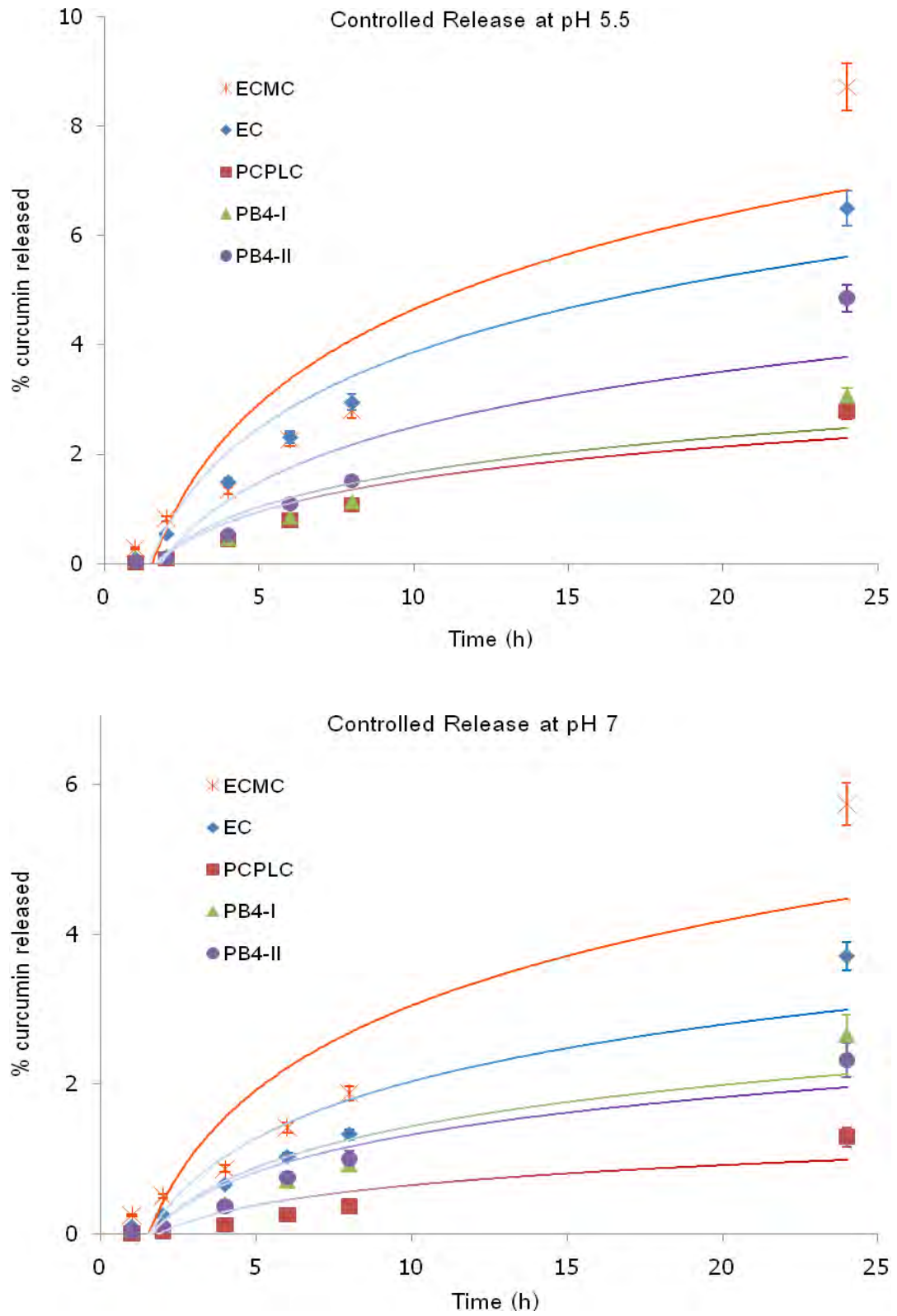
Figure 3.6 The release profile of curcumin-loaded EC, ECMC, PCPLC, PB4-I and PB4-II particles at pH 5.5 and 7
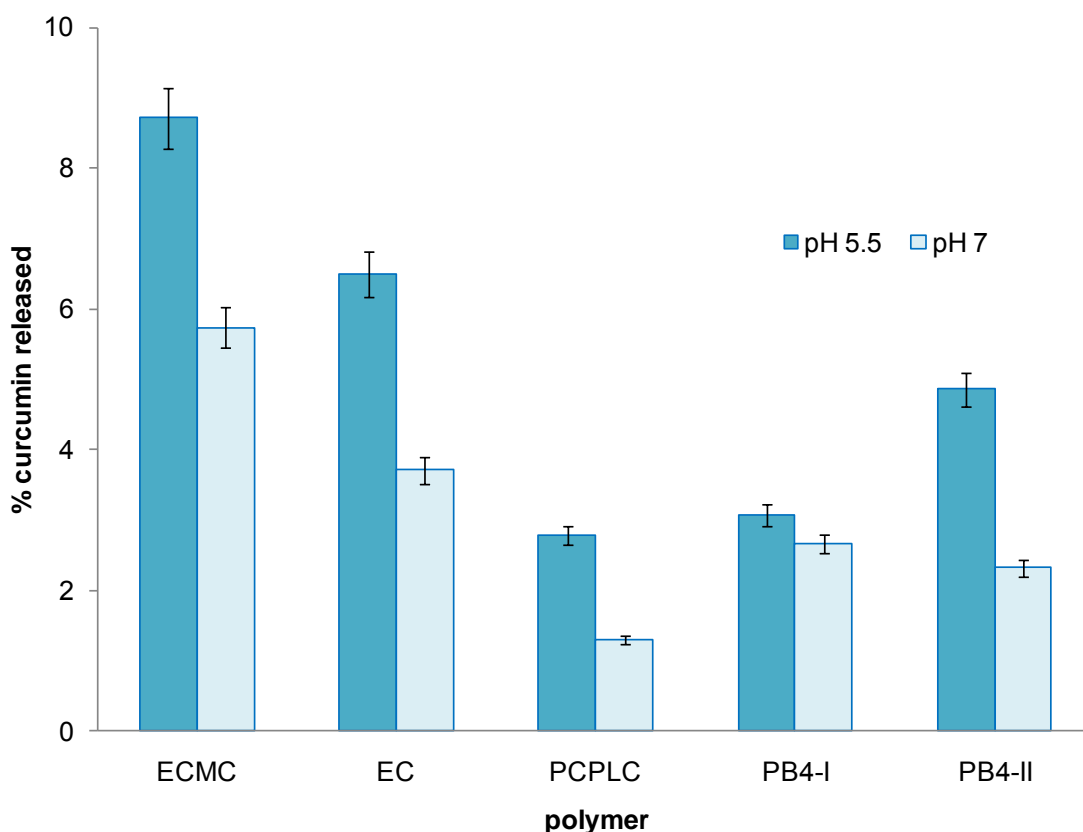
Figure 3.7 Release of curcumin from curcumin-loaded EC, ECMC, PCPLC, PB4-I and PB4-II particles at pH 5.5 and 7 after 24 hours

In conclusion, curcumin was released from five curcumin-loaded particles either acidic or neutral conditions, The C-ECMC gave the highest curcumin released, whereas C-PCPLC gave the lowest curcumin released in both conditions.

Stability of Curcumin Loaded Particles

Photostability of Five Curcumin-Loaded Particles

Light instability of curcumin has been well documented [85, 86]. As a result, photo-degradation of curcumin during the post-application has been an on-going problem. To try to lessen this drawback, encapsulation of curcumin into the UV absorptive PCPLC, PB4-I and PB4-II nanoparticles and EC and ECMC nanoparticles was performed and their photostability was evaluated. The results revealed that upon exposure to sunlight, free curcumin degraded rapidly, resulting in obvious changes in

absorption profiles of the light-exposed curcumin solution (Figure 3.8); principally the completely loss of the characteristic curcumin peak at 425 nm.
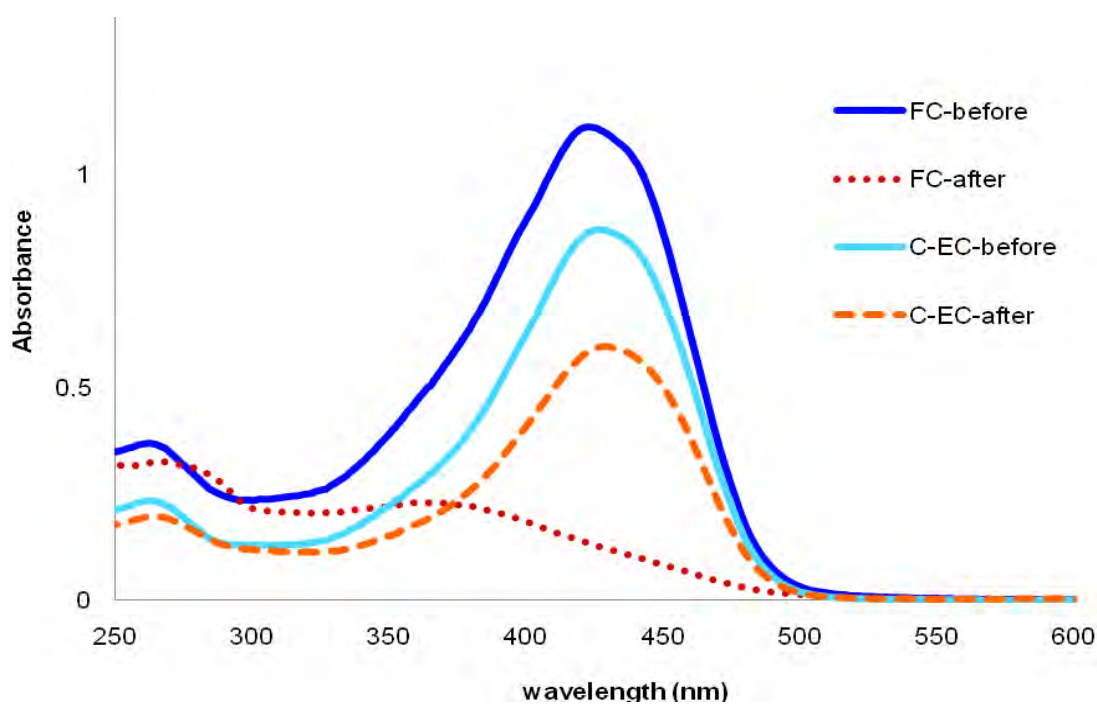
Figure 3.8 The profile spectrum of free curcumin solution and curcumin-loaded EC before and after sunlight exposed for 1 day

As a result, curcumin in samples from the photostability experiment could be quantified using UV-visible absorption spectroscopic technique at 425 nm without interference from the degradation products. Furthermore, after sunlight-exposed for 4 hours, each sample were withdraw and diluted with ethanol prior subjected to determined curcumin content by UV/VIS absorption analysis. The calibration curve of standard curcumin was performed from serial dilution of free curcumin in ethanol (see calibration curve in appendix A). The curcumin content in each sample was calculated with the aids of calibration curve (see appendix A). It was found that when curcumin was encapsulated into nanoparticles, significantly less degradation was observed upon light exposure although this was far from total protection under these conditions. Curcumin-loaded PCPLC nanoparticles showed least degradation compared with curcumin-loaded PB4-I, PB4-II, EC and ECMC nanoparticles (Figure 3.9). Such photoprotection

can be explained by the fact that the curcumin hide in the UV protection property of PCPLC [65]. Finally, it should be noted that close contact between curcumin and the UV absorptive 4-methoxycinnamoyl moieties should not exacerbate the photo-degradation of the curcumin, since the cinnamate is not likely to be a photodynamic sensitizer.

Table 3.3 The percentage remained of curcumin-loaded EC, ECMC, PCPLC, PB4-I and PB4-II after sunlight-exposed for 4 hours

Polymer	% curcumin remained after sunlight exposed for 4 hours
EC	71.77 ± 3.59
ECMC	73.28 ± 3.66
PCPLC	92.91 ± 4.65
PB4-I	78.78 ± 3.94
PB4-II	68.64 ± 3.43
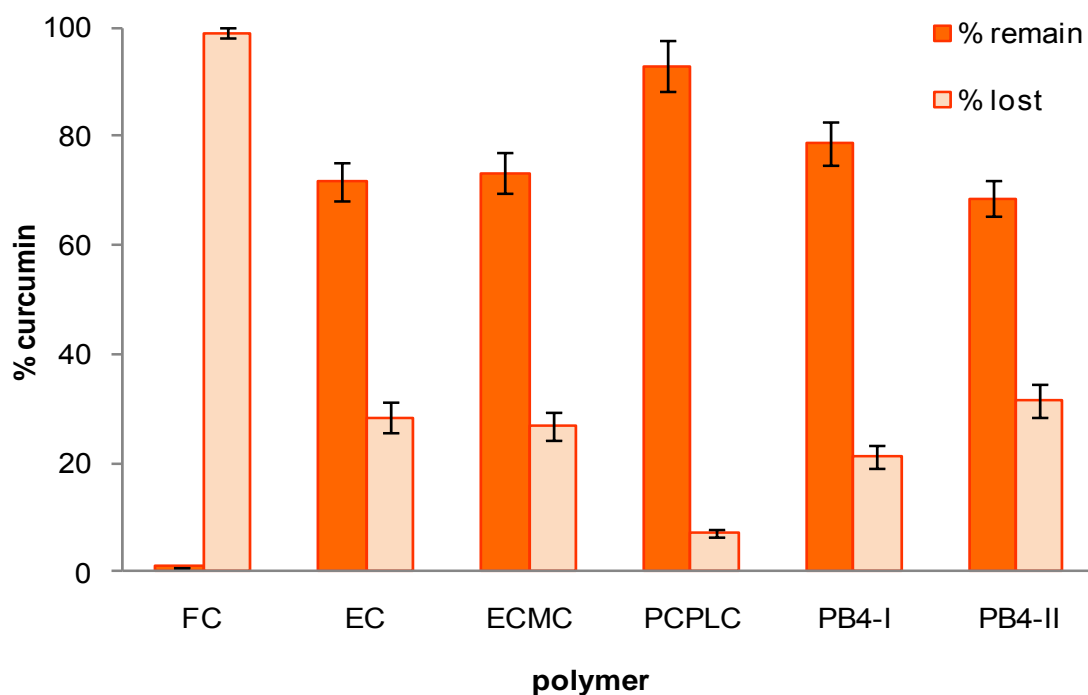
Figure 3.9 The photostability of free curcumin, curcumin-loaded EC, ECMC, PCPLC, PB4-I and PB4-II after sunlight exposed for 4 hours

In conclusion, photostability of curcumin was improved by nanoencapsulation. Five curcumin-loaded particles offered ∼70-90% increase in the curcumin photostability, whereas PCPLC gave the highest photostability.

Although, PCPLC revealed the highest protection for curcumin photodegradation. Nevertheless, EC and ECMC encapsulation offered ∼70-75 % increase in the curcumin photostability (Table 3.3). Moreover, PCPLC gave unstable curcumin-loaded suspension. Therefore, summarizing the results of encapsulation efficiency, curcumin loading, stability of suspension and photostability, it could be concluded that EC and ECMC are more suitable than the other three polymers. Moreover, consideration in safe, inexpensive, FDA approval commercially edible polymer, EC and ECMC were properly used for curcumin encapsulation and the obtained curcumin-loaded particles in both polymers were ready used for pharmaceutical applications so far. Therefore, the next experiments would only focused on curcumin-loaded EC and ECMC particles for its bioavailability and topically application.

Stability of Curcumin-Loaded EC and ECMC Particles in various pH values

The curcumin loaded EC and ECMC nanoparticles suspensions were subjected to dispersibility evaluation under pH 4, 5.5, 7 and 10, using 0.01 M phosphate buffer. The colloidal stability and aggregation behavior of the aqueous suspensions were observed by vision at room temperature. It was found that the nanoparticles suspensions at pH 4 gave completely precipitates after 4 hours, whereas the nanoparticles suspension gave no detectable precipitate after 24 h and 4 days, at pH 5.5, 7 and 10 (Figure 3.10). That means curcumin loaded EC and ECMC nanoparticles suspensions unstable under acidic condition lead to aggregation of the particles which resulted in obvious precipitation. However, the suspensions at pH 7 and 10 were slightly aggregated and gave detectable precipitates after 7 days. Moreover, the color of the nanoparticles suspension at pH 10 was slightly changed from yellow to brown. Interestingly, unbuffered nanoparticles and the suspensions at pH 5.5 could be well

dispersed after 7 days. Explanation on this may lie on enough negative charges on the particles' surfaces which then will protect particles from aggregation to one another due to charge-repulsion. This repulsion together with Brownian motion of the small particles, thus, overrides the aggregation and setting of the particles from gravitational force. In addition, the pH value of EC and ECMC nanoparticles suspension were approximately 5.5, leading to the best dispersibility of EC and ECMC nanoparticles under phosphate buffer at pH 5.5.
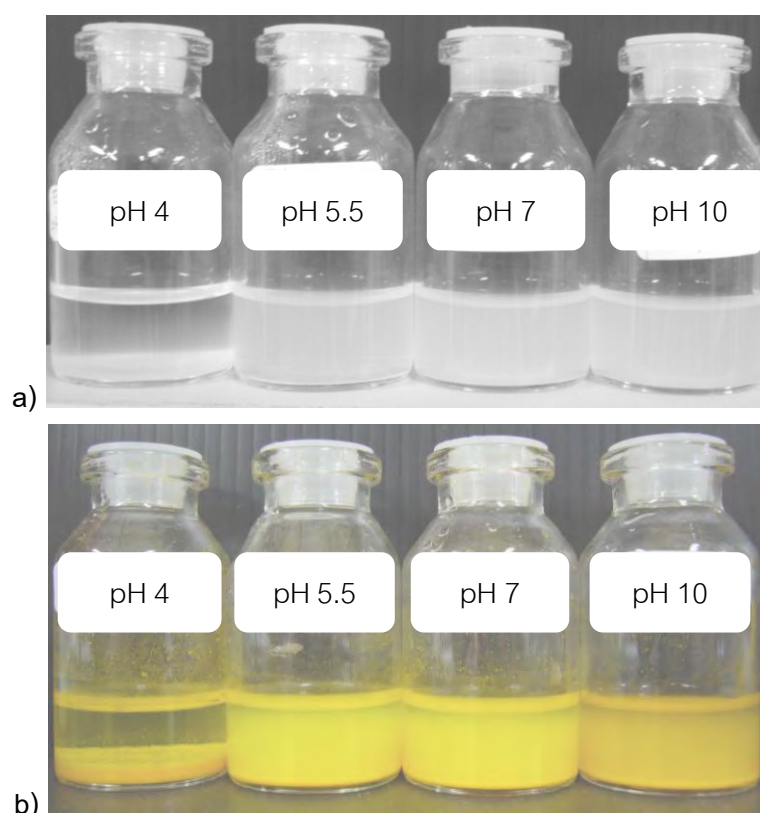
Figure 3.10 The dispersibility after 24 hour of a) unloaded and b) curcumin-loaded EC suspensions in 0.01 M phosphate buffer at pH 4, 5.5, 7 and 10

Stability of Curcumin-Load EC and ECMC Particles under Various Drying Conditions

Stability of curcumin-loaded EC and ECMC particles under various drying conditions was evaluated in order to give basic background of their possible applications and storage.

Freeze Drying

The purpose of freeze-drying is to remove a solvent (water) from suspension. The curcumin-loaded suspension was frozen then placed under vacuum. The frozen water was slowly vaporized under the low air pressure. The freeze drying gave a very light product with natural color. However, the time required for drying is very long. In this study, freeze drying of curcumin-loaded EC and ECMC suspension was carried out at 80 ^{o}C. The curcumin content of the obtained dry product is stable.

Spray Drying

Spray drying is a method of producing a dry powder from a liquid or slurry by rapidly drying with a hot gas. In this study, spray drying of curcumin-loaded EC and ECMC suspension was carried out at 130 ^{o}C. The suspension input stream was sprayed through a nozzle (40 rounds/sec) into a hot vapor stream and vaporised. The solid of curcumin-loaded particles was collected in a cyclone. Spray drying can dry a product very quickly compared to other methods of drying. The curcumin-loaded suspension was turn into a dried powder in a single step, which can be advantageous for profit maximization and process simplification. The obtained dried product of curcumin loaded ECMC is a very light weight. The curcumin content of the obtained dry product is stable.

Low-pressure Super-Heated Steam Drying and Vacuum Drying

The low-pressure superheated steam drying (LPSSD) could increase the potential of the conventional hot air drying by decrease drying time. In this study, LPSSD and vacuum drying was carried out at the pressure of 8 kPa, 80 ^{o}C. Drying time for LPSSD is longer than that for vacuum drying. The obtained dried product of curcumin-loaded EC and ECMC particles was not ready used, due to it was not powder. In addition, the crispy chip dried curcumin-loaded particles was obtained from LPSSD.

Figure 3.11 revealed the curcumin loaded EC and ECMC appearance after drying. SEM visualization of particles after being subjected to freeze-drying, spray-drying, low-pressure superheated steam drying and vacuum drying, indicated that freeze-drying, super-heated steam drying and vacuum drying gave particles with unchanged morphology while spray-drying gave deformed particles. However, upon reconstitution in water by just simple stirring the dry particles with water, the particles resumed their original spherical shape with no indentation (Figure 3.12).
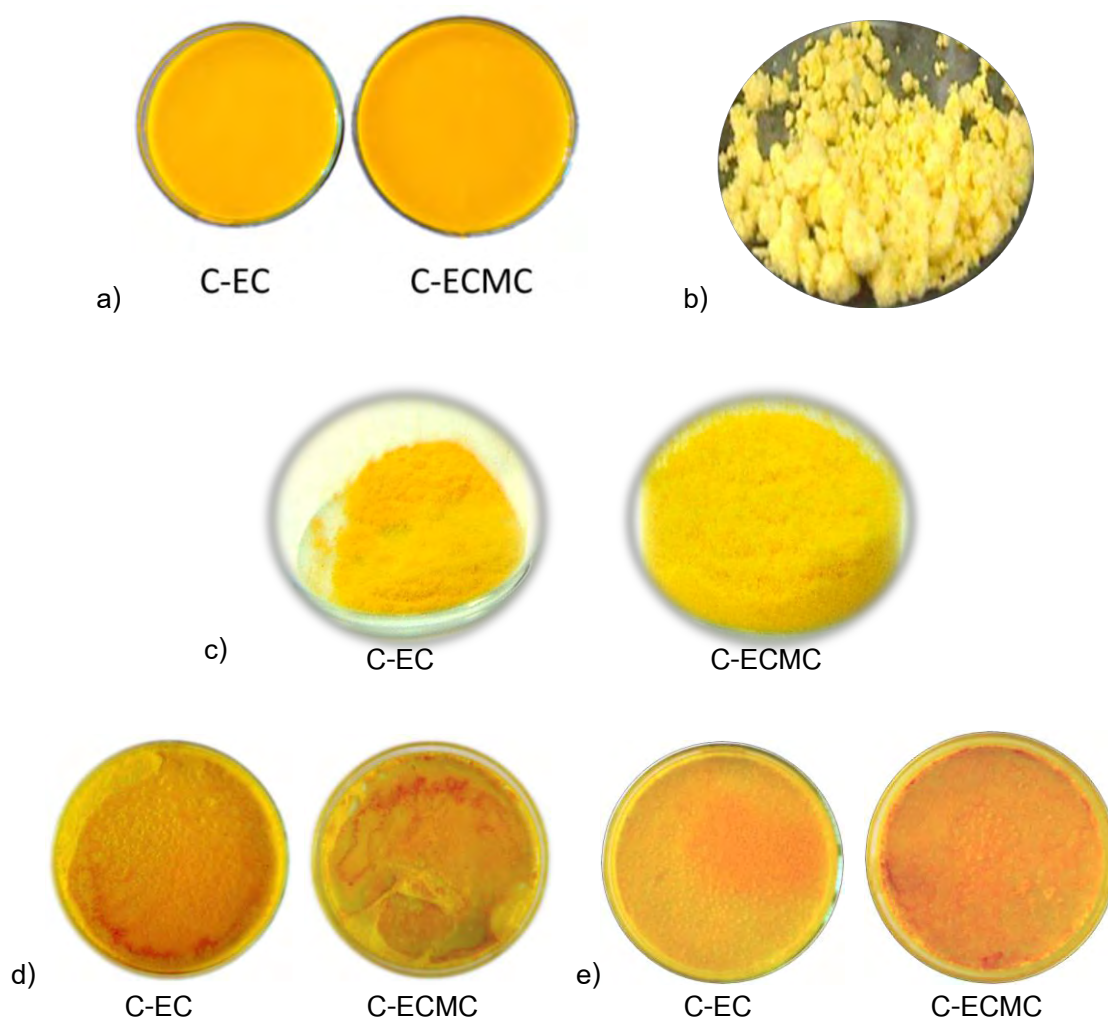
Figure 3.11 The appearance of curcumin-loaded EC and ECMC a) before drying and after drying by b) freeze-drying at -80 $^{\circ}$C, c) spray-drying at 130 $^{\circ}$C, d) low-pressure superheated steam at 8 kPa, 80 $^{\circ}$C and e) vacuum drying at 8 kPa, 80 $^{\circ}$C
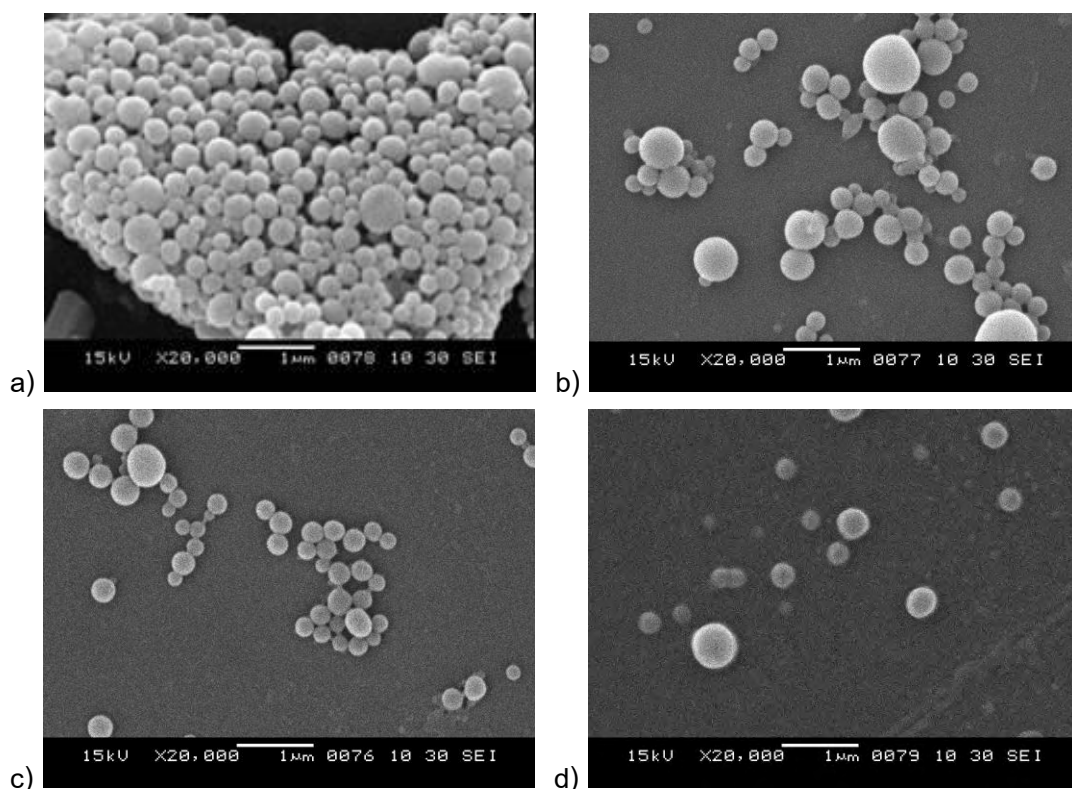
Figure 3.12 SEM photographs of particles after a) freeze-drying at -80 $^{\circ}$C, b) spray-drying at 130 $^{\circ}$C, c) low-pressure superheated steam at 8 kPa, 80 $^{\circ}$C and d) vacuum drying at 8 kPa, 80 $^{\circ}$C

In conclusion, all three drying methods showed different drying time in the order of freeze drying > LPSSD and vacuum drying > spray drying. The particles resumed their original spherical shape after redispersion in water.

In vitro **Release of Curcumin from EC and ECMC Nanoparticles in Simulated Gastric Fluid and Simulated Intestinal Fluid**

The aim of this work was to investigate the stability *in vitro*, in simulated gastro-intestinal fluids, of particles, made of EC and ECMC, and to study the release of curcumin from the particles. The *in vitro* release of curcumin from EC and ECMC nanoparticles was determined after 24 h incubation time in the simulated gastric fluid (SGF), pH 1.2 and simulated intestinal fluid (SIF), pH 6.8. The curcumin content in release medium was determined by UV/VIS spectroscopy at 425 nm with the aids of

calibration curve (see appendix B). The results indicated that curcumin was released from the EC and ECMC carriers at pH 1.2 more than at pH 6.8. However, in this conditions the curcumin was released less than 10% from both particles after 24 h, whereas curcumin was released from the ECMC particles a little faster than from the EC particles at pH 1.2 (Figure 3.13). This result agrees well with preliminary study, which indicated that curcumin was released from EC and ECMC particles under acidic condition more and faster than neutral condition. In fact, the encapsulation of curcumin into EC or ECMC particles did not alter the structure of curcumin and the fact that curcumin shows only minimal solubility in aqueous media, therefore, it was not surprised to see that curcumin still possessed poor solubility in the two aqueous release medium.
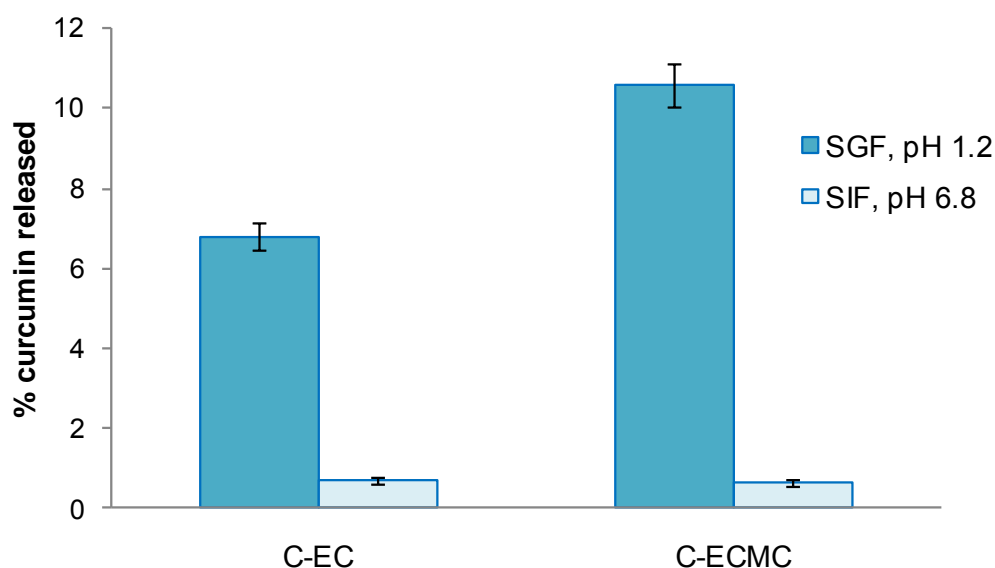
Figure 3.13 The release of curcumin from EC and ECMC particles in simulated gastric fluid (SGF), pH 1.2 and simulated intestinal fluid (SIF), pH 6.8

In conclusion, curcumin was released in SGF more than SIF while release of curcumin from ECMC is higher than EC.

Oral Bioavailability of Curcumin-Loaded EC and ECMC Particles in Mice

Despite its promising pharmacological activity, low oral bioavailability of curcumin due to the poor biopharmaceutical properties, most importantly the low solubility and poor

intestinal permeability, has remained a major hurdle. Usage of the highly bioavailable developed nanoparticulate formulation of curcumin may bring about reduction in dose and improvement in efficacy of curcumin [87]. In this study, bioavailability of curcumin-loaded EC and ECMC particles was evaluated by oral administration of samples in ICR mice, strain ICR/Mlac. and compared with that of free curcumin for i) their ability to deliver curcumin into the blood circulation and ii) their ability to attach to the mucosal layer of the gastrointestinal tract. The animals were divided into three groups ($n = 5$). Group 1 was administered with free curcumin suspension (100 mg/kg body weight); Group 2 with E-EC (100 mg/kg body weight) and Group 3 was administered with C-ECMC (100 mg/kg body weight) by feeding tube. At 15, 30, 60, 90, 180 and 300 min, after oral administration the animals of each group were sacrificed, Curcumin in blood was extracted and subjected to HPLC analysis to quantify curcumin content (3 replications) with the aids of a calibration curve constructed from a series of free curcumin standards freshly prepared in methanol (see calibration curve in appendix C). The amount of curcumin in blood of mice oral administered with each sample was showed in Table 3.4 and Figure 3.14. The results indicated that at 30 min all three groups showed significantly different curcumin levels with C-ECMC as the highest and C-EC as the lowest. However, at 60 and 90 min, all three groups showed significantly different curcumin levels in the order of C-EC > C-ECMC > free curcumin. The highest concentration of curcumin in blood was detected at 30 min after feeding of free curcumin and C-ECMC, whereas, the release of curcumin from C-EC gave the highest concentration, at 60 min of post feeding. This means that curcumin was released from C-ECMC faster than C-EC. This result is agreed well with the previous *in vitro* release study in SGF. At 180 and 300 min, the free curcumin and the C-ECMC groups showed no detectable of curcumin, while the C-EC group gave detectable of curcumin in the blood. Figure 3.14 illustrated that free curcumin suspension upon oral administration resulted in sharp peak concentration within 30 min; however, the plasma concentration of curcumin decreased rapidly, indicating rapid metabolism of curcumin. It could be concluded that the sustainability of curcumin in the blood of mice oral

administered with C-EC was significantly longer than C-ECMC, although C-ECMC particles released curcumin into the blood faster than C-EC particles.

Table 3.4 Curcumin concentration in the blood of mice after oral administered with free curcumin, C-EC and C-ECMC

Time (min)	Curcumin concentration in blood of mice (µg/ml)		
	free curcumin	C-EC	C-ECMC
15	0.024 ± 0.010	0.063 ± 0.017	0.062 ± 0.019
30	0.438 ± 0.138	0.182 ± 0.137	0.784 ± 0.244
60	0.031 ± 0.027	0.698 ± 0.234	0.314 ± 0.192
90	0.003 ± 0.005	0.682 ± 0.286	0.121 ± 0.113
180	0	0.089 ± 0.045	0.010 ± 0.014
300	0	0.024 ± 0.018	0
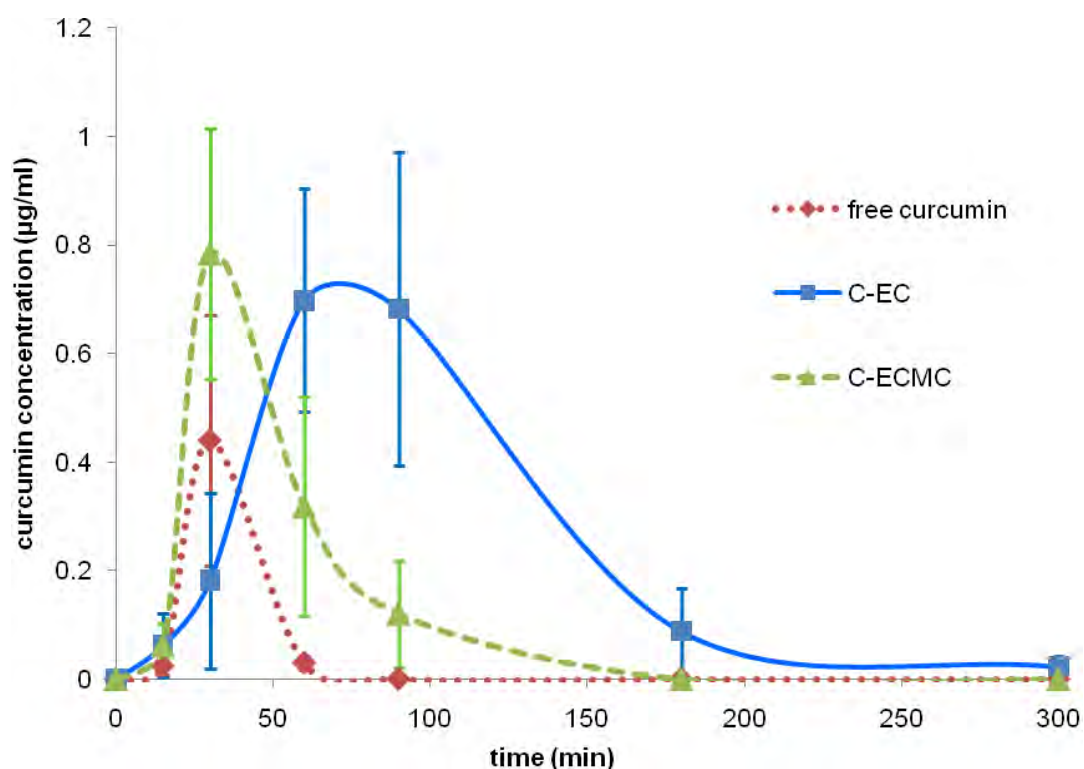
Figure 3.14 Curcumin concentration in the blood of mice oral administered with free curcumin, C-EC and C-ECMC suspension (This picture was also used in article as: N. Suwannateep, et. al., Mucoadhesive curcumin nanospheres: Biological activity, adhesion to stomach mucosa and release of curcumin into the circulation, J.Control.Release (2011)doi: 10.1016/j.jconrel.2011.01.011.)

Oral bioavailability of curcumin was estimated by integrating amount of the curcumin in the blood during the 0 to 300 min post feeding. The estimated amounts of available curcumin in blood were 32.905 µg for free curcumin, 278.939 µg for C-EC and 117.721 µg for C-ECMC. Comparison with free curcumin, EC carrier gave an 8.5-fold increased bioavailability while ECMC carrier gave a 3.6-fold. The mice oral administered with free curcumin showed a significantly lower amount of curcumin in their blood than those administered with C-EC and C-ECMC (Table 3.5).

Table 3.5 Amount of curcumin concentration in the blood of mice after oral administered with free curcumin, C-EC and C-ECMC

Sample	Amount of curcumin in blood of mice (µg)	Bioavailability of curcumin (fold)
free curcumin	32.905	-
C-EC	278.939	8.5
C-ECMC	117.721	3.6

Furthermore, SEM photographs of the freeze-dried stomach and duodenum were taken at 120 min post feeding. The most particles were well attached with the stomach while the attachment of C-EC was at a higher density than that of the C-ECMC particles in both layers (Figure 3.15). Moreover, SEM photographs indicated that the C-EC and C-ECMC particles had passed into the duodenum were the unattached and larger sized aggregated particles, since microsize-particles were observed at the surface of the duodenum. HPLC quantification of curcumin levels in freeze-dried

stomach tissue samples collected at 120 min post oral administration indicated 0.067±0.018, 0.031±0.015 and 0.017±0.010 mg/g for samples from mice fed with C-EC, C-ECMC and free curcumin, respectively. This result confirmed the better attachment of C-EC over C-ECMC particles at the stomach surface observed by SEM. Thus, it was concluded that the better bioavailability of C-EC over the C-ECMC was related to the better attachment of the particles at the stomach layer.

Since the *in vitro* release experiment indicated a minimal release of curcumin into the SGF, the attached particles acted as curcumin reservoirs and continuously released curcumin. It was likely that the curcumin is directly released from the particles into the epithelium of the stomach. Hence, the concentration gradient of curcumin would be the driving force on this diffusion equilibrium. Moreover, the absorbed curcumin molecules quickly enter the blood circulation, thus decreasing the concentration of curcumin at the tissue of contact site. As a result, a curcumin concentration gradient remained in the direction that curcumin was diffused from the particles into the tissue. In addition, good attachment between the particles and the stomach surface would be an important factor for this transportation. Figure 3.15 showed the less attachment of C-ECMC than C-EC, therefore curcumin released from C-EC into blood is higher than that of C-EC and so a high curcumin concentration was observed in the blood for a longer time.

Previously *in vivo* studies have shown that curcumin possesses a rapid metabolism [88], and fast elimination [89, 90]. Comparison with quickly released and rapidly decreased of free curcumin in blood of mice, the long sustainability of curcumin-loaded particles observed here revealed a continuous release of the curcumin into the circulation. The high concentration of curcumin in blood of mice during the first three hours post feeding and SEM photographs indicated that the stomach was the most likely curcumin absorption site. The attachment of the curcumin-loaded self-assembled particles on the stomach surface could protect curcumin molecules in the particles lead to prolong curcumin released from the particles directly into the stomach tissue.
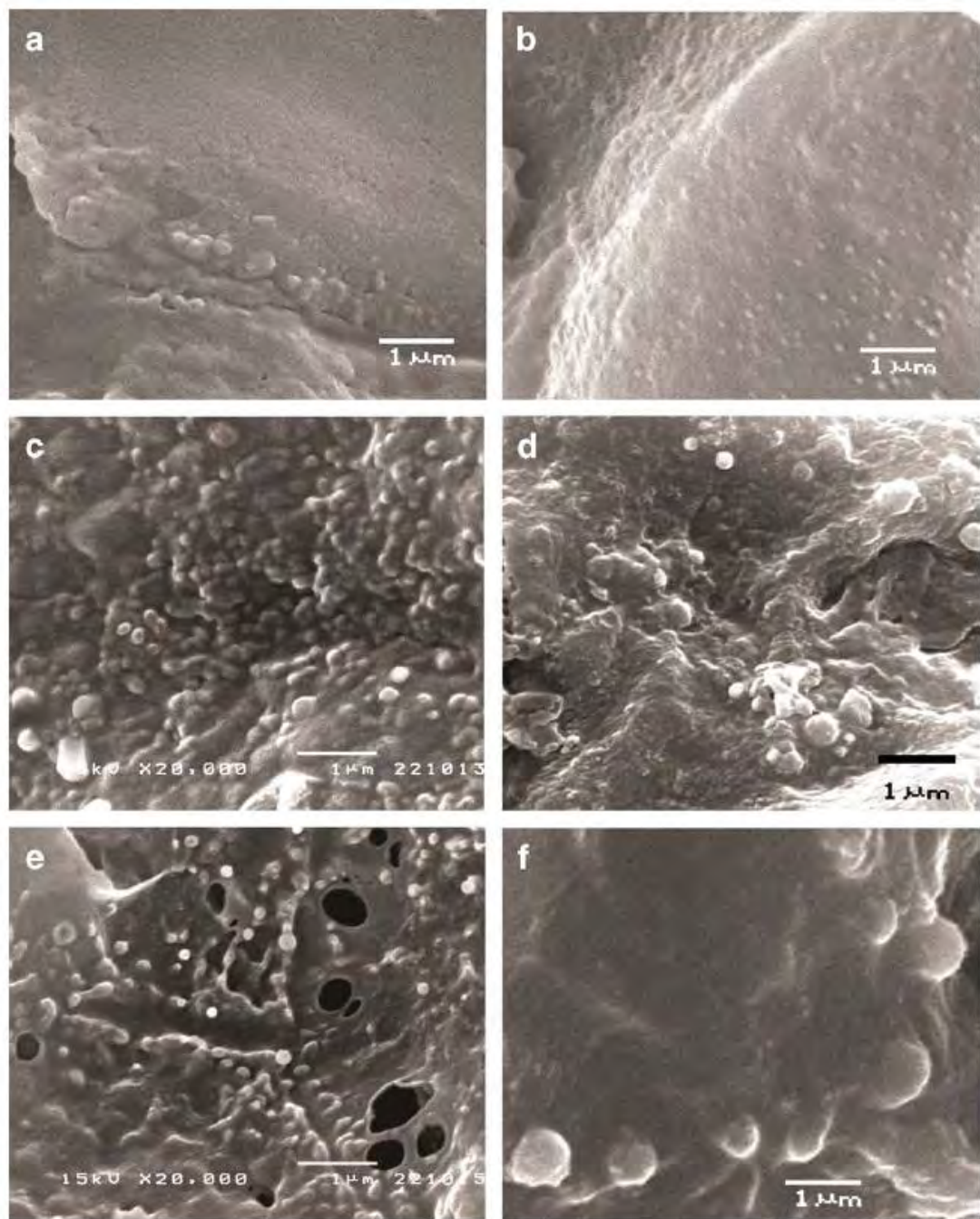
Figure 3.15 SEM photographs of stomach (left column, a, c and e) and duodenum (right column b, d and f) of mice fed with water (a and b), C-EC (c and d) and C-ECMC suspension (e and f) (This picture was also used in article as: N. Suwannateep, et. al., Mucoadhesive curcumin nanospheres: Biological activity, adhesion to stomach mucosa and release of curcumin into the circulation, J.Control.Release (2011) doi: 10.1016/j.jconrel.2011.01.011.)

Free Radical Formation Protection of Curcumin-Loaded EC and ECMC Particles

Ethyl cellulose was used in nanoencapsulation base carriers system to improve the properties and controlled release of some active ingredients such as perfume [78], astaxanthin [79], nimesulide [80] and curcumin [68]. The skin and hair follicle penetration with topical application of loaded curcumin formulation indicated that the lotions could enhanced the penetration and loaded curcumin could penetrated deeper into the skin. Furthermore, the antioxidant activities results, determining by DPPH free radical scavenging assay, showed no statistical significance between loaded curcumin water suspension and free curcumin dissolved in DMSO. However, when loaded curcumin was compared with free curcumin, the antioxidant activity of curcumin loaded nanoparticles was stronger than free curcumin in water [68]. Electron paramagnetic resonance spectroscopy (EPR) is a tool for investigating paramagnetic species, including organic radicals, inorganic radicals, and triplet states. The basic principles behind EPR are very similar to the nuclear magnetic resonance spectroscopy (NMR), except that EPR focuses on the interaction of an external magnetic field with the unpaired electron(s) in a molecule, rather than the nuclei of individual atoms. EPR has been used to investigate kinetics, mechanisms, and structures of paramagnetic species and along with general chemistry and physics, has applications in biochemistry, polymer science, and geosciences [91].

In this study, free curcumin (FC), curcumin-loaded EC (C-EC) and ECMC particles (C-ECMC) (Figure 3.16) in two lotion formulations were determined for its capacity of free radical formation protection using EPR. The loaded curcumin dried powder could well disperse in lotions. Otherwise, C-EC was well dispersed and better than C-ECMC, while C-ECMC was slightly aggregated in both lotion L1 and L2 (Figure 3.17).

FC   C-EC   C-ECMC
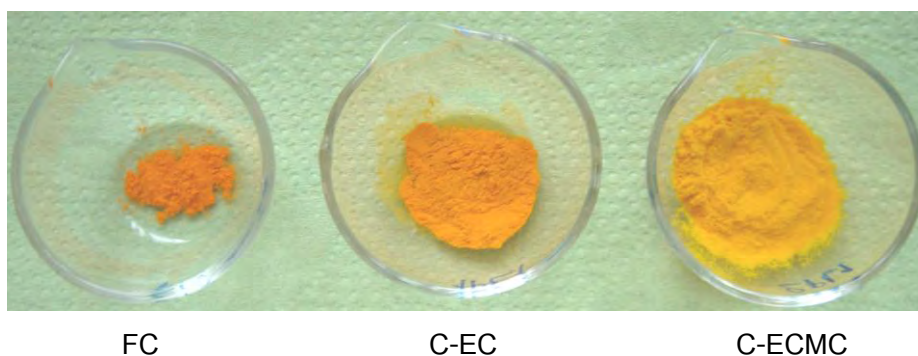
Figure 3.16 The powder of free curcumin, curcumin-loaded EC and ECMC particles

FC-L1   C-EC-L1   C-ECMC-L1

FC-L2   C-EC-L2   C-ECMC-L2
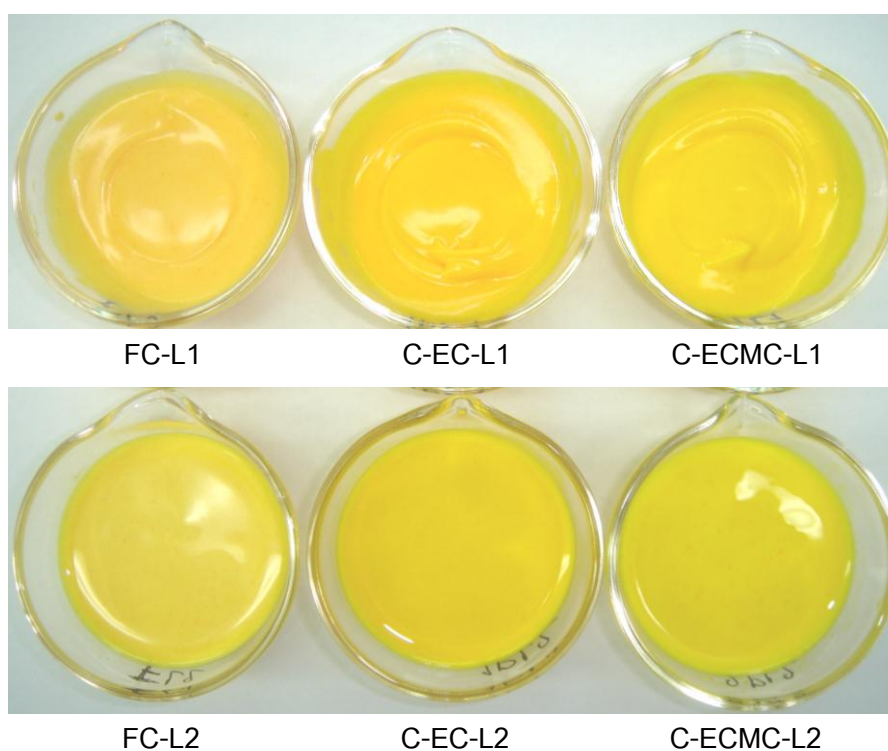
Figure 3.17 The free curcumin and curcumin-loaded particles in lotions

The *in vitro* EPR results, comparison of C-EC and C-ECMC applied in an o/w and w/o lotions with that of free curcumin in the same lotion, indicated that the free radical formation protection capacity of two loaded curcumin is comparable with free curcumin (Table 3.6). Figure 3.18 indicated that the encapsulation system could protect the incorporated curcumin from photo-degradation and prolong released curcumin from the polymeric nanoparticles, afford a slightly capacity of C-EC and C-ECMC less than free curcumin.

Table 3.6 Radical formation protection capacity of various curcumin formulations

Formulation	RFPC ($.10^{14}$ radicals/ml)
L1	23 ± 2
FC-L1	186 ± 8
C-EC-L1	180 ± 2
C-ECMC-L1	147 ± 2
L2	25 ± 5
FC-L2	185 ± 3
C-EC-L2	180 ± 4
C-ECMC-L2	151 ± 7
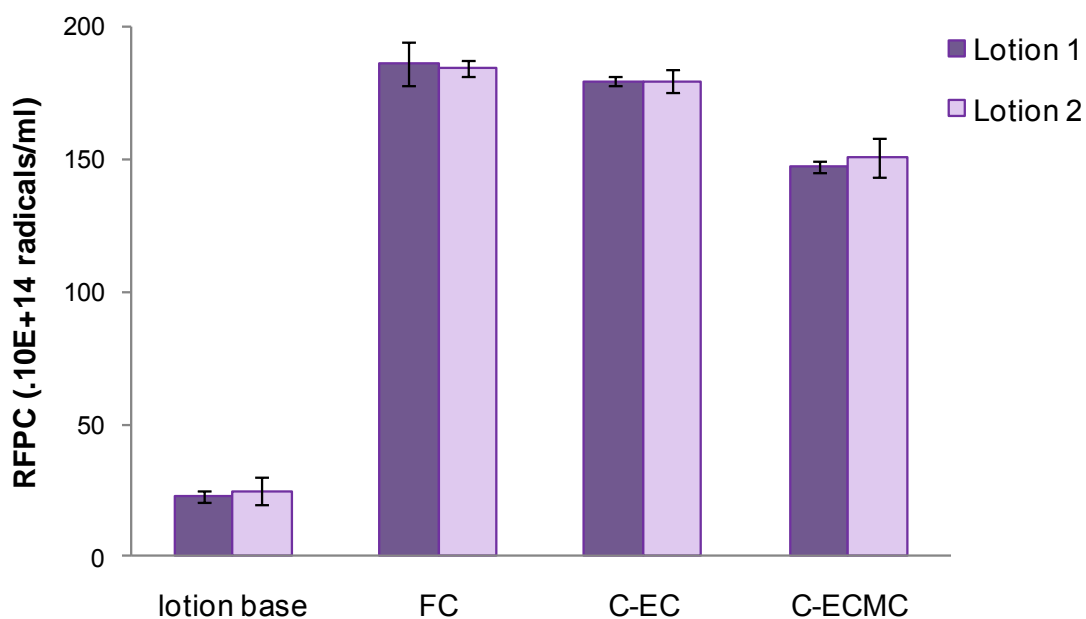
Figure 3.18 Free Radical formation protection capacity of various curcumin formulations in an o/w lotion (lotion 1) and w/o lotion (lotion 2)

For *ex vivo* EPR results, the different radical formation in excised skin after 3 min of UV irradiation is shown in Table 3.7 and Figure 3.19 for various curcumin in o/w lotion and Table 3.8 and Figure 3.20 for various curcumin in w/o lotion.

Table 3.7 Free radical formation in excised skin after applied various curcumin o/w lotion

(L1) and 3 min of UV irradiation

Sample	Normalized EPR intensity (Au)		
	PCA_30 min.	Lotion_15 min.	UV_3 min
control/-UV	1.01 ± 0.05	1.00 ± 0.00	0.96 ± 0.03
control/+UV	1.07 ± 0.13	1.00 ± 0.00	0.31 ± 0.07
L1	0.92 ± 0.16	1.00 ± 0.00	0.36 ± 0.05
FC-L1	0.95 ± 0.17	1.00 ± 0.00	0.40 ± 0.05
C-EC-L1	0.99 ± 0.13	1.00 ± 0.00	0.46 ± 0.08
C-ECMC-L1	1.02 ± 0.07	1.00 ± 0.00	0.45 ± 0.06
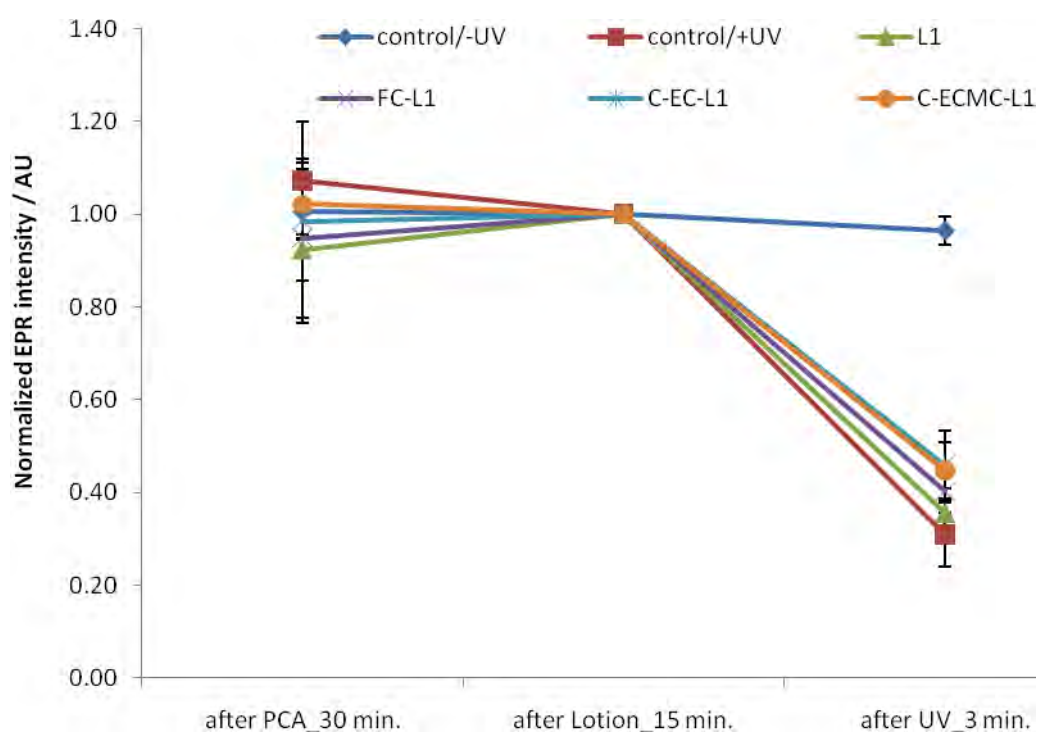
Figure 3.19 Free radical formation in excised skin after applied various curcumin o/w

lotion (L1) and 3 min of UV irradiation

Table 3.8 Free radical formation in excised skin after applied various curcumin w/o lotion (L2) and 3 min of UV irradiation

Sample	Normalized EPR intensity (Au)		
	PCA_30 min.	Lotion_15 min.	UV_3 min
control/-UV	1.06 ± 0.10	1.00 ± 0.00	0.95 ± 0.03
control/+UV	1.02 ± 0.07	1.00 ± 0.00	0.35 ± 0.09
L2	0.97 ± 0.19	1.00 ± 0.00	0.37 ± 0.08
FC-L2	0.92 ± 0.12	1.00 ± 0.00	0.44 ± 0.07
C-EC-L2	0.95 ± 0.07	1.00 ± 0.00	0.51 ± 0.07
C-ECMC-L2	0.87 ± 0.08	1.00 ± 0.00	0.53 ± 0.07
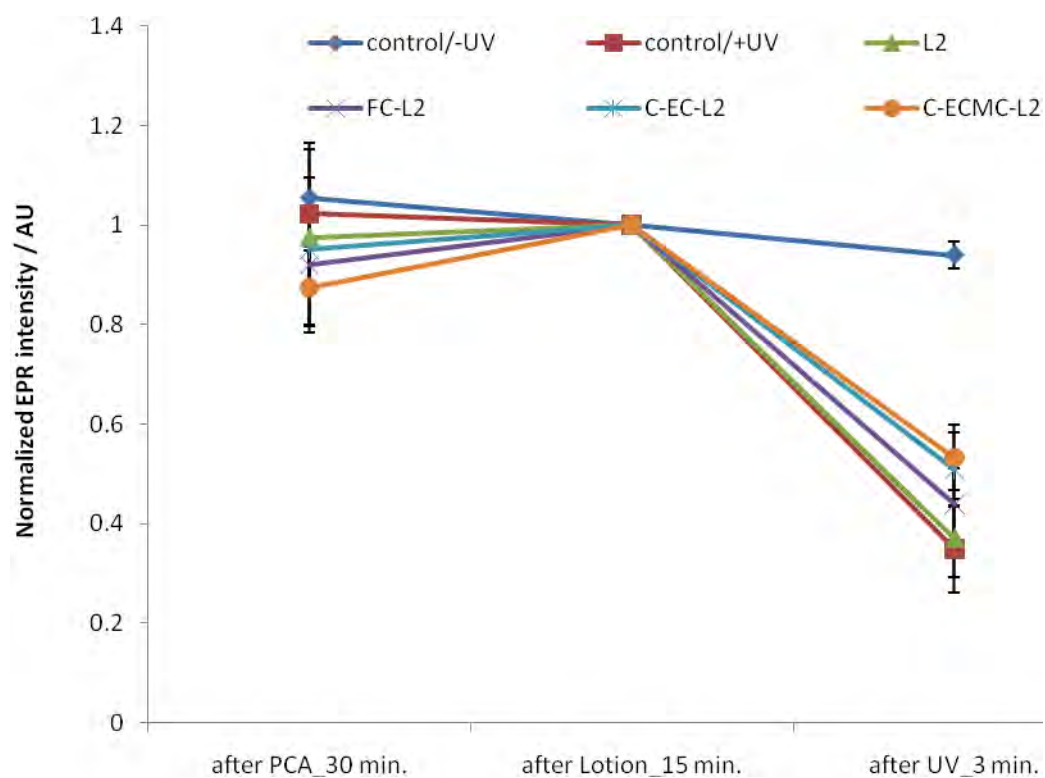
Figure 3.20 Free radical formation in excised skin after applied various curcumin w/o lotion (L2) and 3 min of UV irradiation

All lotions containing curcumin exhibit a significantly higher protection compared to the untreated skin and the lotion base treated skin (Figure 3.21). No significantly differences of the results were found between the two lotions, with the exception of C-ECMC. Therefore, the C-ECMC-L2 shows significantly less radical formation than C-ECMC-L1. Moreover, the skin *ex vivo* results indicated that C-EC and C-ECMC applied in an o/w and w/o lotions have a better radical formation protection capacity more than FC lotions. In this case only for lotion 2 the changes are statistically significant.
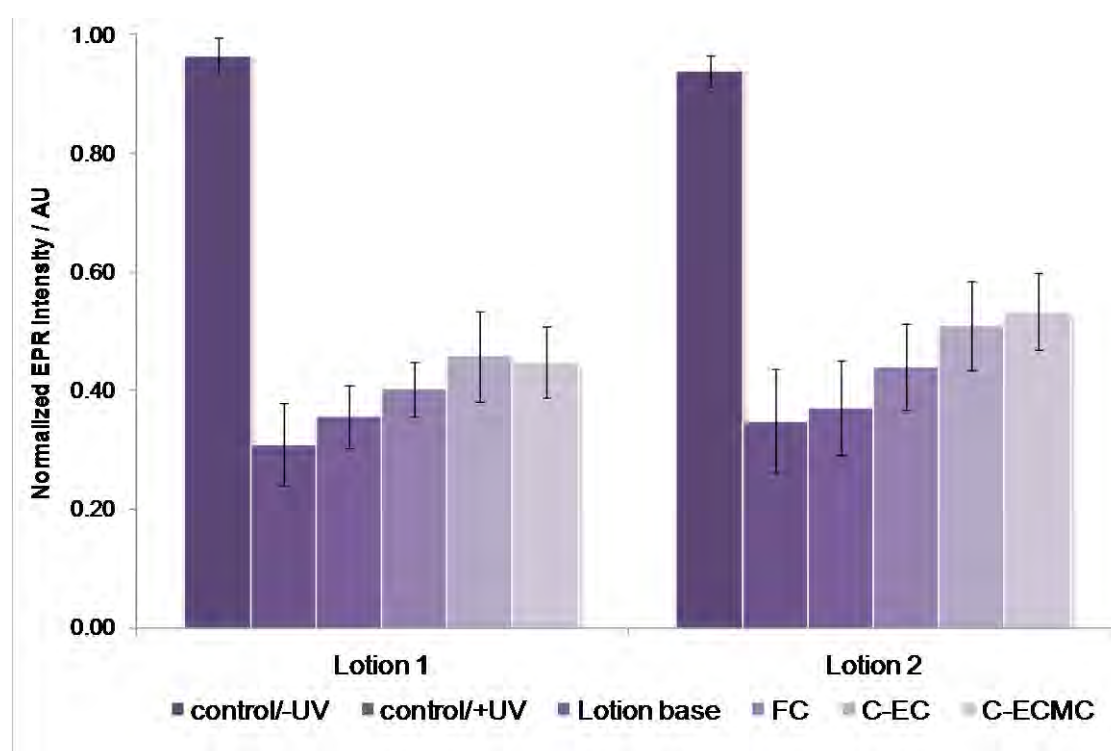
Figure 3.21 Normalized EPR intensity of excised porcine ear skin after applied various curcumin formulations, 15 min penetration time and UV irradiated for 3 min

Since, EC and ECMC polymeric nanoshell probably acted as UV shield or UV filter for loaded curcumin that afford slow release of curcumin and prolong the free radical formation protection property from topical application of various loaded curcumin lotions. Explanation on this EPR results may lie on that free curcumin could dispersed in lotions and some ingredients in formulation may play a role for penetration, but less or could not protected free curcumin degradation from UV irradiation. These results are agree well with data obtained by previous experiment, which showed the photostability

of loaded curcumin water suspension after photo exposed, while completely photodegraded of free curcumin in solution ethanol. In addition, previous investigations have shown that not only the radical protection capacity is important for the radical protection in skin due to irradiation, but also the optical properties of the lotions [92]. Using C-EC or C-ECMC lotions the particles could enhance the scattering properties and more light is reflected or absorbed within the lotion layer.

Skin and Hair Follicle Penetration of Curcumin-Loaded EC and ECMC Particles

Curcumin has already been used to examine the reservoir function of the stratum corneum [93], the distribution of topically applied substances within this layer [94], for follicle penetration [95] and to investigate the influence of different formulations of its skin penetration [96, 97]. Jung et al [95] compared liposomal loaded fluorescein and curcumin and determined relative follicular penetration depths. The relative penetration depths of the dyes, applied in the standard formulation, averaged 30% of the full follicle length during the whole observation period, whereas amphoteric and cationic liposomes reached an average relative penetration depth of approximately 70% of the full hair follicle length. Teichmann et al. [98] could show that a penetration of curcumin applied in the o/w microemulsion, into both the stratum corneum and the hair follicles, is improved compared to the application in an amphiphilic cream. Lipid layers and, presumably, the follicles seem to be the preferred pathways for the lipophilic dye applied in the microemulsion.

In this present study, the skin and hair follicle penetration experiments using freshly porcine ear skin were carried out to determine (i) the distribution of the loaded curcumin from the topically applied particles and (ii) the penetration depth of the particles across the skin or into the hair follicle. In figure 3.22, both water suspensions form revealed stronger fluorescent intensity of loaded curcumin particles than the lotions but no fluorescent signal of stratum corneum could observed (Table 3.9). Although, on the LSM images of C-EC-L1 and C-EC-L2 formulations, stratum corneum could observed, the fluorescent signal indicated that all C-EC lotions were more aggregated

than the C-ECMC lotions and less obvious fluorescent intensity than the C-ECMC lotions. LSM photograph of C-ECMC-L2 indicated the most penetration and stratum corneum could be clearly observed (Figure 3.22f). That means the o/w and w/o lotions could enhance the penetration of the two loaded curcumin particles into porcine skin.

Table 3.9 LSM Observation of various loaded curcumin formulations applied on porcine ear skin after 30 minutes penetration time

Sample	Aggregation	Fluorescent Intensity	Stratum corneum
C-EC-WS	+++	+++	-
C-ECMC-WS	+++	+++	-
C-EC-L1	++	+	+
C-EC-L2	++	++	++
C-ECMC-L1	+	++	++
C-ECMC-L2	+	+++	+++

+++ strong, ++ medium, + weak, - no
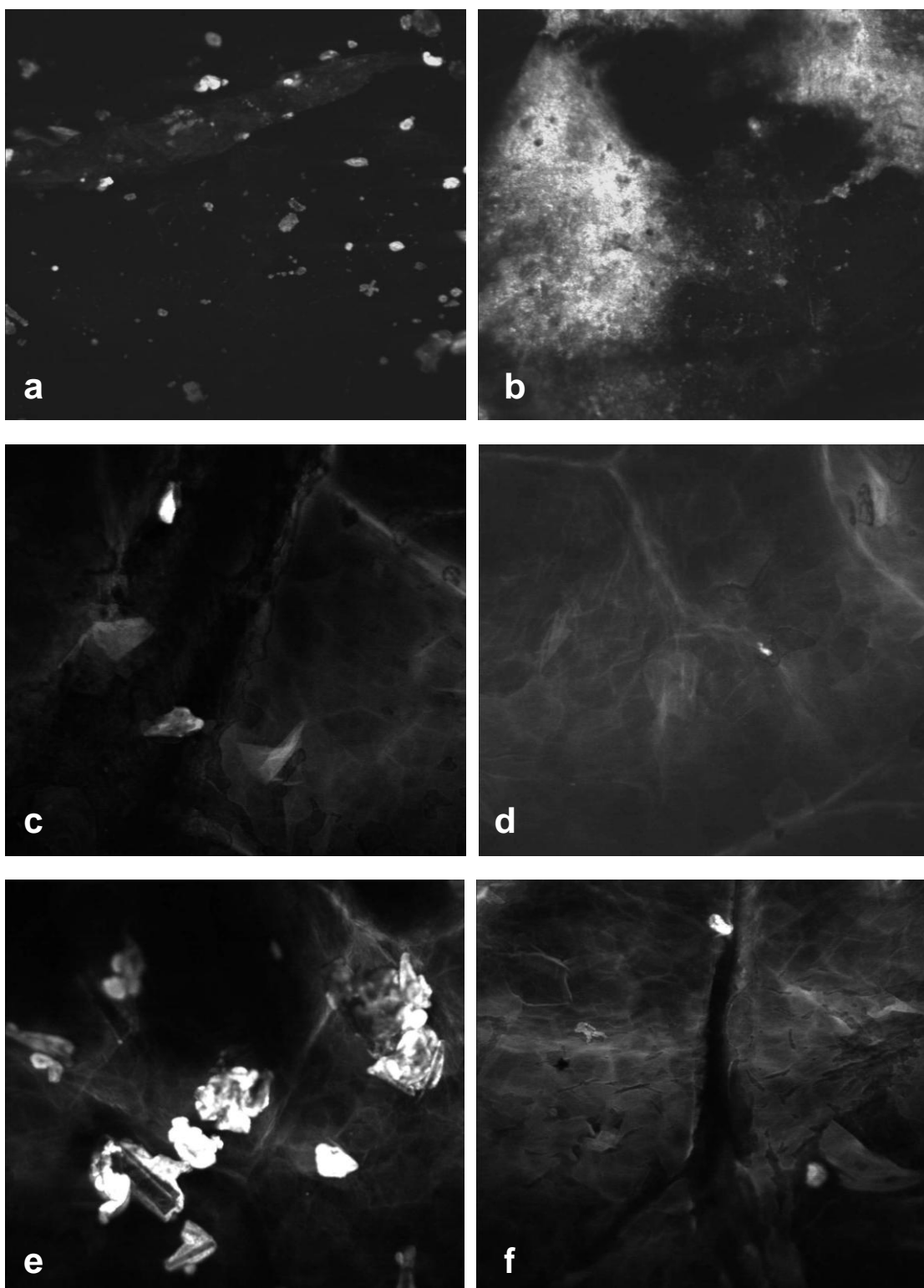
Figure 3.22 LSM photographs of a) C-EC-WS b) C-ECMC-WS c) C-EC-L1 d) C-ECMC-L1 e) C-EC-L2 and f) C-ECMC-L2, applied on porcine ear skin and observed after 30 minutes penetration time

Although, C-EC and C-ECMC were redispersed in water and water suspension could be easily generated, the particles were mostly aggregated and stacked mainly on the skin surface after application on pig ear skin as shown by LSM photographs. The ethyl cellulose and curcumin are strongly hydrophobic substances, but they did not penetrate into the stratum corneum. This could due to their particles size and their high aggregation behavior in water. C-ECMC-WS showed a little deeper penetration which could due to the smaller size of the particle. C-ECMC, in contrast to C-EC or because it was blended with the water soluble polymer (MC), showed less aggregation and a better dispersibility.

Figure 3.23 and 3.24 showed transmittant and fluorescent photographs of skin cryosectioned after application of water suspensions or lotions and allowed 60 min penetration time. Both lotions (lotions with C-EC and lotion with C-ECMC) showed a better distribution of curcumin and hair follicle penetration than water suspension formulations. The figure also revealed that C-ECMC enhances the skin penetration better than C-EC and L2 increases the penetration as well. Since, it is well known that oil phase in water in oil formulation is much more than oil in water formulation, therefore oil phase in L2 is higher than L1. Moreover, curcumin could soluble in the oily phase which would show a better distribution in Lotion 2 and a deeper penetration of C-EC-L2 compared to C-EC-L1. For C-ECMC, the water soluble MC part could enhance the penetration because it is known that slightly amphiphilic substances show the best penetration behavior [99]. Therefore the C-ECMC-L2 could show the highest penetration depth. However, we could not exclude that the particle decay in the formulation or on the skin. The penetration depths could be determined using this images and are presented in Table 3.10 and Figure 3.25.
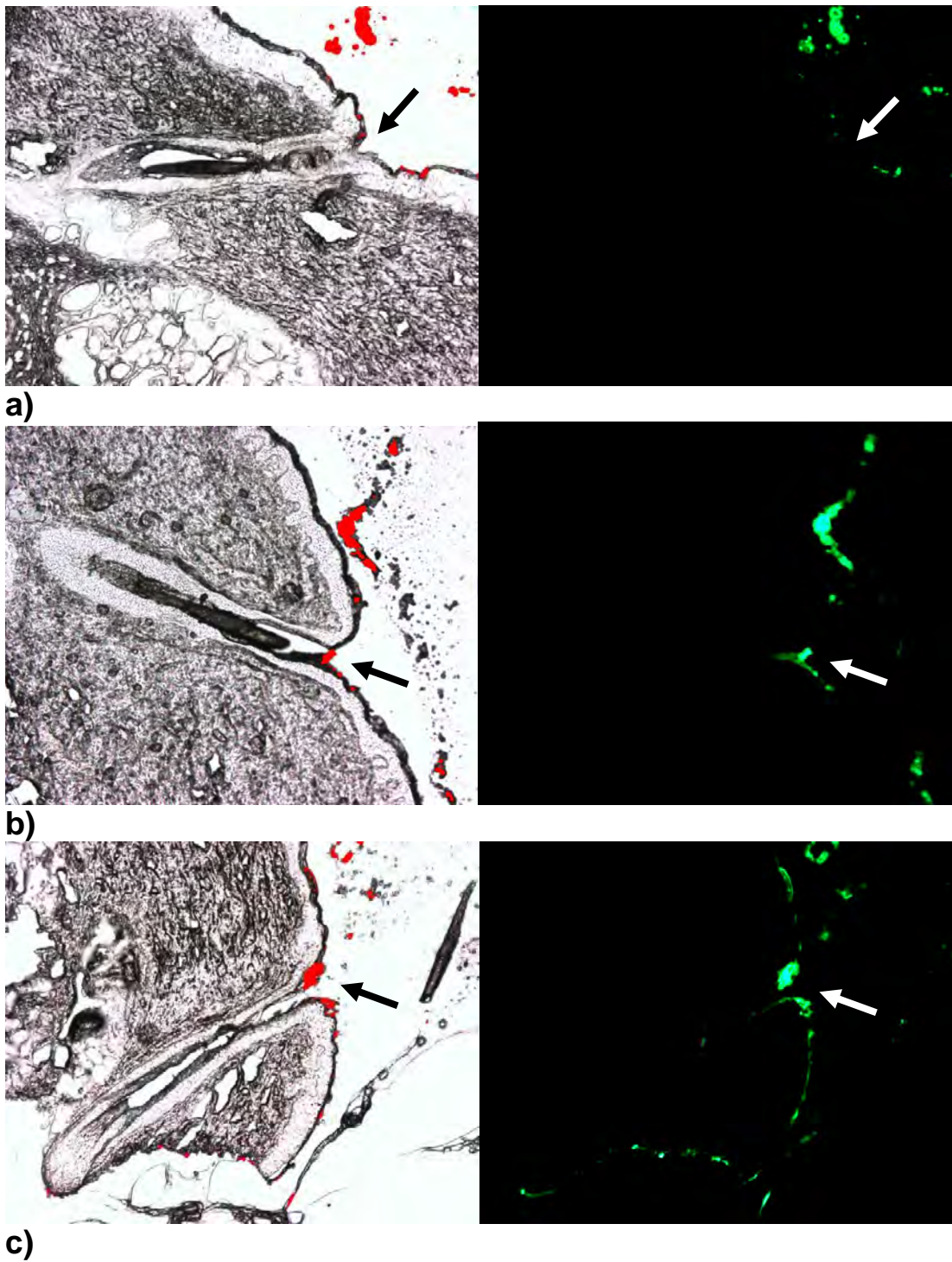
Figure 3.23 The distribution and hair follicle penetration of a) C-EC-WS, b) C-EC-L1 and c) C-EC-L2, applied on porcine ear skin and biopsied/cryosectioned after 60 minutes penetration time
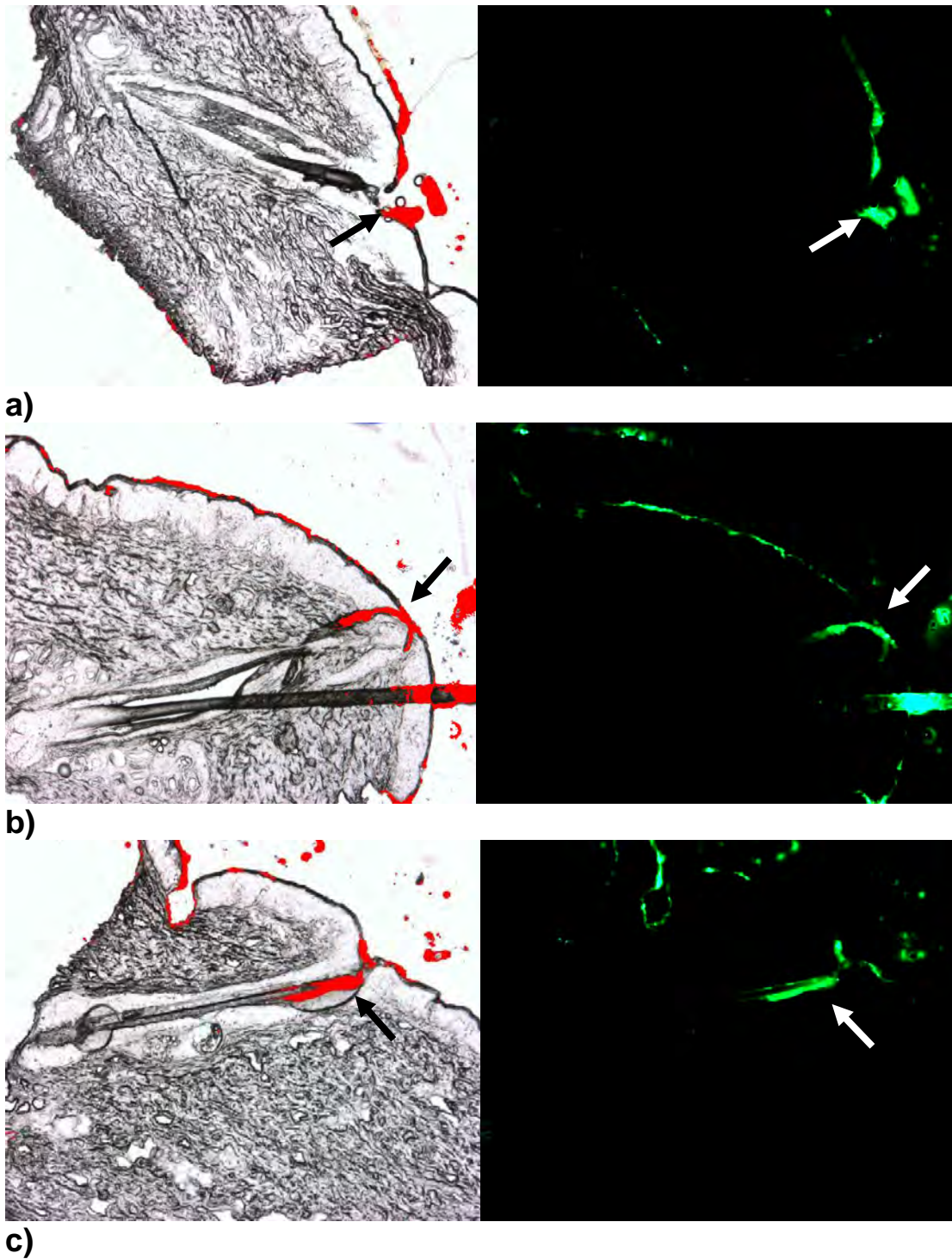
Figure 3.24 The distribution and hair follicle penetration of a) C-ECMC-WS, b) C-ECMC-L1 and c) C-ECMC-L2, applied on porcine ear skin and biopsied/cryosectioned after 60 minutes penetration time

Table 3.10 Skin and hair follicle penetration depths of various loaded curcumin formulations applied on pig ear skin and biopsied/cryosectioned after 60 minutes penetration time.

Curcumin loaded particles	Formulations	Penetration depth (µm)
C-EC	WS (water suspension)	100.66 ± 11.70
	L1 (O/W lotion)	280.95 ± 13.20
	L2 (W/O lotion)	367.91 ± 46.93
C-ECMC	WS (water suspension)	215.44 ± 16.08
	L1 (O/W lotion)	358.93 ± 39.21
	L2 (W/O lotion)	779.58 ± 48.11
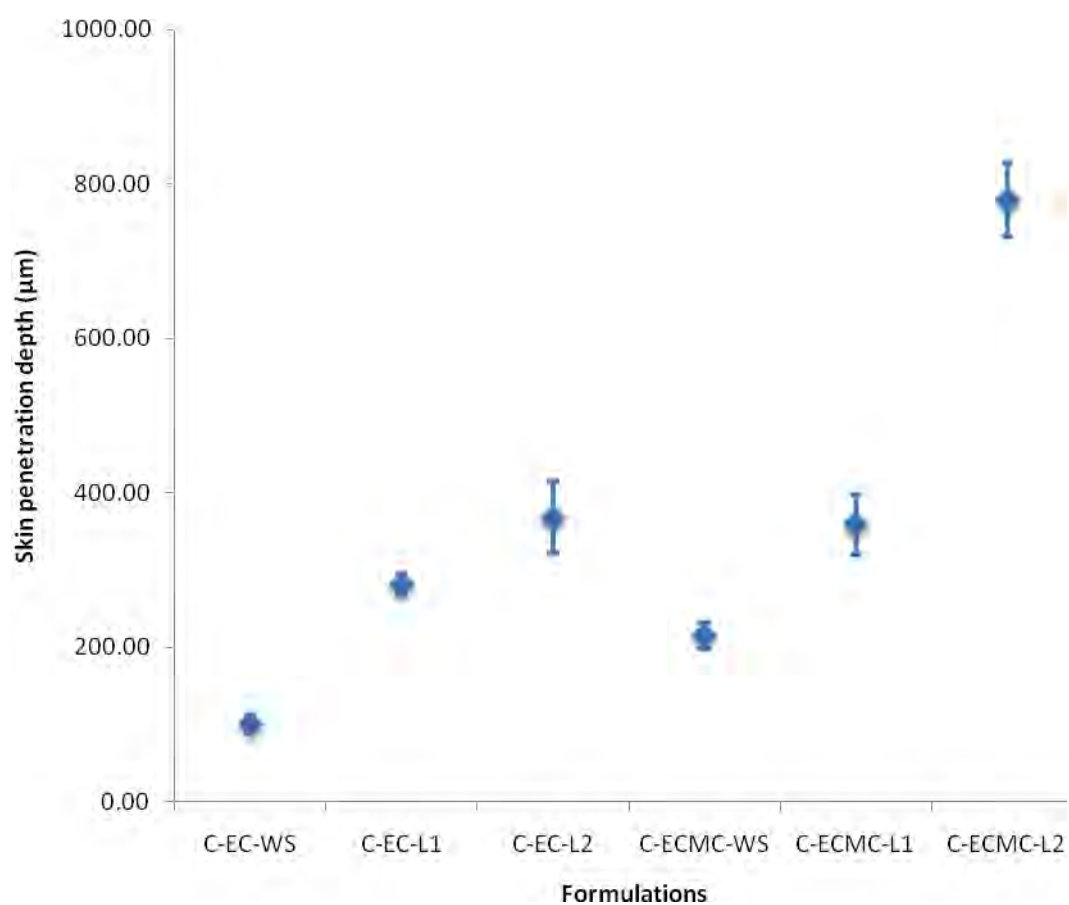
Figure 3.25 Skin penetration depths of the investigated formulations

With the exception of C-EC-L2 and C-ECMC-L1 the penetration depths of all formulations are significantly different ($p < 0.05$). Curcumin loaded particles in lotions showed a deeper hair follicle penetration and more adhesive force to the stratum corneum than water suspensions (101 ± 12 nm for C-EC-WS and 215 ± 16 nm for C-ECMC-WS). Lotion 2 shows significantly better penetration behavior than lotion 1, and C-ECMC significantly enhances the penetration compared to C-EC. The C-ECMC-L2 formulation resulted by far to the deepest hair follicle penetration of 780 nm $\pm$ 50 nm.

Transdermal Penetration of Curcumin-Loaded EC Particles by Suction Blister Technique

For preliminary study of topically application of curcumin loaded particles, only curcumin-loaded EC particles was evaluated in the present study. Transdermal penetration experiments using suction blister fluid from healthy volunteer skin were carried out to determine the release of curcumin from the topically applied particles across the skin. C-EC was dispersed in lotion base and was evaluated for the transdermal penetration of the loaded curcumin. To investigate the release of curcumin loaded within the particles after the particles were applied on the skin, the *in vivo* controlled release experiments were carried out by applying free curcumin and curcumin-loaded EC lotion on the blister roof (Figure 3.26). After 3h application time, curcumin in the SBF from volunteer skin was determined by UV–visible absorption analysis at 425 nm with the aids of a calibration curve constructed from a series of free curcumin solutions prepared in isotonic PBS (see calibration curve in appendix B). The absorption profile spectrum indicated the obvious release of curcumin from the particles (Figure 3.27). The curcumin content in SBF was compared with SBF without lotion application for each individual volunteer.
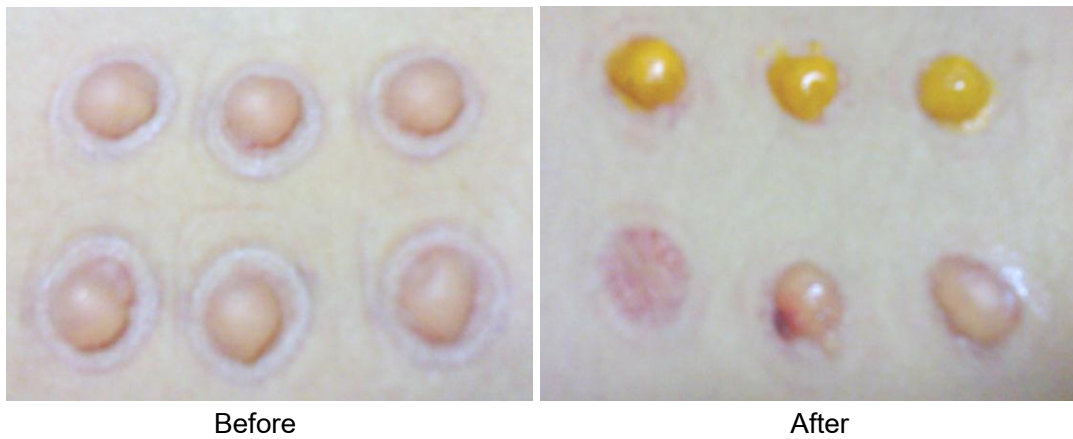
| Before | After |

Figure 3.26 The blister's roof of volunteer before and after sample application
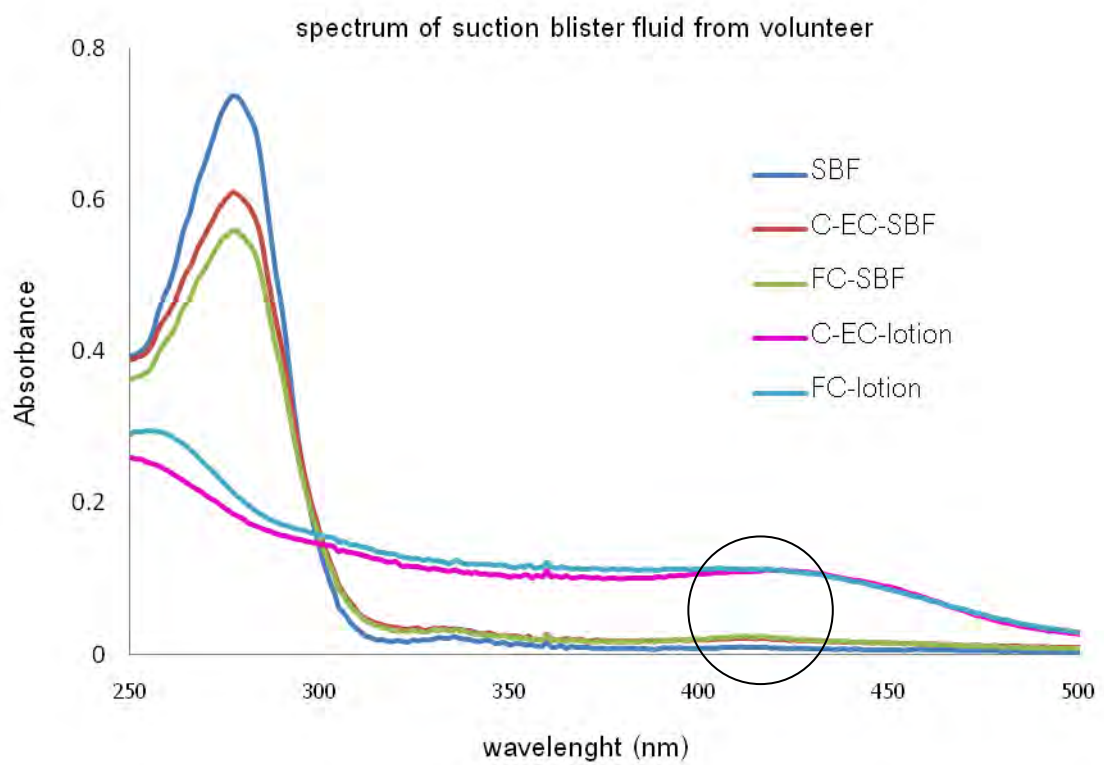
Figure 3.27 The absorption profile spectrum of curcumin in SBF from volunteer skin and lotion

Table 3.11 Concentration of curcumin in lotion samples and suction blister fluid

Sample	curcumin concentration (mg/ml)
free curcumin lotion	10
C-EC lotion	10
free curcumin in SBF	0.03
C-EC in SBF	0

It should be noted here that only about 0.3% of the free curcumin could transdermally penetrate into SBF after 3 h (Table 3.11). This indicated quite a slow transport of the curcumin molecules across the skin barrier. As a result, when the loaded curcumin was applied onto the human skin, it was not surprised to see even a smaller percentage of curcumin in the SBF after 3 h. Since the penetration of free curcumin was significantly faster than that of the loaded curcumin, EC particles possessed controlled release of curcumin during the topically applied state.

Previously, Lademann et al [70] compared excised human skin and porcine ear skin as tissue models for the analysis of follicular penetration and its prevention by barrier emulsions. They found that the preventive efficacy of the barrier emulsions could be significantly better investigated on porcine ear skin than on excised human skin. In this study, although curcumin in SBF from blister roof which applied with curcumin-loaded EC particle could not detected. This may be due to several factors that affect the skin penetration such as the concentration, formulation, biological factors of volunteers and the skin barrier properties. Nevertheless, *in vitro* skin and hair follicle penetration study significantly revealed the penetration of curcumin from both EC and ECMC particles could penetrated into stratum corneum and hair follicle of porcine ear skin. Therefore, porcine ear skin is showed as useful skin model for the development and optimization of topically applied drugs and cosmetic products. Moreover, it can be concluded that for the analysis of the follicular penetration porcine ear skin is more suitable *in vitro* model than the human skin.

CHAPTER IV

CONCLUSION

The encapsulation of curcumin into polymeric nanoparticles by solvent displacement using dialysis method was compared for five different polymers, namely; ethylcellulose (EC), methylcellulose (MC), poly(ethylene oxide)-4-methoxycinnamoylphthaloylchitosan (PCPLC), poly(vinylalcohol-co-vinyl-4-methoxycinnamate) with two degrees of 4-methoxy cinnamoyl substitution (PB4-I and PB4-II). Although all five polymers could effectively form curcumin-loaded nanoparticles with more than 90% encapsulation efficiency at the loading of 1:1 (w/w) polymer to curcumin ratio, only curcumin-loaded EC (C-EC) and ECMC (C-ECMC) particles showed no settling of the spheres in 10,000 ppm aqueous particle suspension after 8 months. The C-EC and C-ECMC nanoparticles did not deformed under freeze-drying at -80 $^{\circ}$C, low pressured superheated steam and vacuum drying at 8 kPa, 80 $^{\circ}$C, and the dry particles could be redispersed well in water. Spray-drying at 130 $^{\circ}$C although resulted in deformed particles, the deformed particles resumed their original spherical shapes upon redispersion in water. Photostability study indicated that the loaded curcumin was significantly more stable than free curcumin. The C-EC and C-ECMC particles also showed controlled release of the curcumin more quickly and higher than PCPLC, PB4-I and PB4-II polymers.

When C-EC and C-ECMC were orally administered to mice, as confirmed by blood curcumin quantification, slowly release curcumin into the blood circulation for up to 3 h, and as confirmed by SEM and stomach tissue analysis for curcumin, C-EC particles attached well to the gastric mucosa. In contrast, it was clear that although C-ECMC particles could attach to the gastric mucosa, the attachment was not as favorable as that seen for C-EC. In addition, C-ECMC released curcumin more quickly than C-EC did *in vitro* under an acidic condition and this could be attributed to the higher swelling nature and smaller size of the ECMC spheres compared to the EC

spheres. Although the improvement in the curcumin sustainability in blood attained by the use of C-ECMC nanoparticles was significant compared to free curcumin, it was not as great as that attained with C-EC nanoparticles. Excellent mucoadhesion of the self-assembled EC nanosparticles could be explained through the hydrophilic surface of the self-assembled particles.

In addition, the *in vitro* EPR results indicated that both C-EC and C-ECMC formulations significantly comparable with free curcumin radical formation protection capacity and more effective than free curcumin when applied on porcine ear skin. That means the nanoencapsulation system could play as a UV shield to protect the compound and remained the radical formation protection capacity of curcumin in an o/w and w/o lotion. Moreover, the C-EC and C-ECMC nanoparticles were applied in an o/w, w/o lotion and water suspension. The *in vitro* skin penetration was investigated on porcine ear skin using Laser fluorescent scanning microscope (LFSM). It was found that the o/w and w/o lotions enhanced the penetration of the two loaded curcumin into porcine ear skin via the hair follicle route and penetrate much deeper than the water suspension form, whereas the w/o enhanced the penetration better than the o/w lotion. The LFSM photographs indicated that hair follicle was the main transportation route. Likely, the loaded curcumin lotions was attached to stratum corneum and penetrated into hair follicle, curcumin bioactivity was probably reserved and then controlled release.

Furthermore, transdermal penetration experiments using suction blister fluid from healthy volunteer skin were carried out to determine the release of the loaded curcumin from the topically applied particles. Only about 0.3% of the free curcumin could transdermally penetrate into SBF after 3 h. This indicated a quite slow transport of the curcumin molecules across the skin barrier. Since the penetration of free curcumin was significantly faster than that of the loaded curcumin, EC particles possessed controlled release of curcumin during the topically applied state.

Finally, it could be concluded that two curcumin-loaded nanoparticles, C-EC and C-ECMC, were successfully fabricated through a self-assembling mechanism with an excellent loading capacity and encapsulation efficiency. The obtained C-EC and C-ECMC possessed a high curcumin loading of close to 50% (wt curcumin/ total wt) and were around 300 and 200 nm diameter-particles, respectively, with a hydrophilic surface charge approximately -30 mV in water at pH 5.5, so disperse well in water. The loaded curcumin molecules still possessed free radical scavenging activity. Hence, the encapsulation of curcumin into safe, inexpensive and FDA approved commercially edible polymer, EC and MC polymers, promisingly improves the physicochemical properties of curcumin and effectively enhances its bioavailability, ready to use in pharmaceutical and cosmetic formulations and enhances skin penetration of curcumin via hair follicle route.

REFERENCES

[1] Hatcher, H., Planalp, R., Cho, J., Torti, F. M., and Torti, S. V. Curcumin: From ancient
        medicine to current clinical trials. Cell Mol. Life Sci. 65 (2008): 1631-1652.

[2] Shishodia, S., Sethi, G., and Aggarwal, B. B. Curcumin: Getting back to the roots.
        Ann. N.Y. Acad. Sci. 1056 (2005): 206-217.

[3] Anand, P., Kunnumakkara, A. B., and Newman, R. A. Bioavailability of curcumin:
        Problems and promises. Mol. Pharmaceutics. 4 (2007): 807-818.

[4] Kreuter, J. Nanoparticles. In J. Kreuter (ed.), Colloidal drug delivery systems,
        pp.219-342. New York: Marcel Dekker, 1994.

[5] Mohanraj, V. J., and Chen, Y. Nanoparticles – A review. Trop. J. Pharm. Res.
        5 (2006): 561-573.

[6] Pinto, R. C., Neufeld, R. J., Ribeiro, A. J., and Veiga, F. Nanoencapsulation I.
        Methods for preparation of drug-loaded polymeric nanoparticles.
        Nanomed-Nanotechnol. 2 (2006): 8-21.

[7] Walters, K. A., and Roberts, M. S. The structure and function of skin. In K. A. Walters
        (ed.), Dermatological and transdermal formulations: Drugs and the
        pharmaceutical sciences, pp.1-39. New York: Marcel Dekker, 2002.

[8] Luengo, C. J. Models for skin absorption and skin toxicity testing. In C. Ehrhardt and
        K.J. Kim (eds.), Drug absorption studies, pp.3-33. New York: Springer, 2008.

[9] Washington, N., Washington, C., and Wilson, C. G. Transdermal drug delivery.
        In N. Washington (ed.), Physiological pharmaceutics: Barriers to drug
        absorption, pp.181-198. London: Taylor and Francis, 2001.

[10] Moghimi, H. R., Williams, A. C., and Barry, B. W. A lamellar matrix model for
        stratum corneum intercellular lipids. II. Effect of geometry of the stratum corneum
        on permeation of model drugs 5-fluorouracil and oestradiol. Int. J. Pharm.
        131 (1996): 119.

[11] Naik, A., Kalia, Y. N., and Guy, R. H. Transdermal drug delivery: overcoming the skin's barrier function. Pharm. Sci. Technolo. Today. 3 (2000): 318-326.

[12] Cevc, G., and Vierl, U. Nanotechnology and the transdermal route: A state of the art review and critical appraisal. J. Control. Release. 141 (2010): 277-299.

[13] Roberts, M. S., and Cross, S. E. Skin transport. In K. A. Walters (ed.), Dermatological and transdermal formulations: Drugs and the Pharmaceutical Sciences, pp.89-195. New York: Marcel Dekker, 2002.

[14] Luengo Contreras, E. J. Human skin drug delivery using biodegradable PLGA nanoparticles. Doctoral dissertation, Department of Pharmacy Faculty of Natural Sciences and Technology Saarland University, 2007.

[15] Hadgraft, J. Skin deep. Eur. J. Pharm. Biopharm. 58 (2004): 291-299.

[16] Langer, R. Transdermal drug delivery: past progress, current status, and future prospects. Adv. Drug Deliv. Rev. 56 (2004): 557-558.

[17] Lademann, J., et al. Hair follicles - An efficient storage and penetration pathway for topically applied substances. Skin Pharmacol. Physiol. 21 (2008):150-155.

[18] Lademann, J., et al. Hair Follicles - A long-term reservoir for drug delivery. Skin Pharmacol. Physiol. 19 (2006): 232-236.

[19] Lademann, J., et al. Nanoparticles - An efficient carrier for drug delivery into the hair follicles. Eur. J. Pharm. Biopharm. 66 (2007): 159-164.

[20] Kumar, S., Dubey, K. K., Tripathi, S., Fujii, M. and Misra, K. Design and synthesis of curcumin-bioconjugates to improve systemic delivery. Nucl. Acids Symp. Ser. 44 (2000): 75-76.

[21] Venkateswarlu, M., Ramachandra, S., and Subbaraju, G. V. Synthesis and biological evaluation of polyhydroxycurcuminoids. Bioorg. Med. Chem. 13 (2005): 6374-6380.

[22] Safavy, A., et al. Design and development of water-soluble curcumin conjugates as potential anticancer agents. J. Med. Chem. 50 (2007): 6284-6288.

[23] Kim, C. Y., Bordenave, N., Ferruzzi, M. G., Safavy, A., and Kim, K. H. Modification of curcumin with polyethylene glycol enhances the delivery of curcumin in preadipocytes and its antiadipogenic property. J. Agric. Food Chem. 59 (2011): 1012-1019.

[24] Tønnesen, H. H., Masson, M., and Loftsson, T. Studies of curcumin and curcuminoids. XXVII. Cyclodextrin complexation: solubility, chemical and photochemical stability. Int. J. Pharm. 244 (2002): 127-135.

[25] Baglole, K. N., Patricia, G. B., and Brian, D. W. Fluorescence enhancement of curcumin upon inclusion into parent and modified cyclodextrins. J. Photochem. Photob. A: Chemistry. 173 (2005): 230-237.

[26] Hegge, A. B., Schüller, R. B., Kristensen, S., and Tønnesen, H. H. In vitro release of curcumin from vehicles containing alginate and cyclodextrin. Studies of curcumin and curcuminoides. XXXIII. Pharmazie. 63 (2008): 585-592.

[27] Maiti, K., Mukherjee, K., Gantait, A., Saha, B. P., and Mukherjee, P. K. Curcumin–phospholipid complex: Preparation, therapeutic evaluation and pharmacokinetic study in rats. Int. J. Pharm. 330 (2007): 155-163.

[28] Sneharani, A. H., Karakkat, J. V., Singh, S. A., and Rao, A. G. Interaction of curcumin with β-lactoglobulin-stability, spectroscopic analysis, and molecular modeling of the complex. J. Agric. Food Chem. 58 (2010): 11130-11139.

[29] Tønnesen, H. H. Solubility, chemical and photochemical stability of curcumin in surfactant solutions. Pharmazie. 57 (2002): 820-824.

[30] Wang, X., Jiang, Y., Wang, Y. W., Huang, M. T., Ho, C. T., and Huang, Q. Enhancing, anti-inflammation activity of curcumin through O/W nanoemulsions. Food Chem. 108 (2008): 419-424.

[31] Cui, J., et al. Enhancement of oral absorption of curcumin by self-microemulsifying drug delivery systems. Int. J. Pharm. 371 (2009): 148-155.

[32] Lin, C. C., Lin, H. Y., Chen, H. C., Yu, M. W., and Lee, M. H. Stability, and characterisation of phospholipid-based curcumin-encapsulated microemulsions. Food Chem. 116 (2009): 923-928.

[33] Chen, C., et al. An in vitro study of liposomal curcumin: Stability, toxicity and biological activity in human lymphocytes and Epstein-Barr virus-transformed human B-cells. Int. J. Pharm. 366 (2009): 133-139.

[34] Takahashi, M., Uechi, S., Takara, K., Asikin, Y., and Wada, K. Evaluation of an oral carrier system in rats: bioavailability and antioxidant properties of liposome-encapsulated curcumin. J. Agric. Food Chem. 57 (2009): 9141-9146.

[35] Patel, R., Singh, S. K., Singh, S., Sheth, N. R., and Gendle, R. Development and characterization of curcumin loaded transfersome for transdermal delivery. J. Pharm. Sci. & Res. 1 (2009): 71-80.

[36] Tiyaboonchai, W., Tungpradit, W., Plianbangchang, P. Formulation and characterization of curcuminoids loaded solid lipid nanoparticles. Int. J. Pharm. 337 (2007): 299-306.

[37] Onoue, S., et al. Formulation, design and photochemical studies on nanocrystal solid dispersion of curcumin with improved oral bioavailability. J. Pharm. Sci. 99 (2010): 1871-1881.

[38] Aziz, H. A., Peh, K. K., and Tan, Y. T. F. Solubility of core materials in aqueous polymeric solution effect on microencapsulation of curcumin. Drug Dev. Ind. Pharm. 33 (2007): 1263-1272.

[39] Wang, Y., Lu, Z., Lv, F., and Bie, X. Study on microencapsulation of curcumin pigments by spray drying. Eur. Food. Res. Technol. 229 (2009): 391-396.

[40] Bisht, S., et al. Polymeric nanoparticle-encapsulated curcumin ("nanocurcumin"): a novel strategy for human cancer therapy. J. Nanobiotechnology. 5 (2007): 3.

[41] Sahu, A., Bora, U., Kasoju, N., and Goswami, P. Synthesis of novel biodegradable and self-assembling methoxy poly(ethylene glycol)–palmitate nanocarrier for curcumin delivery to cancer cells. Acta Biomater. 4 (2008): 1752-1761.

[42] Shaikh, J., Ankola, D. D., Beniwal, V., Singh, D., and Kumar, M. N. Nanoparticle, encapsulation improves oral bioavailability of curcumin by at least 9-fold when compared to curcumin administered with piperine as absorption enhancer. Eur. J. Pharm. Sci. 37 (2009): 223-230.

[43] Das, R. K., Kasoju, N., and Bora, U. Encapsulation of curcumin in alginate-chitosan-pluronic composite 3 nanoparticles for delivery to cancer cells. Nanomed-Nanotechnol. 6 (2010): 153-160.

[44] Anand, P., et al. Design of curcumin-loaded PLGA nanoparticles formulation with enhanced cellular uptake, and increased bioactivity in vitro and superior bioavailability in vivo. Biochem Pharmacol. 79 (2010): 330-338.

[45] Yen, F. L., Wu, T. H., Tzeng, C. W., Lin. L. T., and Lin. C. C. Curcumin nanoparticles improve the physicochemical properties of curcumin and effectively enhance its antioxidant and antihepatoma activities. J. Agric. Food Chem. 58 (2010): 7376-7382.

[46] Sakuma, S., et al. Behavior of mucoadhesive nanoparticles having hydrophilic polymeric chains in the intestine. J. Control. Release. 81 (2002): 281-290.

[47] Umamaheshwari, R. B., Ramteke, S., and Jain, N. K. Anti-Helicobacter pylori effect of mucoadhesive nanoparticles bearing amoxicillin in experimental gerbils model. AAPS Pharm. Sci. Tech. 5 (2004): 60-68.

[48] Sarmento, B., Ribeiro, A., Veiga, F., Sampaio, P., Neufeld, R., and Ferreira, D. Alginate/chitosan nanoparticles are effective for oral insulin delivery. Pharm Res. 24 (2007): 2198-2206.

[49] Bravo-Osuna, I., Vauthier, C., Farabollini, A., Palmier, G. F., and Ponchel, G. Mucoadhesion mechanism of chitosan and thiolated chitosan-poly(isobutyl cyanoacrylate) core-shell nanoparticles. Biomaterials. 28 (2007): 2233-2243.

[50] Thirawong, N., Thongborisute, J., Takeuchi, H., and Sriamornsak, P. Improved intestinal absorption of calcitonin by mucoadhesive delivery of novel pectin-liposome nanocomplexes. J. Control. Release. 125 (2008): 236-245.

[51] Moghaddam, F. A., Atyabi, F., and Dinarvand, R. Preparation and in vitro
      evaluation of mucoadhesion and permeation enhancement of thiolated chitosan-
      pHEMA core-shell nanoparticles. Nanomedicine. 5 (2009): 208-215.

[52] Chang, C. H., et al. Nanoparticles incorporated in pH-sensitive hydrogels as
      amoxicillin delivery for eradication of Helicobacter pylori. Biomacromolecules.
      11 (2010): 133-142.

[53] Makhlof, A., Werle, M., Tozuka, Y., and Takeuchi, H. A mucoadhesive
      nanoparticulate system for the simultaneous delivery of macromolecules
      and permeation enhancers to the intestinal mucosa. J. Control. Release.
      149 (2011): 81-88.

[54] Alvarez-Román, R., Naik, A., Kalia, Y. N., Guy, R. H., and Fessi, H. Enhancement
      of topical delivery from biodegradable nanoparticles. Pharm. Res. 21 (2004):
      1818-1825.

[55] Alvarez-Román, R., Naik, A., Kalia, Y. N., Guy, R. H., and Fessi, H. Skin
      penetration, and distribution of polymeric nanoparticles. J. Control. Release.
      99 (2004): 53-62.

[56] Olvera-Martínez, B. I., Cázares-Delgadillo, J., Calderilla-Fajardo, S. B., Villalobos-
      García, R., Ganem-Quintanar, A., and Quintanar-Guerrero, D. Preparation of
      polymeric nanocapsules containing octyl methoxycinnamate by the
      emulsification-diffusion technique: penetration across the stratum corneum.
      J. Pharm. Sci. 94 (2005): 1552-1559.

[57] Vogt, A., et al. 40 nm, but not 750 or 1,500 nm, nanoparticles enter epidermal
      CD1a+ cells after transcutaneous application on human skin. J. Invest. Dermatol.
      126 (2006): 1316-1322.

[58] Lademann J., et al. Nanoparticles – An efficient carrier for drug delivery into the
      hair follicles. Eur. J. Pharm. Biopharm. 66 (2007): 159-164.

[59] Liu, W., Hu, M., Liu, W., Xue, C., Xu, H., and Yang, X. Investigation of the carbopol gel of solid lipid nanoparticles for the transdermal iontophoretic delivery of triamcinolone acetonide acetate. Int. J. Pharm. 364 (2008): 135-141.

[60] Ghouchi Eskandar, N., Simovic, S., and Prestidge, C. A. Nanoparticle coated submicron emulsions: sustained in-vitro release and improved dermal delivery of all-trans-retinol. Pharm. Res. 26 (2009): 1764-1775.

[61] Zhang, W., et al. Penetration and distribution of PLGA nanoparticles in the human skin treated with microneedles. Int. J. Pharm. 402 (2010): 205-212.

[62] Senzui, M., Tamura, T., Miura, K., Ikarashi, Y., Watanabe, Y., and Fujii, M. Study on penetration of titanium dioxide (TiO(2)) nanoparticles into intact and damaged skin in vitro. J. Toxicol. Sci. 35 (2010): 107-113.

[63] Zhao, Y., Brown, M. B., and Jones, S. A. The effects of particle properties on nanoparticle drug retention and release in dynamic minoxidil foams. Int. J. Pharm. 383 (2010): 277-284.

[64] Schlupp, P., et al. Drug release and skin penetration from solid lipid nanoparticles and a base cream: a systematic approach from a comparison of three glucocorticoids. Skin Pharmacol. Physiol. 24 (2011): 199-209.

[65] Anumansirikul, N., Wittayasuporn, M., Klinubol P., Tachaprutinun A., and Wanichwecharungruang S. P. UV-screening chitosan nanocontainers: increasing the photostability of encapsulated materials and controlled release. Nanotechnology. 19 (2008): 205101-205109.

[66] Luadthong, C., Tachaprutinun, A., and Wanichwecharungruang, S. P. Synthesis and characterization of micro/nanoparticles of poly(vinylalcohol-co-vinylcinnamate) derivatives. Eur. Polym. J. 44 (2008): 1285-1295.

[67] Devahastin, S., Suvarnakuta, P., Soponronnarit, S., and Mujumdar A. S. A comparative study of low-pressure superheated steam and vacuum drying of a heat-sensitive material. Drying Technol. 22 (2004): 1845-1867.

[68] Suwannateep, N., Banlunara, W., Wanichwecharungruang, S. P., Chiablaem, K., Lirdprapamongkol, K., and Svasti, J. Mucoadhesive curcumin nanospheres: Biological activity, adhesion to stomach mucosa and release of curcumin into the circulation. J. Control. Release. (2011), doi:10.1016/j.jconrel.2011.01.011

[69] Meinke, M., Haag, S., Groth, N., Klein, F., Sterry, W., and Lademann, J. Method for detection of free radicals in skin by EPR spectroscopy after UV irradiation. SOFW. 3 (2008): 2-10.

[70] Lademann, J., et al. Comparison of two in vitro models for the analysis of follicular penetration and its prevention by barrier emulsions. Eur. J. Pharm. Biopharm. 72 (2009): 600-604.

[71] Savage, A. B. In H. F. Mark, N. G. Gaylord, and N. M. Bibles (eds.), Encyclopedia of Polymer Science and Technology, Vol. 3, pp.459-492. New York: Wiley-Interscience, 1965.

[72] The Dow Chemical Co., Ethocel, ethylcellulose polymers technical handbook [Online]. (n.d.). Available from: http://msdssearch.dow.com/PublishedLiterature DOWCOM/dh_004f/0901b8038004fb7c.pdf?filepath=/192-00818.pdf&fromPage =GetDoc [2011, January 28]

[73] Rekhi, G. S., and Jambhekar, S. S. Ethylcellulose – A polymer review. Drug Dev. Ind. Pharm. 21 (1995): 61-77.

[74] Feller, R. L., and Wilt, M. Evaluation of cellulose ethers for conservation. 2nd ed. USA: J. Paul Getty Trust, 1993.

[75] Verhoeven, E., De Beer, T. R., Schacht, E., Van den Mooter, G., Remon, J. P., and Vervaet, C. Influence of polyethylene glycol/polyethylene oxide on the release characteristics of sustained-release ethylcellulose mini-matrices produced by hot-melt extrusion: in vitro and in vivo evaluations. Eur. J. Pharm. Biopharm. 72 (2009): 463-70.

[76] Jelvehgari, M., Valizadeh, H., Rezapour, M., and Nokhodchi, A. Control of encapsulation efficiency in polymeric microparticle system of tolmetin. Pharm. Dev. Technol. 15 (2010): 71-79.

[77] Morales, M. E., Ruiz, M. A., López, G., and Gallardo, V. Development of oral suspensions of microparticles of ethylcellulose with tramadol. Drug Dev. Ind. Pharm. 36 (2010): 885-92.

[78] Sansukcharearnpon, A., Wanichwecharungruang, S., Leepipatpaiboon, N., Kerdcharoen, T., and Arayachukeat, S. High loading fragrance encapsulation based on a polymer-blend: preparation and release behavior. Int. J. Pharm. 391 (2010): 267-273.

[79] Tachaprutinun, A., Udomsup, T., Luadthong, C., and Wanichwecharungruang, S. Preventing the thermal degradation of astaxanthin through nanoencapsulation. Int. J. Pharm. 374 (2009): 119-24.

[80] Ravikumara, N. R., Madhusudhan, B., Nagaraj, T. S., Hiremat, S. R., and Raina, G. Preparation and evaluation of nimesulide-loaded ethylcellulose and methylcellulose nanoparticles and microparticles for oral delivery. J. Biomater. Appl. 24 (2009): 47-64.

[81] Chen, S., Wang, Y., and Wu, G. Preparation and characterization of ampicillin loaded ethylcellulose nanospheres. Sheng Wu Yi Xue Gong Cheng Xue Za Zhi. 22 (2005): 60-65.

[82] Arayachukeat, S., Wanichwecharungruang, S. P., and Tree-Udom, T. Retinyl acetate-loaded nanoparticles: dermal penetration and release of the retinyl acetate. Int. J. Pharm. 404 (2011): 281-288.

[83] Zheng, R., and Liu, G. Water-dispersible, oil-filled, ABC, triblock, copolymer, vesicles and nanocapsules. Macromolecules. 40 (2007): 5116-5121.

[84] Muller, R. H., Jacobs, C., and Kayser, O. Nanosuspensions as particulate drug formulations in therapy rationale for development and what we can expect for the future. Adv. Drug Deliv. Rev. 47 (2001): 3-19.

[85] Wang, Y. J., et al. Stability of curcumin in buffer solutions and characterization of its degradation products. J. Pharm. Biomed. Anal. 15 (1997): 1867-1876.

[86] Pfeiffer, E., Hohle, S., Solyom, A. M., and Metzler, M. Studies on the stability of turmeric constituents. J. Food Eng. 56 (2003): 257-259.

[87] Shaikh, J., Ankola, D. D., Beniwal, V., Singh, D., and Kumar, M. N. Nanoparticle, encapsulation improves oral bioavailability of curcumin by at least 9-fold when compared to curcumin administered with piperine as absorption enhancer. Eur. J. Pharm. Sci. 37 (2009): 223-230.

[88] Wahlstrom B., and Blennow G. A study on the fate of curcumin in the rat. Acta Pharmacol. Toxicol. 43 (1978): 86-92.

[89] Sharma, R. A., et al. Pharmacodynamic and pharmacokinetic study of oral curcuma extract in patients with colorectal cancer. Clin. Cancer Res. 7 (2001): 1894-1900.

[90] Maiti, K., Mukherjee, K., Gantait, A., Saha, B. P., and Mukherjee, P. K. Curcumin–phospholipid complex: preparation, therapeutic evaluation and pharmacokinetic study in rats. Int. J. Pharm. 330 (2007): 155-163.

[91] Bovet, C., and Barron, A. EPR Spectroscopy: An overview [Online]. 2009. Available from: http://cnx.org/content/m22370/1.3/ [2011, February 17]

[92] Meinke, M. C., Haag, S. F., Schanzer, S., Groth, N., Gersonde, I., and Lademann, J. Radical protection by sunscreens in the infrared spectral range. Photochem. Photobiol. 87 (2011): 452-456.

[93] Jacobi, U., Waibler, E., Sterry, W., and Lademann, J. In vivo determination of the long-term reservoir of the horny layer using laser scanning microscopy. Laser Phys. 15 (2005): 565-569.

[94] Weigmann, H. J., et al. Development of a spectroscopic method for the ex vivo determination of the protection efficacy of sunscreens. Laser Phys. 14 (2004): 497-501.

[95] Jung, S., et al. Innovative liposomes as a transfollicular drug delivery system: penetration into porcine hair follicles. J. Invest. Dermatol. 126 (2006): 1728-1732.

[96] Patel, N. A., Patel, N. J., and Patel, R. P. Formulation and evaluation of curcumin gel for topical application. Pharm. Dev. Technol. 14 (2009): 80-89.

[97] Suhaimi, H., Ahmad, F. B., and Friberg, S. E. Curcumin in a model skin lotion formulation. J. Pharm. Sci. 84 (1995): 376-380.

[98] Teichmann, A., et al. Comparison of stratum corneum penetration and localization of a lipophilic model drug applied in an o/w microemulsion and an amphiphilic cream. Eur. J. Pharm. Biopharm. 67 (2007): 699-706.

[99] Frum, Y., Bonner, M. C., Eccleston, G. M., and Meidan, V. M. The influence of drug partition coefficient on follicular penetration: in vitro human skin studies. Eur. J. Pharm. Sci. 30 (2007): 280-287.
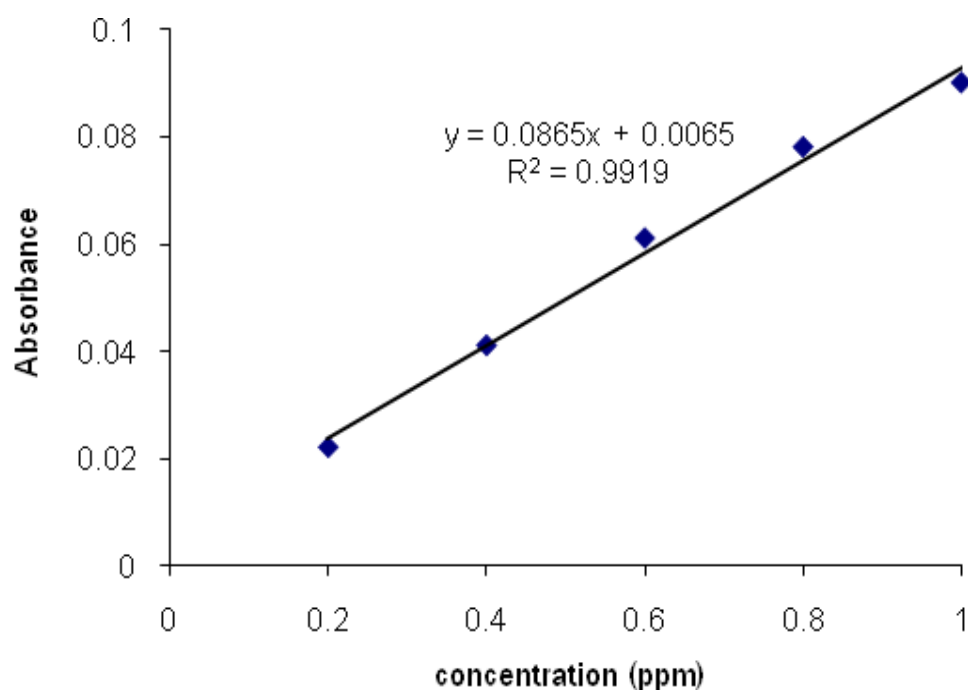
APPENDICES

APPENDIX A

Calculation of Encapsulation Efficiency (%EE), Loading of Curcumin (%w/w) and Final
Curcumin Concentration in Curcumin-Loaded Suspension
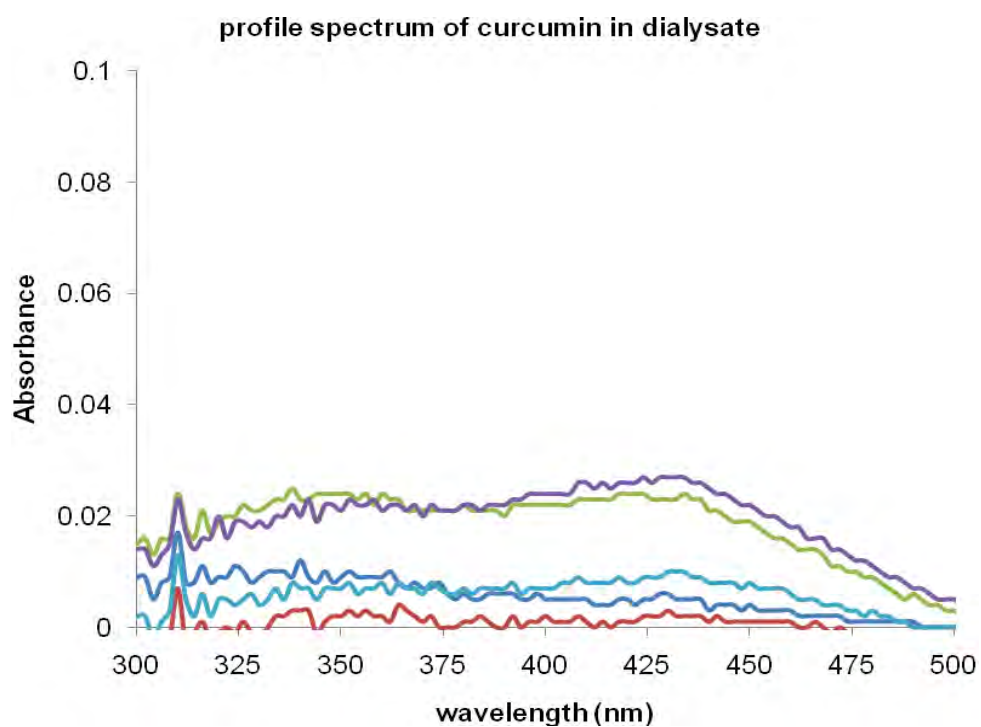
profile spectrum of curcumin in dialysate

Calibration curve of standard curcumin in ethanol

$y = 0.0865x + 0.0065$
$R^2 = 0.9919$

By plotting a graph between absorbance and concentration of standard curcumin solutions, a linear relationship was obtained and used for calculation of concentration of curcumin.

1. % Encapsulation Efficiency (%EE)

$$\%EE = \frac{\text{amount of curcumin used} - \text{amount of curcumin found in dialysate}}{\text{amount of curcumin used}} \times 100$$

C-EC: curcumin used   =   30   mg

curcumin found in dialysate   =   0.399   mg

%EE   = $\dfrac{30 - 0.399}{30}$ x 100

=   98.67   %

C-ECMC: curcumin used   =   30   mg

curcumin found in dialysate   =   0.663   mg

%EE   = $\dfrac{30 - 0.663}{30}$ x 100

=   97.79   %

C-PCPLC: curcumin used   =   30   mg

curcumin found in dialysate   =   1.014   mg

%EE   = $\dfrac{30 - 1.014}{30}$ x 100

=   96.62   %

C-PB4=I: curcumin used   =   30   mg

curcumin found in dialysate   =   2.634   mg

%EE   = $\dfrac{30 - 2.634}{30}$ x 100

=   91.22   %

C-PB4-II: curcumin used   =   30   mg

              curcumin found in dialysate   =   2.493   mg

$$\%EE = \frac{30 - 2.493}{30} \times 100$$

$$= 91.69 \ \%$$

2. % loading (w/w)

$$\% \ loading = \frac{amount \ of \ curcumin \ encapsulated}{amount \ of \ curcumin \ used + amount \ of \ polymer \ used} \times 100$$

C-EC: curcumin encapsulated   =   29.60   mg

       curcumin used   =   30   mg

       polymer used   =   30   mg

$$\% \ loading = \frac{29.60}{30+30} \times 100$$

$$= 49.34 \ \%$$

C-ECMC: curcumin encapsulated   =   29.34   mg

              curcumin used   =   30   mg

              polymer used   =   30   mg

$$\% \ loading = \frac{29.34}{30+30} \times 100$$

$$= 48.90 \ \%$$

C-PCPLC: curcumin encapsulated   =   28.99   mg

              curcumin used   =   30   mg

              polymer used   =   30   mg

$$\% \ loading = \frac{28.99}{30+30} \times 100$$

$$= 48.31 \ \%$$

C-PB4-I: curcumin encapsulated   =   27.37 mg

             curcumin used   =   30 mg

             polymer used   =   30 mg

$$\% \text{ loading} = \frac{27.37}{30+30} \times 100$$

$$= 45.61 \ \%$$

C-PB4-II: curcumin encapsulated   =   27.51 mg

             curcumin used   =   30 mg

             polymer used   =   30 mg

$$\% \text{ loading} = \frac{27.51}{30+30} \times 100$$

$$= 45.85 \ \%$$

### 3. Final Curcumin Concentration in Curcumin-Loaded Suspension

$$\text{Curcumin concentration (ppm)} = \frac{\text{weight of loaded curcumin (mg)}}{\text{final volume of the obtained suspension (ml)}} \times 1000$$

C-EC: curcumin encapsulated   =   29.60 mg

             final volume   =   20 ml

   Curcumin concentration   = $\dfrac{29.60}{20} \times 1000$

$$= 1480 \ \text{ppm}$$

C-ECMC: curcumin encapsulated   =   29.34 mg

             final volume   =   20 ml

             Curcumin concentration   = $\dfrac{29.34}{20} \times 1000$

$$= 1467 \ \text{ppm}$$

C-PCPLC: curcumin encapsulated   =   28.99   mg

final volume   =   20   ml

Curcumin concentration   = $\frac{28.99}{20}$ x 1000

=   1450   ppm

C-PB4-I: curcumin encapsulated   =   27.37   mg

final volume   =   20   ml

Curcumin concentration   = $\frac{27.37}{20}$ x 1000

=   1369   ppm

C-PB4-II: curcumin encapsulated   =   27.51   mg

final volume   =   20   ml

Curcumin concentration   = $\frac{27.51}{20}$ x 1000

=   1376   ppm

Calculation of % Photostability of Curcumin-Loaded Particles
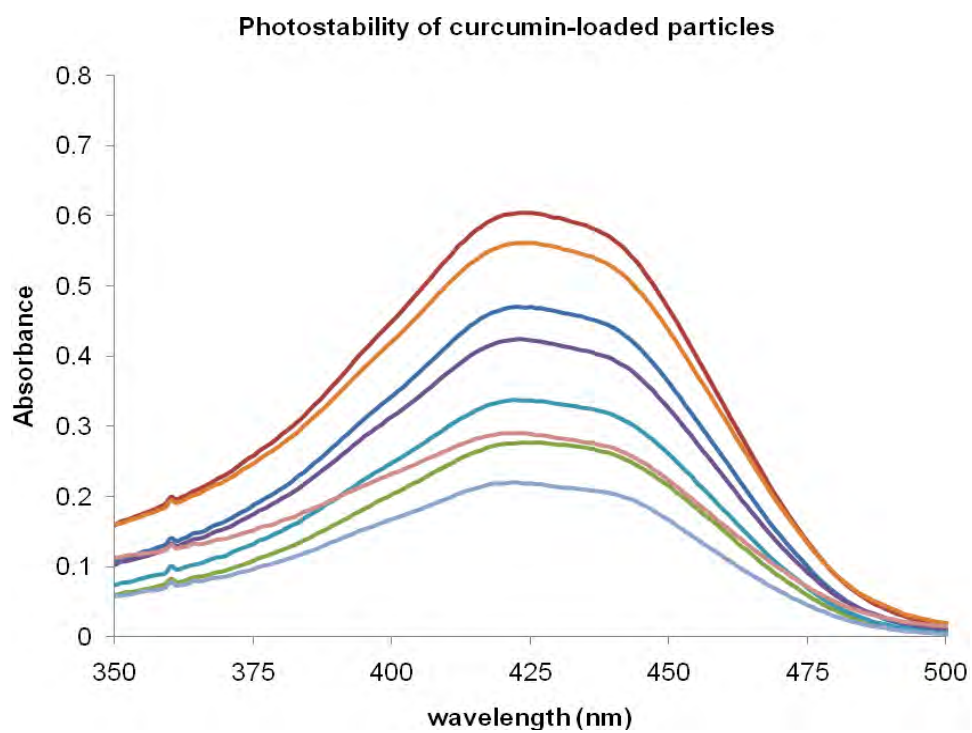
Photostability of curcumin-loaded particles

Calibration curve of standard curcumin in ethanol
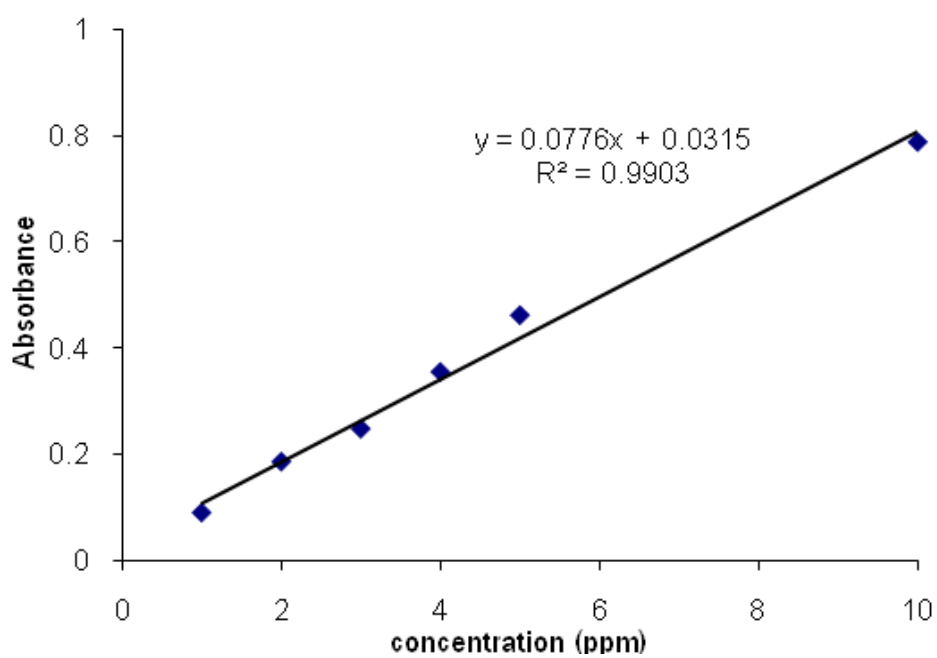
$y = 0.0776x + 0.0315$
$R^2 = 0.9903$

By plotting a graph between absorbance and concentration of standard curcumin solutions, a linear relationship was obtained and used for calculation of concentration of remain and lost curcumin after sunlight exposed.

1. % Remained Curcumin

$$\% \text{ remained} = \frac{\text{concentration of curcumin after sunlight exposed (ppm)}}{\text{concentration of curcumin used (ppm)}} \times 100$$

C-EC:	curcumin remained	=	717.7	ppm
	curcumin used	=	1000	ppm
	% remained	=	$\frac{717.7}{1000} \times 100$	
		=	71.77	%

C-ECMC:	curcumin remained	=	732.8	ppm
	curcumin used	=	1000	ppm
	% remained	=	$\frac{732.8}{1000} \times 100$	
		=	73.28	%

C-PCPLC:	curcumin remained	=	929.1	ppm
	curcumin used	=	1000	ppm
	% remained	=	$\frac{929.1}{1000} \times 100$	
		=	92.91	%

C-PB4-I:	curcumin remained	=	787.8	ppm
	curcumin used	=	1000	ppm
	% remained	=	$\frac{787.8}{1000} \times 100$	
		=	78.78	%

C-PB4-II: curcumin remained   =   686.4 ppm

                curcumin used   =   1000   ppm

                % remained   = $\dfrac{686.4}{1000}$ x 100

                                                    =   68.64 %

2. % Lost Curcumin

% lost (ppm) = 100 - % remained curcumin

C-EC: curcumin remained   =   71.77 %

                % lost   =   100 - 71.77

                                                      =   28.23 %

C-ECMC: curcumin remained   =   73.28 %

                % lost   =   100 - 73.28

                                                      =   26.72 %

C-PCPLC: curcumin remained   =   92.91 %

                % lost   =   100 - 92.91

                                                      =   7.09   %

C-PB4-I: curcumin remained   =   78.78 %

                % lost   =   100 - 78.78
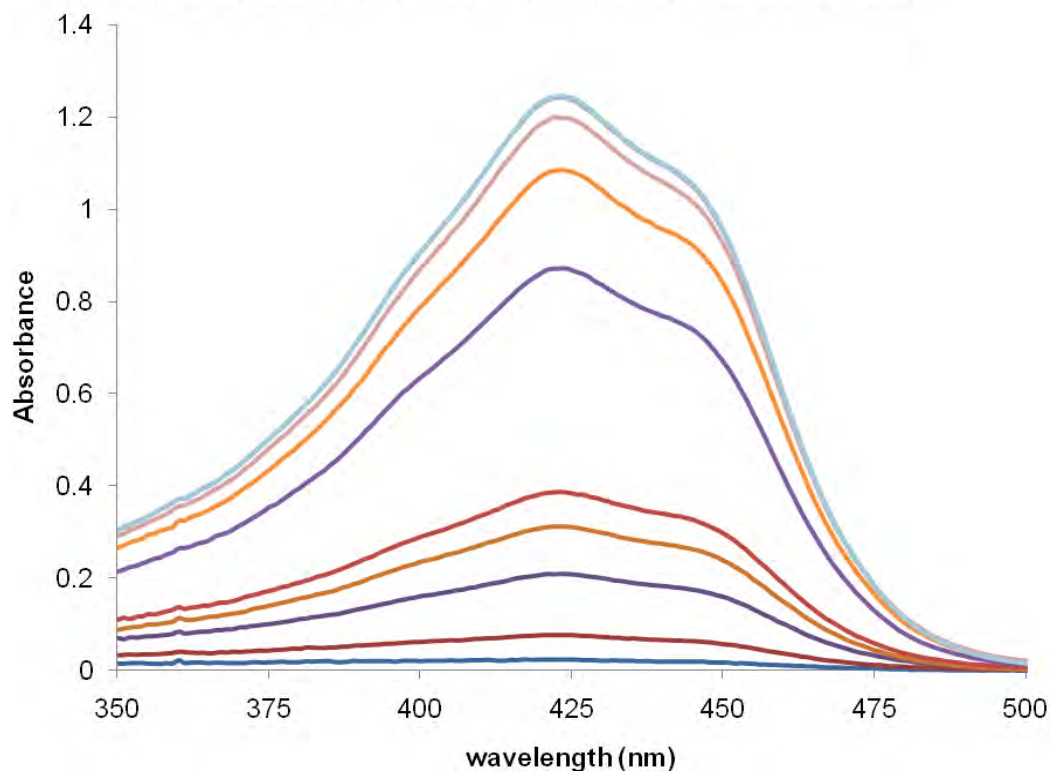
                                                      =   21.22 %

C-PB4-II: curcumin remained   =   68.64 %

                % lost   =   100 - 68.64

                                                      =   31.36 %
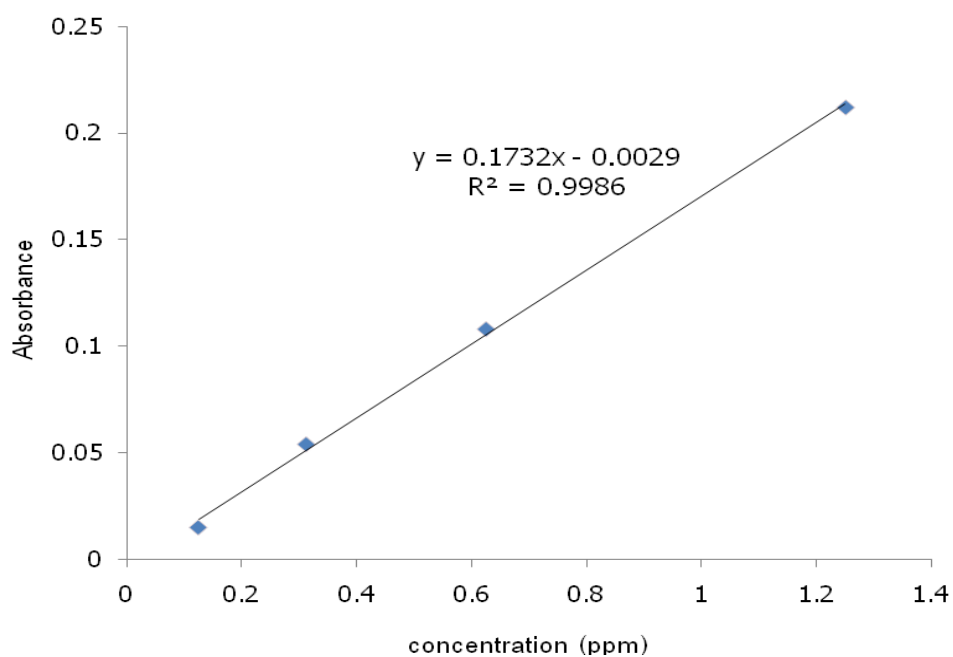
APPENDIX B

Calibration Curve of Standard Curcumin in Various Release Medium

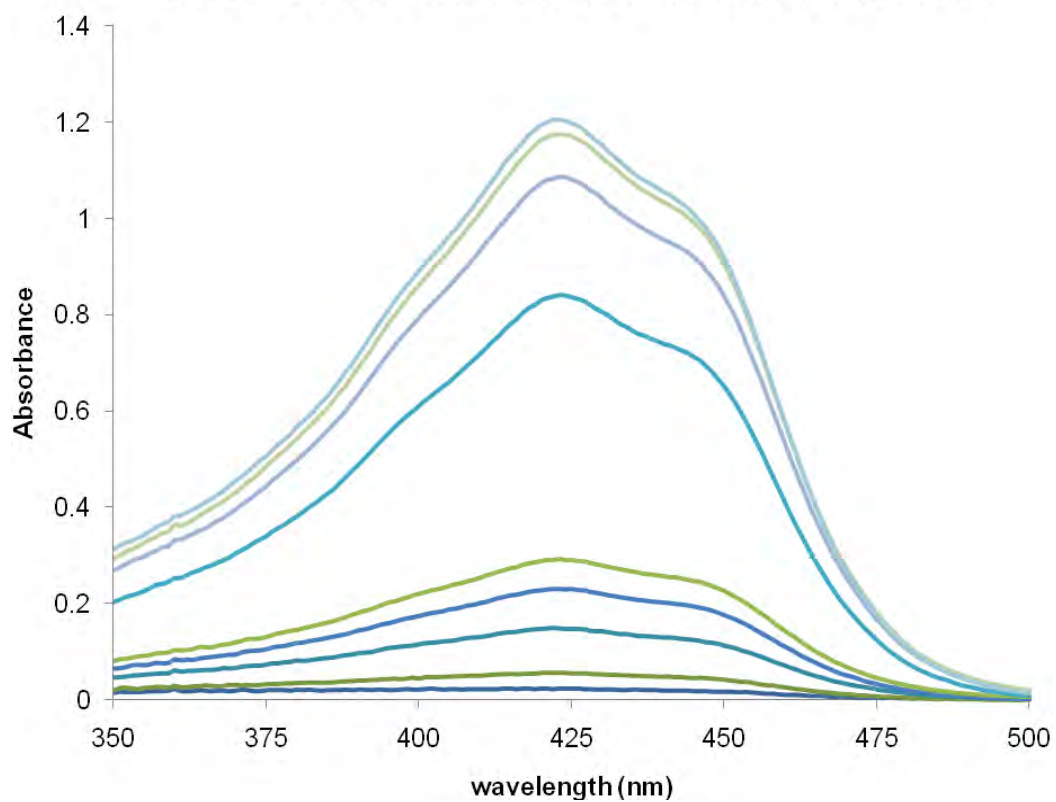1. Calibration curve of standard curcumin in release medium pH 5.5

$y = 0.0854x$
$R^2 = 0.9946$
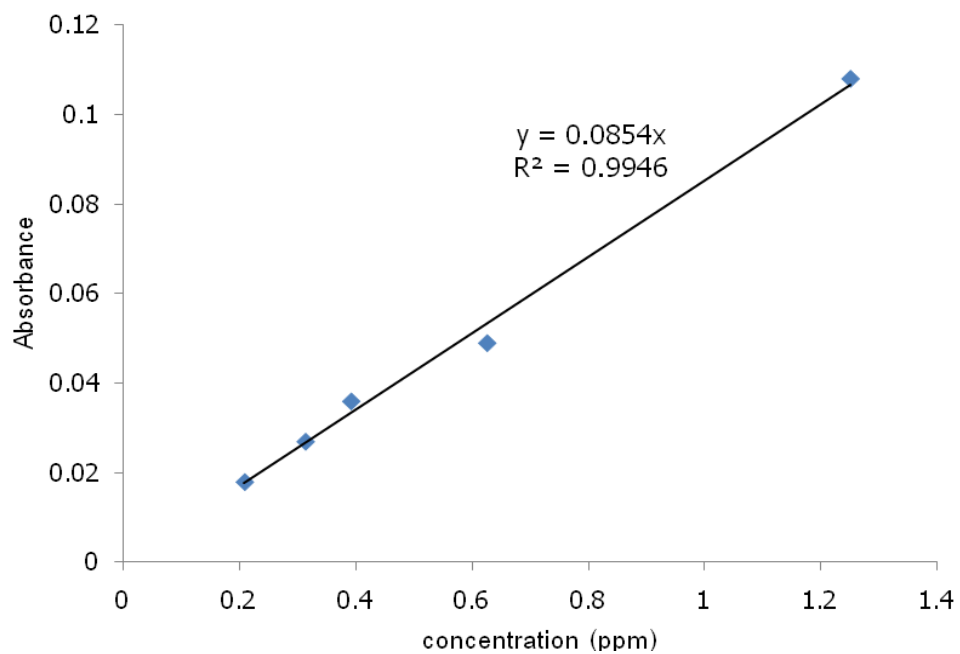
spectrum profile of curcumin in release medium pH 5.5 at various time

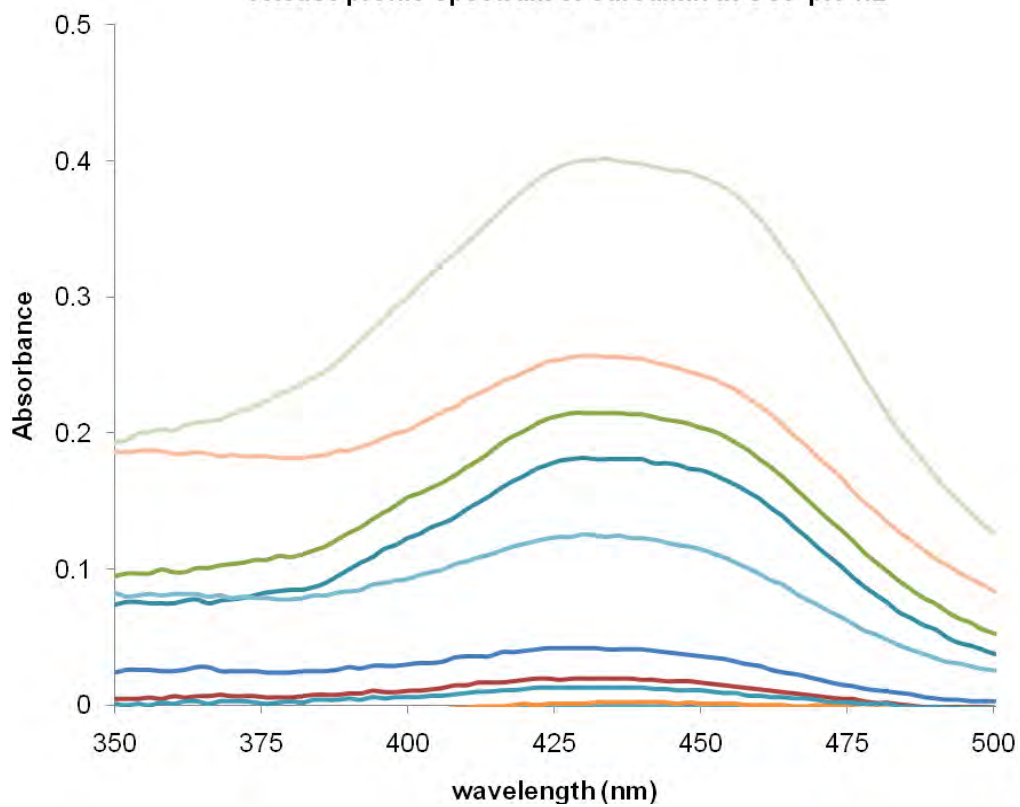2. Calibration curve of standard curcumin in release medium pH 7

$y = 0.1732x - 0.0029$
$R^2 = 0.9986$

spectrum profile of curcumin in release medium pH 7 at various time
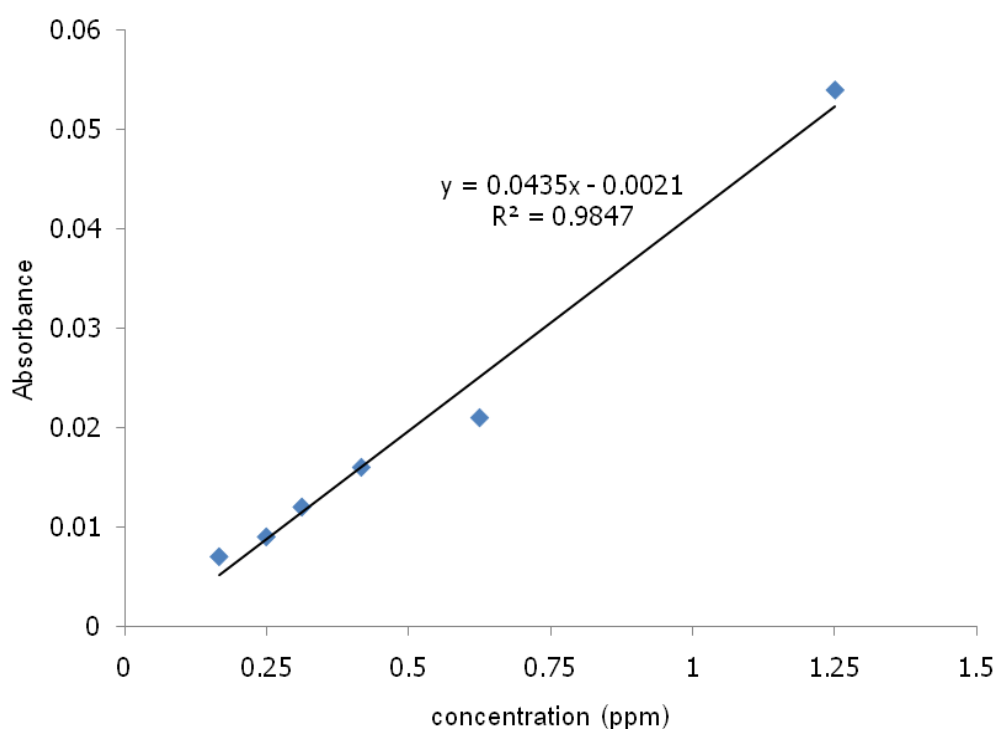
3. Calibration curve of standard curcumin in simulated gastric fluid pH 1.2
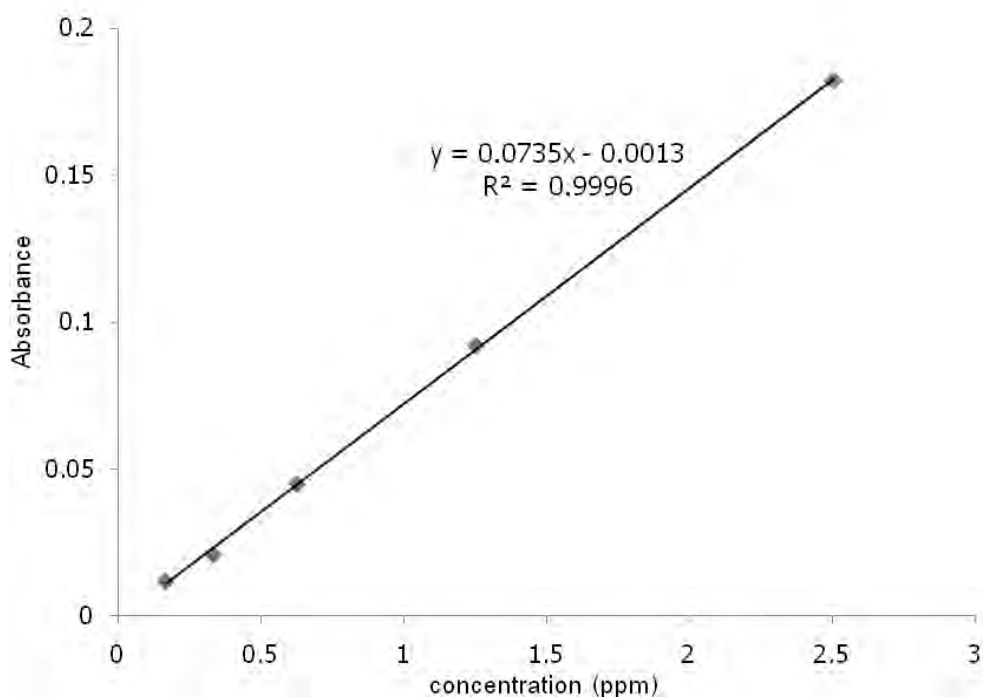
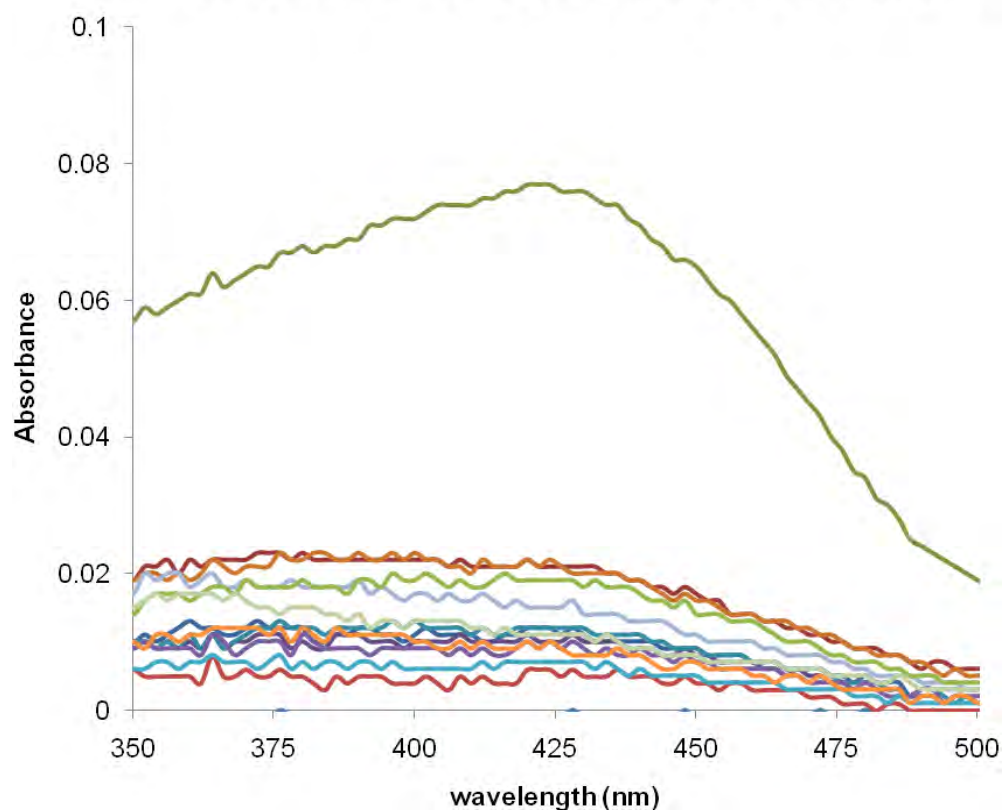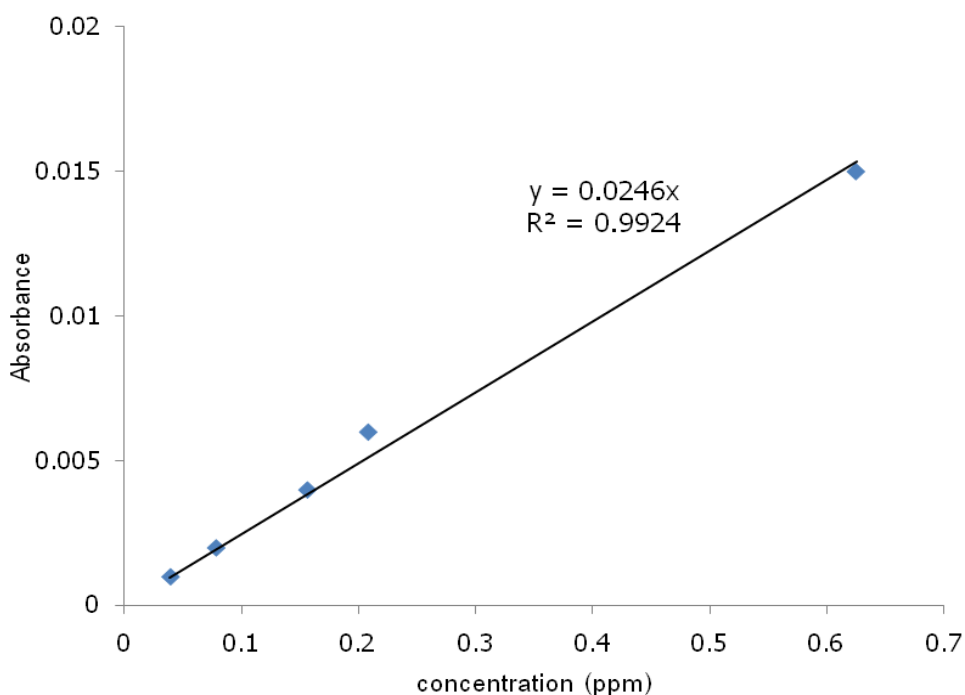release profile spectrum of curcumin in SGF pH 1.2

4. Calibration curve of standard curcumin in simulated intestinal fluid pH 6.8

$$y = 0.0435x - 0.0021$$
$$R^2 = 0.9847$$

releare profile spectrum of curcumin in SIF pH 6.8under pH 6.8

5. Calibration curve of standard curcumin in isotonic phosphate buffer saline pH 7.4
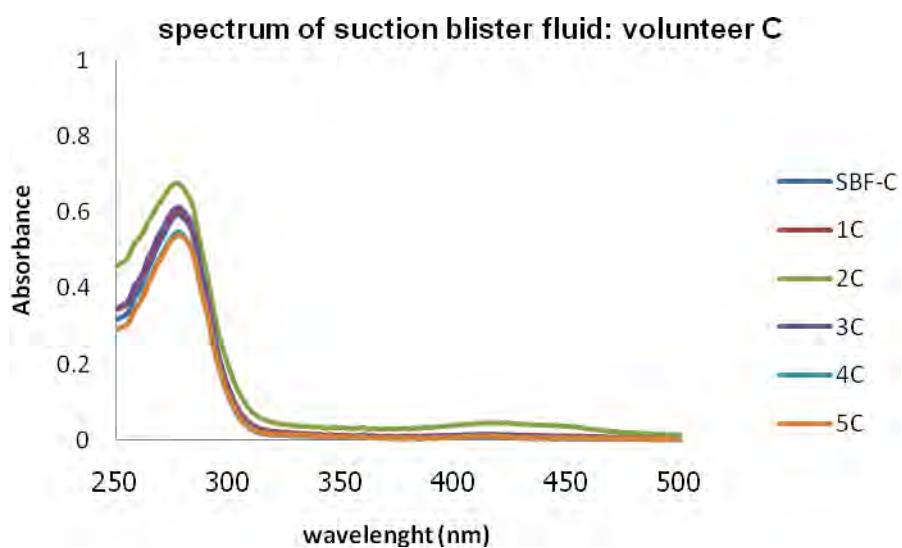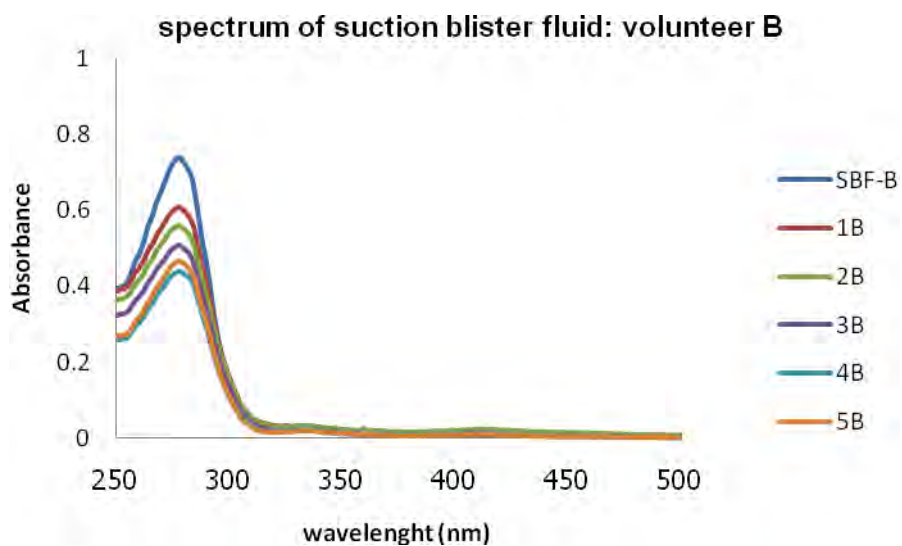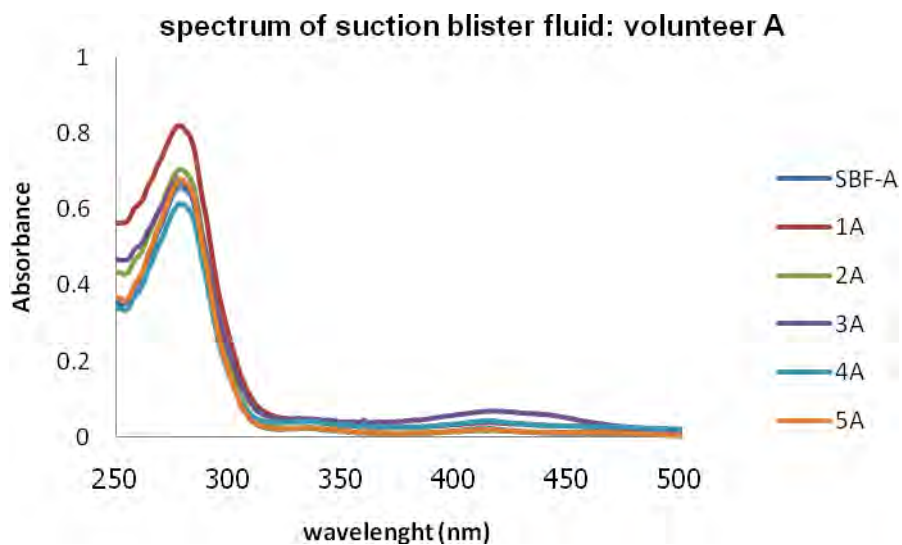

By plotting a graph between absorbance and concentration of standard curcumin solutions, a linear relationship was obtained and used for calculation of release of curcumin.

$$\text{Release (\%)} = \frac{\text{Released curcumin}}{\text{Total curcumin used}} \times 100$$

Example: release of curcumin in SGF at 24 h;

C-EC: curcumin released   =   0.167 mg

             curcumin used   =   5   ml

             % release   = $\frac{0.167}{5}$ x 100

                                      =   3.34   %

C-ECMC: curcumin released   =   0.293 mg

             curcumin used   =   5   ml

             % release   = $\frac{0.293}{5}$ x 100

                                      =   5.86   %

spectrum of suction blister fluid: volunteer A

spectrum of suction blister fluid: volunteer B

spectrum of suction blister fluid: volunteer C

spectrum of suction blister fluid: volunteer D

spectrum of suction blister fluid: volunteer E

spectrum of C-EC and FC lotion
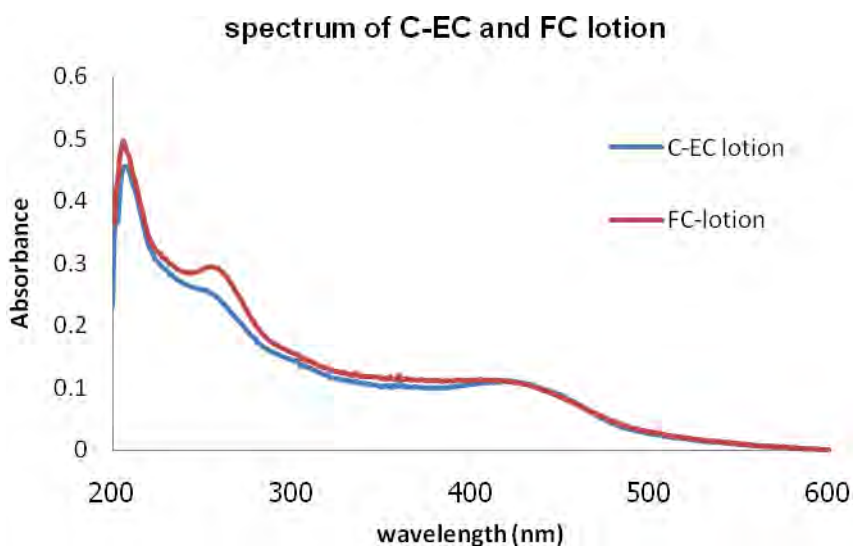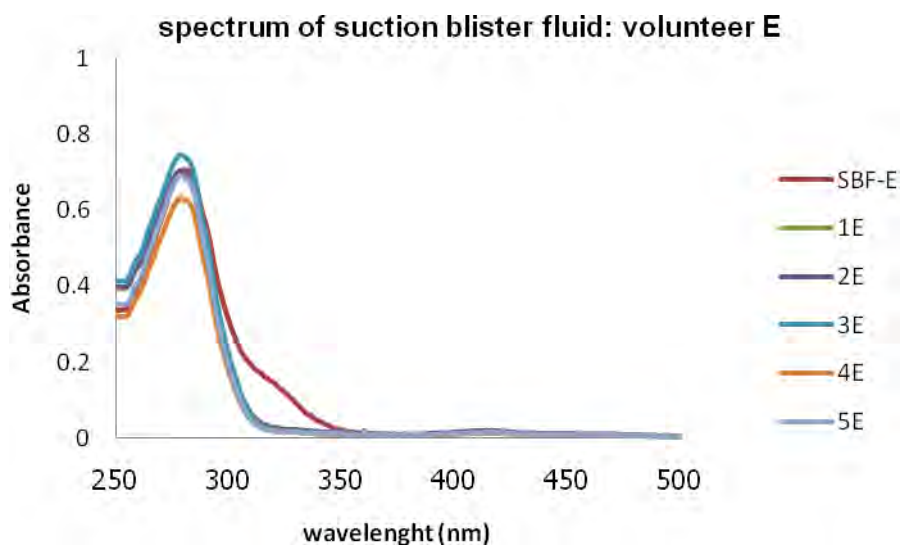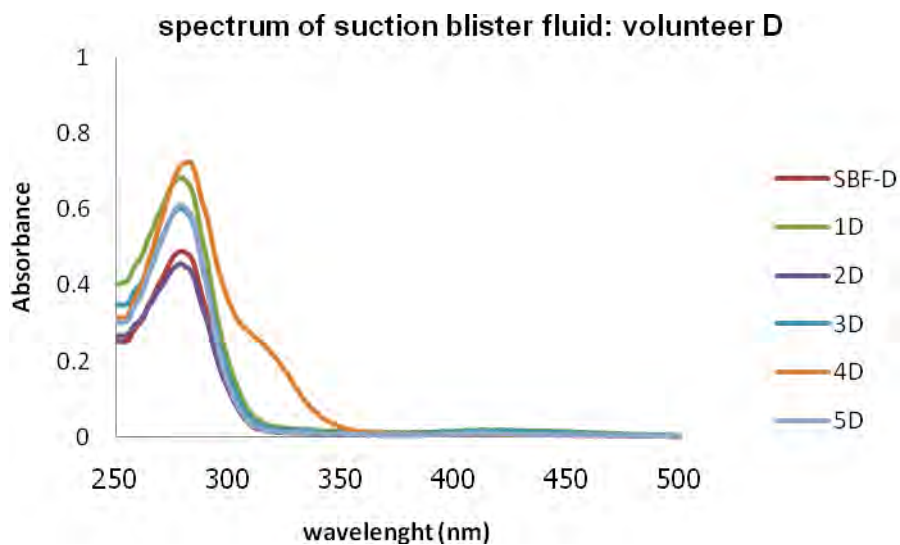
APPENDIX C

Phosphate Buffer Solution Preparation

    1. 0.1 M Phosphate Buffer Solution pH 4

        KH_2PO_4 6.80   g

        2M HCL   0.34   ml

        Dissolve KH_2PO_4 with distilled water, add 2M HCl then adjust volume to 500 ml with distilled water to get the require pH.

    2. 0.1 M Phosphate Buffer Solution pH 5.5

        KH_2PO_4 6.65   g

        K_2HPO_4 0.17   g

        Dissolve KH_2PO_4 and K_2HPO_4 with distilled water then adjust volume to 500 ml with distilled water to get the require pH.

    3. 0.1 M Phosphate Buffer Solution pH 7

        KH_2PO_4 4.17   g

        Na_2HPO_4 2.75   g

        Dissolve KH_2PO_4 and Na_2HPO_4 with distilled water then adjust volume to 500 ml with distilled water to get the require pH.

    4. 0.1 M Phosphate Buffer Solution pH 10

        Na_2HPO_4 7.07   g

        1M NaOH   0.20   ml

        Dissolve Na_2HPO_4 with distilled water, add 1M NaOH then adjust volume to 500 ml with distilled water to get the require pH.

5. Isotonic Phosphate Buffer Saline pH 7.4

NaCl	8.00	g
KCl	0.20	g
KH_2PO_4	0.20	g
Na_2HPO_4	1.44	g

Dissolve NaCl, KCl, KH_2PO_4 and Na_2HPO_4 with distilled water then adjust volume to 1000 ml with distilled water to get the require pH.

6. Simulated Gastric Fluid pH 1.2

NaCl	2.00	g
Pepsin	3.20	g
Conc. HCL	7.00	ml

Dissolve NaCl and pepsin with distilled water, add conc. HCl then adjust volume to 1000 ml with distilled water to get the require pH.

7. Simulated Intestinal Fluid pH 6.8

KH_2PO_4	6.80	g
0.2 N NaOH	77.00	ml

Dissolve KH_2PO_4 with distilled water, add 0.2 N NaOH, adjust pH with 0.2 N NaOH or 0.2 N HCl to get the require pH (if required) then adjust volume to 1000 ml with distilled water.

VITA

Miss Natthakitta Suwannateep was born on 25th November, 1971 in Nakhon Ratchasima. She has got Bachelor Degree of Science in Biotechnology (second class honor) from Srinakharinwirot University in 1993. She worked as chemist at Bayer Laboratories Co., Ltd. (under Bayer Thai Co., Ltd.). She has got Master Degree of Science in Biotechnology from Chulalongkorn University in 1999. After that, she has been working as lecturer at the Faculty of Science and Technology, Suan Dusit Rajabhat University. At academic year 2006, she has started Doctoral degree at Chulalongkorn University. Her study is under the scholarship from the Office of the Higher Education Commission (Strategic Scholarship for Frontier Research Network for the Join Ph.D. Program Thai Doctoral degree). She has conducted a part of research for 1 year at Center of Experimental and Applied Cutaneous Physiology (CCP), Department of Dermatology, Charité-Universitätsmedizin Berlin, Germany. During her study, she had poster presentations at the Commission on Higher Education Congress I: University Staff Development Consortium (CHE-USDC Congress I) 2008, Cholburi, Thailand and the Third International NanoBio Conference Zurich 2010, ETH Zurich, Switzerland.

Her address is 12/88 Inthamara 4, Suthisarn road, Phayathai, Bangkok, 10400.

Academic Publications

1. N. Suwannateep, S. Wanichwecharungruang, and J. Lademann, Curcumin Encapsulation Using Biodegradable Polymeric Nanoparticles: Controlled Release, Photostability and Transdermal Skin Penetration, European Cells and Materials. 20 (2010): 251.

2. N. Suwannateep, et al., Mucoadhesive curcumin nanospheres: Biological activity, adhesion to stomach mucosa and release of curcumin into the circulation. Journal of Controlled Release. (2011), doi:10.1016/j.jconrel.2011.01.011